PROSPECT OF RENEWABLE THERMAL ENERGY IN BLACK TEA PROCESSING IN ASSAM: AN INVESTIGATION FOR ENERGY RESOURCES AND TECHNOLOGY

A THESIS SUBMITTED IN PARTIAL FULFILLMENT OF THE
REQUIREMENTS FOR THE DEGREE OF
DOCTOR OF PHILOSOPHY

PARTHA PRATIM DUTTA

Registration Number 099 of 2000

SCHOOL OF ENGINEERING
DEPARTMENT OF ENERGY
TEZPUR UNIVERSITY
JUNE - 2014

I

dedicate this thesis to my

Parents (Late Horaswar Dutta)

(Mrs. Purniema Neog Dutta)

my wife (Dr. Manasai Devi)

my sweet daughter (Jumki)

Whose love and care encouraged me

to complete this thesis work successfully

DECLARATION

I do hereby declare that the thesis entitled "**Prospect of Renewable Thermal Energy in Black Tea Processing in Assam: an Investigation for Energy Resources and Technology**", being submitted to the Department of Energy, School of Engineering, Tezpur University, is a record of original research work carried out by me. All sources of assistance have been assigned due acknowledgment. I also declare that neither this work as a whole nor a part of it has been submitted to any other University or Institute for any other degree, diploma or award.

Place: Tezpur

Date: 23/06/2014

(Partha Pratim Dutta)

D.C. Baruah, B.E., M.Tech,
Professor

TEZPUR UNIVERSITY
Department of Energy
Ph.D Napaam-784028
Tezpur, Assam, India

CERTIFICATE BY THE SUPERVISOR

This is to certify that the matter embodied in the thesis entitled "**Prospect of Renewable Thermal Energy in Black Tea Processing in Assam: an Investigation for Energy Resources and Technology**", submitted by Partha Pratim Dutta for the award of degree of Doctor of Philosophy of Tezpur University is a record of bona-fide research work carried out by him under my supervision and guidance. The results embodied in this thesis have not been submitted to any other University or Institute for the award of any degree or diploma.

Date: 23/06/2014

(D.C.Baruah)

TEZPUR UNIVERSITY
(A Central University established by an Act of Parliament)
NAPAAM, TEZPUR-784028, INDIA
Ph: 03712-267004, 267005 Fax: 03712-267005, 267006

CERTIFICATE

This is to certify that the thesis entitled "**Prospect of Renewable Thermal Energy in Black Tea Processing in Assam: an Investigation for Energy Resources and Technology**", submitted to the Tezpur University in the Department of Energy under the School of Engineering; in partial fulfillment for the award of the Degree of Doctor of Philosophy, has been examined by us on 17th Nov, 2014 and found to be satisfactory.

The committee recommends for the award of the degree of Doctor of Philosophy.

Supervisor

Date: 17.11.2014

External Examiner

Date: 17/11/14

ACKNOWLEDGEMENT

I wish to express my sincere thanks and deep sense of gratitude to my supervisor, Prof. D.C. Baruah, Department of Energy, Tezpur University for his constant inspiration, scholarly guidance, and helpful suggestions throughout the course of this thesis work. I am indebted to him for allowing me to draw upon his precious and valuable time. I will always remember his quick analysis, thoughtful solutions, and critical reviews he has given throughout the period. I am also grateful to HOD, Energy, Prof. D Deka, and Dr. D. Datta, my colleague and HOD Mechanical Engineering for their inspiration. I am extremely grateful to Er. Utpal Bhattachyya (Manager, Engineering, Williamson Magor Group, Biswanath Chariali, Tezpur, Assam) for arranging fermented tea samples from their Tea estate like *Rupajuli, Tarajuli* and *Goghora* as well respective tea estates management. I am also grateful to colleagues and staff of Department of Energy and Mechanical Engineering for encouragement and assisting in fabrication process of hardware required as well as assistance from Ashutosh is also acknowledged.

I am grateful to different tea industries where the survey work for thermal energy consumption pattern was conducted.

I am also grateful to my family members, particularly my wife, mother, and sweet daughter Jumki for their support and encouragement.

(Partha Pratim Dutta)

ABSTRACT

Tea is one of the principal and cheap soft drinks in the world. India is the second largest producer of tea, manufacturing about 1137 million kg of made tea (next to China with 1761 million kg annual production). India exports about 236 million kg tea with annual revenue of about $480 million (as per the statistics of the year 2012) from tea processing industry. Tea industry is about 200 years old and has about 0.58 million hectares of tea cropped land providing direct employment to about one million people. About half of the Indian tea production is contributed by the tea industries situated in Assam (a northeastern state of India). Black tea, which is a specially processed made tea, dominates Assam's tea production.

Cost of tea processing has bearing influence on economy of tea production. Black tea processing consists of series of standard unit operations. They are withering (partial removal of moisture), rolling (size reduction), fermentation (biochemical reaction in presence of oxygen), drying, and sorting (fiber removal and grading). Energy is one major cost contributor in tea processing. About (90 to 95) % of total thermal energy is required in the form of hot air for tea drying. Traditionally, tea drying oil, natural gas, and coal are used as sources of thermal energy for tea processing in the factories located in Assam with some variation in specific energy consumption amongst the processing units. For example, about 24, 28 and 44 MJ of specific thermal energy were reported to be consumed by oil fired, gas fired and coal fired tea dryer, respectively for each kg of made tea processing.

There have been some issues concerning the uses of these conventional energy resources in tea processing such as, ever increasing cost of conventional fuel and adverse environmental impact. For example, the volatile prices of fossil fuel have badly affected the economy of Assam tea. Further, fossil fuel based tea processing industries in India has reported to emit about 3252 million kg greenhouse gas annually. Considering these issues, an alternative system of energy is essentially required for tea processing.

There have been several attempts to search for alternative energy sources comprising of cleaner new and renewable energy for different industrial applications.

ABSTRACT

There are many successful examples of renewable energy adaption both in thermal and electrical modes in industries. However, success of the application of renewable energy depends upon several local factors, primarily due to spatially and temporally varying availability and varying characteristics of the resources. Further, there are many renewable energy conversion technologies and the success of these technologies depends on appropriate research and development intervention.

Keeping in view of the above, the present research work has been directed to explore renewable energy resources and technological feasibility for substitution of conventional fuel in tea processing in Assam. Biomass gasification and solar thermal are two prominent renewable energy technologies. However, both of these sources have individual limitations with reference to uncertainty of spatial and temporal availability as per demand. Therefore, a hybrid mode of application for tea processing may be feasible, provided soundness of technologies is assured. The present investigation has focused to examine the usability of the said two renewable energy sources in three stages *viz*., (1) Characterization of some locally available biomass species, generation of appropriate mode of thermal energy through gasification, and tea drying experimentation and modelling with producer gas combustion product mixed with air as drying medium (2) technology for harnessing adequate quantity of solar thermal energy for tea processing and finally, (3) prospect of hybridization of gasification and solar thermal energy for fulfilling the need of tea processing.

Ten specific type of locally available biomass samples [*Bambusa tulda, Delonix regia, Azadirachta indica, Ficus lepidosa, Dalbergia sissoo, Psidium guajava, Samanea saman, Camellia sinensis, Moringa oleifera and Polyalthia longifoli*], were considered for proximate, ultimate analysis and determination of calorific values. Further, experiments were conducted using a 30 $kW_{thermal}$ (maximum output) biomass gasifier with selected species (*Camellia sinensis,* uprooted shrubs) of biomass to see technical feasibility and its performance to utilize as fuel for tea drying in a laboratory scale drying unit.

Laboratory scale tea drying experiments were also conducted in an attempt to investigate the comparative drying kinetics based on producer gas fueled drying and that of conventional mode of drying. An appropriate producer gas premixed burner was developed by modifying and existing 5 kW diffusion type gas burner. In the series of experiments, thin layer drying kinetics of fermented tea (*Camellia sinensis*) was investigated at both varying air temperatures (80, 90,100, and 110) °C and varying flow rates [0.50, 0.65, and 0.75) m s^{-1}] of drying fluid using a producer gas burner laboratory scale tea dryer. The black tea drying data could be fitted to five different semi-theoretical models [*viz.*, (1) Lewis, (2) Page, (3) Modified Page, (4) Henderson and Pabis and (5) Two Terms] to identify best-fit model. The best-fit model was further used to estimate activation energy required for tea drying while using producer gas as a fuel. During black tea drying experiment, rate of consumption of producer gas and fermented tea moisture loss were also recorded continuously to estimate specific energy consumption of the dryer.

In order to explore the prospect of another renewable energy source/technology, an attempt was made to design a suitable solar air heater for supplementing thermal energy for tea processing. The performance of a solar air heater mostly depends on surface geometry of absorber plate. Therefore, two types of surface geometries (*viz.*, hemispherical, and smooth absorber) were examined and the best configuration was identified based on thermo hydraulic efficiency of hemispherical protruded absorber. The performance test result of the solar air heater with the best absorber plate configuration was further used to examine its usefulness to substitute thermal energy required for tea processing.

Finally, the possible hybridization of producer gas and solar hot air systems was analyzed by mixing solar hot air with producer gas combustion products. This was investigated based on the data assessed from laboratory scale experiments with a view to examine overall performance of the hybrid renewable energy system.

The analysis of the biomass characteristics data indicated the prospect of using all the ten biomass samples through gasification routes for generation of thermal energy although they exhibit some varying degree of fuel characteristics. Based on their highest calorific value characteristics, *Camellia sinensis* (18.400 MJ kg^{-1}, *Psidium guajava* (18.403 MJ kg^{-1}) and *Bambusa tulda* (18.401 MJ kg^{-1}) were selected for further testing on gasification system for tea drying experiments.

For each atom of C, the variation of H atoms ranged between 1.866 (*Delonix regia*) and 1.580 (*Ficus lepidosa*). Such variation for N was *Azadirachta indica* (0.051) to *Camellia sinensis* (0.03). The variation of O atom was 0.698 (*Ficus lepidosa*) and 0.599 (*Bambusa tulda*). These results of fuel characteristics were useful to understand the behaviour of the fuels for gasification. While fueling the experimental downdraft gasifier using *Camellia sinensis,* output producer gas could be obtained with 4.5 MJ Nm^{-3} calorific values (measured using a Junker gas calorimeter). Further, the composition of producer gas with *Camellia sinensis* was analyzed and it was found in line with characteristics of the input fuel. Since all three fuels have almost similar calorific value, therefore, thermally all could be considered as suitable fuel for gasification. Therefore, use of these fuels as mixture may be recommended.

The suitability of producer gas (obtained from the mixture of *Camellia sinensis, Psidium guajava* and *Bambusa tulda*) for tea drying was ascertained from the drying experiments. Thin layer experimental studies of fermented tea with producer gas as a fuel gave the modified Page model [with drying rate constant (k = 25.91×10^{-4} s^{-1}) and exponent (n = 1) at 100 °C] as the best-fit model. In general, both the temperatures of drying media and its flow velocities influenced to drying rate constant (k) and exponent (n). Further, the modeled data was used to compute the diffusivity constant (D_o = 0.746 × 10^{-3} m^2 s^{-1}) and activation energy (E_a = 52.104 kJ mol^{-1}). Specific energy consumption of producer gas fired tea drying has been estimated as 10.20 MJ kg^{-1} of water removed.

As mentioned earlier, the feasibility of using solar thermal energy for tea processing was examined through an optimally designed low cost flat plate solar air heater at solar radiation (790 W m^{-2}). The size of the hemispherical protruded plate solar air heater single duct was 2400 mm × 375 mm × 37.5 mm. Thermal efficiency of roughened solar air heater was found to be a strong function of air mass flow rate. Mass flow rate of air (0.028 kg m^{-2} s^{-1} from one duct) and with the surface roughness geometry (hemispherical protruded) of dimensionless relative roughness height $\frac{e}{D}$ = 0.035, relative roughness pitch $\frac{p}{e}$ = 12 and around Reynolds number 12000, the best thermo-hydraulic efficiency (74%) was recorded.

Experiment was conducted with above configuration solar air heater and up to 65 °C outlet air temperature was achieved in summer at Tezpur University campus. Analytical studies based one experimental results showed that minimum contribution of solar energy was 12.9% at (9.00- 9.40) a.m., while maximum contribution was 27.23% at (12.00 -12.40) p.m in solar biomass hybrid mode. By using five 1.65 m^2 improved solar air heater, average 20% saving in biomass energy was possible.

Finally, based on the results of (i) gasification cum tea drying experiments and (ii) performance results of solar air heater for the test location, a techno-economic analysis was done to examine the prospect of hybrid mode of renewable energy use for tea drying. It was estimated that for a 0.99 M kg made tea factory, 28% of tea drying thermal load may be covered by plantation of 22.5 ha *Bambusa tulda*, through biomass gasification in a 454 kW downdraft gasifier. It has been perceived that if 400 m^2 of tea factory galvanized roof were converted by using black painting, plywood insulation and tempered glass enclosure to convert into solar air heater then average 20 % of biomass energy may be saved. The annual carbon-dioxide reduction 2189 t is achievable. The payback period of the hybrid renewable thermal energy based system is less than fifteen months and benefit to cost ratio is 1:1.

There is potential benefit for application of biomass gasification and solar air preheating technology in tea manufacturing industries in Assam. However, proper government policy is required for long-term fast growing biomass plantation and its assured supply at regulated prices. Factory roof integrated efficient solar air heaters may effectively trap solar thermal energy. It is concluded that biomass gasification and solar air heater combined renewable energy technology is feasible for partial thermal energy substitution in tea manufacturing industries in Assam, India.

Table of Contents

Table of Contents

Table of Contents

Table of Contents

Table of Contents

List of Figures

List of Figures

List of Tables

Nomenclature

A	Area of cross section (m^2)
A1	Drying kinetic constant
A_c	Collector area (m^2)
A_{ff}	Free flow area (m^2)
A_p	Area of absorber plate (m^2)
ASHRAE	American Society of Heating Refrigeration and Air-conditioning Engineering
ASTM	American Society of Testing and Materials
B	Constant
c	Constant = $\eta_F \eta_m \eta_{tr} \eta_{th}$
C_{pa}	Specific heat of air ($Jkg^{-1}K^{-1}$)
C_{pv}	Specific heat capacity of vapour ($Jkg^{-1}°C^{-1}$)
CTC	Curl Tear and Crushing
CV	Calorific value
D_h	Hydraulic diameter (m)
d	Print diameter of hemispherical protrusion (mm)
D_{eff}	Effective diffusivity (m^2s^{-1}))
e	Protrusion height (mm)
Ea	Activation energy (kJ mol^{-1})
FFA	Free Fatty acid
F_0	Heat removal factor based on outlet air
FC	Fixed carbon
F_n	Future amount of money at end of *n* year
F_R	Collector heat removal factor
f_s	Friction factor for smooth passages.
f	Friction factor
G	Mass flow rate of air per unit collector are (kg $s^{-1}m^{-2}$)
H	Duct height (m)

h	Convective heat transfer coefficient. ($Wm^{-2}K^{-1}$)
$\bar{h}$	Average convective heat transfer coefficient ($Wm^{-2}K^{-1}$)
HHV	Higher heating value (MJ kg^{-1})
HSD	Hybrid solar dryer
i	Rate of interest
I_c	Incident radiation (Wm^{-2})
K	Thermal conductivity of air ($Wm^{-2}K^{-1}$)
k	Drying rate constant (s^{-1})
kW	kilowatt
L	Latent heat of vaporization of water (kJ kg^{-1})
L_c	Length of collector (m)
$\dot{m}$	Mass flow rate (kg s^{-1})
M, M_o, M_e	Material moisture (Initial, equilibrium)
MJ kg^{-1}	Mega Joule per kilogram
MNRE	Ministry of New and Renewable Energy
MR	Moisture ratio
Mt	Million tonne
m_v	Mass of water removed (kg)
n	Numbers of years
n	Kinetic constant (exponent)
N	Number of observation
Nu	Nusselt number
OSD	Open sun drying
P	Principal amount
p	Pitch (mm)
ΔP	Pressure drop across collector length (Nm^{-2})
ΔPG	Pressure drop across gasifier (Nm^{-2})

ΔPN	Pressure drop across nozzle (Nm^{-2})
P_m	Mechanical energy consumed for propelling air through collector. (W)
Pr	Prandtl number
PT	Platinum resistance thermometer
PV	Peroxide value
PVT	Photovoltaic thermal
q_u	Useful heat gain (W)
R	Average radius of tea particle (mm)
R	Universal Gas constant (J $mol^{-1}K$)
R_{av}	Average radius (m)
Re	Reylonds number
RMSE	Root mean square error
S	Short way length between protrusions (m)
S-BHCD	Solar biomass hybrid cabinet dryer
SCDM	Simplified Constant Diffusivity Model
SFC	Specific fuel consumption (MJ kg^{-1})
SIFC	Sophisticated Instrumentation Facilities Centre
SWG	Standard wire gauge
T	Temperature in K
$\bar{t}_a$	Average ambient temperature (K)
$\bar{t}_p$	Average plate temperature (K)
t	Drying time (minute)
T_a,	Ambient temperature (K)
T_{amb}	Ambient air temperature (°C)
t_{fm}	Mean fluid temperature (K)
T_i	Inlet air temperature (K)
T_{in}	Hot air inlet temperature (°C)

T_n	Different temperatures (°C) in setup
T_o	Outlet air temperature (K)
$T_{p,}$	Plate temperature (K)
t_{pm}	Mean plate temperature (K)
TBA	Thiobarbituric acid
TMA-N	Trimethylamine nitrogen
TVB-N	Total volatile bases nitrogen
UV	Ultra violet
V_h	Specific air volume (m^3kg^{-1})
VM	Volatile matter
W	Width of the solar air heater duct (m)
wb	Wet basis
WBG	Woody biomass gasifier
w_R	Uncertainty in results
X	Moisture percent (wet basis)
z	Number of constant in the model

Greek symbols

η	Thermal efficiency
τ	Tansmissivity of glass
α	Absorptivity of glass
τ	Transmittance
α	Absorptance
η	Efficiency
ρ	Density
β	Angle of attack
Φ	Equivalence ratio
η_{cold_gas}	Cold gasification efficiency

Subscripts

Nomenclature

a	Ambient
c	Collector
ff	Fluid flow
fm	Fluid mean
i	Inlet
l	Loss
m	Mechanical
h	Hydraulic
o	Outlet
p	Plate
pm	Plate mean
s	Smooth
u	Useful
b	Back
s	Side
t	Top
cl	Collector loss

1.1 Importance of tea

Tea is one of the principal and cheap soft drink in the world. Per capita tea consumption in the world (0.3 kg y^{-1}, in 2009) is steadily increasing with augmentation of production in recent years. India is largest producer of tea manufacturing about 1137 M kg next to China (1761 M kg). India exported about 236 M kg teas for revenue of about $ 480 million in the year 2012. About 20% (of total tea production is exported rest 80% is used for domestic consumption. Indian tea industry is about 200 years old and it has 579350 hectares total tea cropped area. Tea plantation area covered by small grower is about 163326 ha (up to 10.12 ha) and area under big grower is about 416024 ha (above 10.12 ha). Present average productivity of made tea is about 2000 kg ha^{-1} in India. About 50 % of Indian tea production is from tea estate situated in Assam. Therefore, tea processing is one of the traditional plantation based beverage industries in India providing direct and indirect employment to one million workforces. Tea crops provide the highest employment per unit arable area. It generates largest employment to the men and women of weaker section of the society. Tea industries generate indirect employment for tea- machinery development sector, agricultural chemicals, warehouse facilities, road transport, etc. These are in addition to the direct employment generation in tea production and processing sector. Moreover, tea industry is supporting machinery-manufacturing industries for supply and maintenance of tea processing machines. It also supports fertilizer and manure production chemical industries for tea cultivation practices. Thus, growth and development of tea industry is essential to ensure these economic benefits. Improved tea processing machinery development, adoption of energy efficiency and conservation practices, intervention of renewable energy for tea processing, etc., are the future need for sustainable development of this important agro based industrial sector in India. Tea plays a key role in Indian economy and society [1, 2].

It has been reported that tea productivity has increased by 60 % in last two decades. However, internal consumption of tea has increased 7% annually. To maintain India's lead in tea export and upward foreign exchange earnings, stress on tea productivity coupled with stress on better quality and reduced production cost are essential. Employment of improved and innovative tea processing machinery, efficient and economic energy system are some of the key factors to be targeted to achieve such a goal [3]. Since tea manufacturing is highly energy intensive chemical engineering unit operation, therefore a brief description of black tea processing has been discussed below.

1.2 Black tea processing

Black tea processing consists of five unit operations namely withering (partial removal of moisture), rolling (size reduction), fermentation (biochemical reaction in presence of oxygen), drying and sorting (fiber removal and grading). Thermal energy is required in the form of hot air for withering and drying operations. Out of these two energy requirements, drying shares the major fraction of total thermal energy while withering requires very small amount thermal energy (5-10) % for black tea processing [4, 5]. The main sources of thermal energy in Indian tea industries are natural gas, coal, tea drying oil, and fuel wood. Woody biomass is more prominently used in South Indian tea industries. Assam and Northeast India tea industries use other three non-renewable thermal energy sources for black tea manufacturing. Specifically, the Southeast Assam tea industries significantly use natural gas and tea drying oil whereas Northern Assam tea industries use coal for tea drying energy requirement. The principal unit operations with a special reference to thermal energy consumption have been discussed below.

1.2.1 Withering

A standard tea shoot is consisted of two leaves and a terminal bud with (74-77) % moisture (dry surface) and (23-26) % solid matter. About half the solid matter is insoluble in water and it is made up of crude fiber, cellulose, proteins, fat, etc. Fresh tea after plucking is spread in thin layers to dry (withering) it partially for (12-20) hours. During first (4-8) hours, moisture loss is quite rapid and then it slows down for next (10-12) hours until the equilibrium is reached. Green leaf is loaded over the trough at the rate of (25-30) kg m^{-2} area up to 20 cm depth. About 2000 tonne of air is required to process one tonne of made tea and 75% of this air is required during withering. It has been reported that dryer exhaust air may be very efficiently used for withering green leaf in very dry weather.

Optimal withering air temperature and humidity are two important factors to determine quality of made tea and thermal energy requirement for this unit operation. Normally best quality tea is obtained for withering air temperature near to 27 °C with a dry bulb and wet bulb temperature difference 3 °C, at withering trough. As the air has passed through the exhaust, the hygrometric temperature difference should not be below 1.6 °C. Thermal energy is wasted rapidly if hygrometric temperature difference is more than 2.2 °C, at exhaust stream. The wet bulb temperature raises approximately 0.55 °C for (1.65 – 2.2) °C increase in dry bulb temperatures [5]. Moisture is usually reduced to (68-60) % particularly in tea factory situated in Assam. Normally, the tea manufacturing peak time ranges from May to November over the year. From May to September, the climate of Assam is hot and humid. Daytime room temperature is well above 27 °C and therefore addition of extra heat to withering air is not recommended for quality purpose. During rainy or winter season, additional thermal energy is required for withering purposes. Separate tea drying oil burners are used in certain tea factories for withering. Therefore, withering thermal energy requirement is met from varied sources as per availability and ease of operation [5].

During physical wither; there is a change in cell permeability by losing moisture. Bio-chemicals changes occur inside leaf during chemical wither. It is achieved by blowing air sporadically or incessantly at low flow rate to keep leaf cool with loss of moisture for 4-18 hours [6]. However, chemical wither is necessary for producing full and round liquors. The duration could be reduced to 6-8 hours by holding leaf at 30 and 37 °C temperature and airflow rate of 0.01 m^3 s^{-1} [7]. Immediately after plucking, the fresh leaf starts to lose water vapour. The stomata of the lower leaf surface begin to close [8-9]. The maximum initial drying rate is 0.075 kg kg^{-1} (water per kilogram of green leaf per hour) [10].

1.2.2 Fermentation

During fermentation process, the most important quality property of tea is produced. This process is carried out simply by laying the *dhool** (3.75 – 7.00) cm thickness at an average air temperature of 27 °C. On an average, fermentation takes (2.75 - 3.50) hours for completion at a temperature of 26.7 °C. A rapid fermentation at higher temperature suits certain tea; a longer fermentation at a lower temperature might suitable for other variety. By shortening or lengthening the period of fermentation, the degree of colour and quality may be varied. The compounds responsible for tea quality, such as theaflavins (TFs) and thearubigins were found to augment with fermentation time [11].

1.2.3 Drying

The principal objectives of drying are to arrest the fermentation process to have desired properties and to obtain a stable finished product for preservation and marketing. Normally hot air generated by furnace and heat exchanger or flue gas mixed with air is used as drying medium. Multi-stage tea drying process uses different drying medium temperature range in identified zones of dryer for fuel economy and quality. In general, two types of tea dryer are used in black tea manufacturing. They are endless chain pressure and vibrated fluidized bed types tea dryer. The understanding on the working of tea dryer is essential in relation to the present work. Therefore, both the types of dryers are briefly highlighted below.

Endless chain pressure type dryer

Conventional tea dryer is an endless chain pressure (ECP) type. This dryer is normally double firing type and used traditionally in Northeast India tea factory for better quality. Normal range of drying air temperature is (82-99) °C with an exhaust temperature of (49-54) °C to stop stewing and case hardening of *dhool*. Exhaust air temperature 52 °C is ideal for both economy and quality of black tea produced. For double firing, initial temperature may be (93.3 – 104) °C whereas a temperature of (77

* Fermented tea undergoing drying is called *dhool*

– 82.2) °C is suitable for CTC[†] and (71-77) °C for orthodox (special type of tea) tea in second drying depending on the moisture of first drying per batch drying. Average drying time in endless chain pressure type varies from (30-40) minutes. Though ECP dryer ensures better quality, to achieve better thermal efficiency and associated higher production rate there has been a shift towards vibrated fluidized bed dryer for processing of black tea after 1990 (Fig.1.3).

Vibrated fluidized bed dryer

These dryers may have three or five zones in mixed flow or cross flow mode in addition to a cooling section. When a fluid flows upwards through a bed of granular particles, the pressure drop is initially proportional to the rate of flow. At a certain increased air velocity, the frictional drag of the particles become equivalent to the perceptible weight and bed begins to expand. This stage is known as onset of fluidization or incipient fluidization. Further boost in velocity causes the individual particles to separate from one another and float on stream of air. At this stage, the system is said as a fluidized bed. Good thermal contact between the tea particles and drying medium results in improve fuel performance. Particle to particle attrition in a fluidized bed medium is minimized because its own fluid cushion bound each particle. This gives rise to blacker tea with better appearance and bloom as quality parameters. Plug flow fluidization is very much necessary for optimal energy consumption of black tea drying. Particles look like a boiling liquid in plug flow fluidized bed condition. The upper surface of the bed remains horizontal. The solids rapidly mix that lead to near isothermal condition in each zone of the bed.

The fermented leaf is loaded in grid plate of drying chamber. The top of the drying chamber is totally enclosed and two sets of centrifugal fans are provide with cyclones; one for re-firing and other is for dust collection operations. Plenum is situated beneath the bedplate where the air pressure is equalized as per requirements. Damper controls the direction of hot air entering into the bedplate. It has dual purposes namely direction of damper determines the residence time of tea particles as

[†] Curl tear and crush

well as evacuates the dryer completely at completion of drying. The fermented leaf enters into the drying chamber with a very high moisture contents. It is reduced rapidly by admitting maximum volume of hot air for swift evaporation of moisture. The rapid loss of moisture causes increase in bulk density of fermented tea. Therefore, the material tends to move away from the feed end because it is displaced by incoming fresh fermented tea containing high moisture.

In addition to the understanding of tea dryers, the major factors influencing the tea drying process need also a brief discussion as below.

Factors affecting tea-drying process

The factors affecting tea drying process are, inlet air temperature, volume of air, fermented tea feeding rate into the dryer, drying time and outlet humid air temperature from dryer. Tea drying is normally carried out at a temperature range of (90 -140) °C depending on various factors to reduce withered tea average moisture from 67 % to (2.5-3) %. Normally, (1.5-2.5) kg moisture is removed against each kilogram of made tea in drying. When the fermented leaf enters into the drying chamber, it has very high moisture content (58-72) %. It is rapidly reduced in the first drying zone of the dryer. In the first drying zone, maximum air volume and high temperature is introduced. As a result, the material density is decreased and it tends to move away from the feed end towards exit of the dryer. Moreover, it is displaced by fresh material containing high moisture contents. As the material is fully dried, it is expelled into a cooling chamber at ambient temperature. Cooling of tea undergoing drying is essential for stopping case hardening as well as over drying. If only quality aspect is considered, then endless-chain pressure type dryer for tea drying is preferable over fluidized bed tea drying.

1.3 Thermal energy utilization for black tea drying

Black tea drying is a highly energy intensive unit operation in tea manufacturing process. Different literature pertaining to tea drying energy consumption, drying efficiency, and energy conservation works is available both international and national level. Importance of thermal energy management in tea drying had been highlighted almost all the major tea processing regions including China [12], India [13, 14, 16], Japan [15] and Africa [17]. Coal and biomass are the predominant sources of thermal energy for tea processing in China. The studies indicated the requirement of appropriate management practices including introduction of improved drying machinery, utilization of waste heat, planning of unit operation, etc. for tea processing in order to conserve thermal energy. This would reduce unit cost of production.

Similarly, black tea manufacturing industries situated in Assam (India) had been reported to have variation in specific thermal energy consumption for different types of fuel. The minimum rate of energy consumption was 23.88 MJ kg^{-1} of made tea in oil-fired burners, 43.72 MJ kg^{-1} for coal-fired furnace and, 27.49 MJ kg^{-1} for gas-fired burner [13]. Energy efficiency improvement in air heater of a tea-manufacturing unit revealed that dryers were operating at very low efficiency due age-old design and improper selection of materials. Appropriate excess air control techniques might conserve 38 % of thermal energy in coal or biomass fired furnace with little or no investment. Therefore, optimal selection and discharge control of induced draft and forced draft fan was key factor for consideration. Moreover, furnace cum cast iron air heater (Fig.1.1) might be replaced with steam boiler for hot air generation [14].

Development of a primary drying tea roller with heat recovery devices in order to save energy in the primary drying process in tea manufacturing had been reported in Japan. The energy saving devices adopted were a heat exchanger that recovered heat from the furnace exhaust gas, heat pipes that recovered heat from the dryer exhaust air and a circulation path for the dryer exhaust air. The heat flow and energy saving effect of these devices used singly or in combination were calculated and discussed. A saving of between 12 and 29 % of the fuel consumption in the primary drying process was achieved with this waste-heat recovery device [15].

Fig.1.1 Coal fired air heater furnace

Fig.1.2 A Natural gas fired furnace for black tea manufacturing

The energy and economic issues related to the drying of tealeaves, with focus on the "zero physical wither system" being implemented in some areas in Africa, specifically in Kenya had been reported [17].

Sri Lanka also produces tea and importance of electrical and thermal energy management in tea drying is realized in that country [18]. Conservation of thermal energy required in tea processing and search for a new and sustainable sources of energy seem to be universal requirements.

It has been observed that almost all tea-manufacturing industries in India have been using tradition fuel (Natural gas, Coal, Tea drying oil, and Wood) for tea drying process. It is evident that except wood, other three thermal energy resources are fossil origin based. Moreover, wood is burnt conventional fixed bed biomass fired furnace to heat air. Studies shows that conventional fixed bed coal fired furnace and air heaters have been operating at a very low overall efficiency in most of the tea factories excluding a prominent part of upper Assam (Eastern part), India for long time. The reasons behind very low efficiency are, age old design of furnace and air heater, inconsistent quality of coal (low calorific value), inherently low heat transfer coefficient from flue gas to air in cast iron shell and tube heat exchanger. Moreover, with increase in coal prices in international market, as well as operation of low energy efficient fixed coal fired furnace (Fig.1.1), the cost of production of black tea is augmented. Secondly, even though a natural gas burner (Fig.1.2) for tea drying is energy efficient, yet natural gas is not available to most of the tea factories in Assam, India. Natural gas being a fossil origin fuel, it is non-renewable in nature. Therefore, for economy and sustainability for tea manufacturing urgently need to use certain amount of green energy like biomass gasification derived producer gas, solar thermal energy for tea drying in place of inefficient fixed bed coal fired furnace and air heater. The details of biomass gasification, solar air heating technology and the nature of hot fluid used to dry tea and the related drying kinesics will be discussed later.

1.4 Black tea drying performance

The drying experiments were reported at three different inlet air temperatures of 100, 115 and 130 °C and fluidization condition at five vibration intensity levels of 0 (no vibration), 0.063, 0.189, 0.395 and 1.184 respectively. The results showed that bed channeling and de-fluidization problems were declined in vibration condition. The vibration system decreased the requirement of minimum fluidization velocity of tea particles and this velocity reduced by increasing the vibration intensity. In the experiments, the maximum evaporation rate (13×10^{-3} kg m^{-2} s^{-1}) was experimented at the vibration intensity of 1.184 and inlet air temperature of 130 °C. In addition, the *minimum specific energy consumption (4955 kJ kg^{-1}) was observed at 1.184 vibration* intensity and inlet air temperature 100 °C. Based on lower minimum fluidization velocity and specific energy consumption, the vibration intensity of 1.184 and inlet air temperature of 100 °C were recommended for drying black tea particles [19].

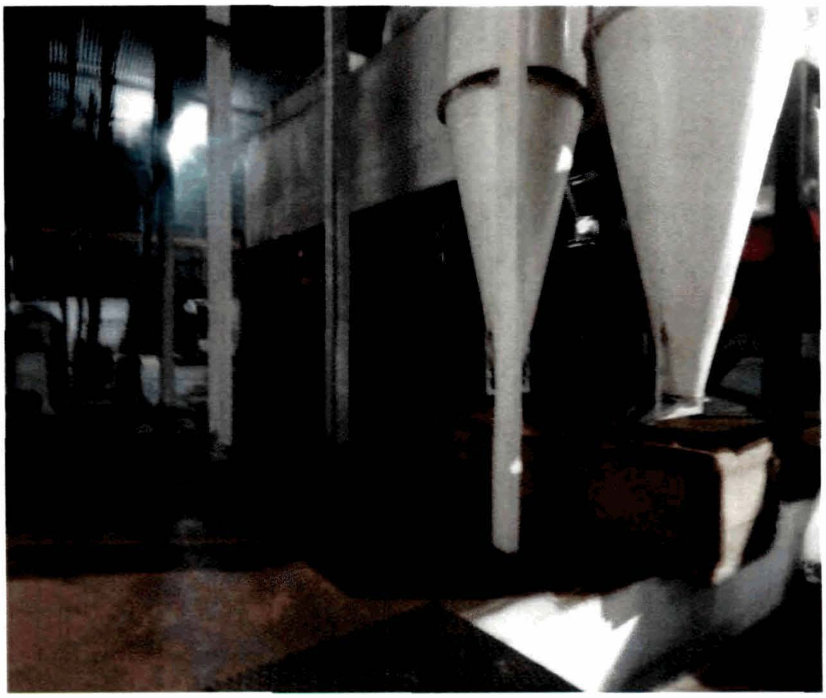

Fig.1.3 A vibrated fluidized bed dryer

The characteristics; performance, availability, and cost analysis of wedge wire as an ideal dryer bedplate material in tea industry has been reported. This material was recommended for its short drying times, found incredibly economical and expected for a very long life. In another study reported factors influencing the effectiveness and efficiency of fluidized bed dryers for tea and gave the optimum design parameters for the three drying stages [20, 21].

Different aspects of black tea drying under Northeast Indian tea factories such as drying medium temperature, types of dryer and drying time have been reported. Six dust collection systems for tea dried in a vibrating fluidized bed dryer and observations regarding their influence on tea quality was reported [22, 23]. Another study observed that the rate of drying of tealeaves during the primary drying process is related to the temperature and humidity of the drying air, the air and tea ratio, the number of revolutions of the main shaft of the dryer and the physical characteristics of the tea. In the initial stage, the tealeaves were dried at a constant rate agreeing with the wet bulb temperature of the air. However, in the later stages, the rate of drying tended to decrease as the surface area of the leaves changed, but overall the rate could be considered constant. A model based on drying at a constant rate agreed well with the experimental results. Experimental results meshed with calculated values for drying rate, the conditions of exhaust air, and drying efficiency. It assumed adiabatic heating and total mixing of air inside the dryer. A study on recirculation of humid exhaust air indicated that this could increase thermal efficiency without greatly affecting the quality of the tea [24]. A tea dryer house in which the roof space was incorporated to form an integrated exhaust system was reported. This offered the advantage of improved dust extraction and negligible discharge of saleable products. The exhaust system had no moving parts, there was no obstruction to the passage of the exhaust to the open air and a chamber formed by the roof of the building, and a platform over the loading end of the dryer allowed all exhaust air to develop gently and mix thoroughly [25]. Fuel burning efficiency in wood-fired furnace and heat losses with respect to improved tea dryer efficiency and performance had been reported [26]. A rotary dryer made from an unserviceable concrete mixer mounted on an iron frame over a brick fireplace was proposed. The dryer produced good quality tea more cheaply than that of hand processing one [27]. Another study was observed in Switzerland on a brief report of the work done by three dryers. These dryers were installed by the Department of Agriculture in different parts of Switzerland in 1941. Performance results of these three dryers were considered as exclusively satisfactory. The material dried included grass, cereals, vegetables, and tea. The dried grass was of a good, green colour and high quality as reported [28].

1.5 Tea drying kinetics studies

A study on modelling and simulation of fluidized bed tea drying was reported for both batch and continuous process. It was observed that for thin layer drying of tea, constant rate drying period did not exist. However, a constant rate-drying period may exist for batch fluid bed tea-drying experiments. Constant rate period exist if there is more saturated air per unit mass of tea particles. Therefore, constant rate period is not the property of tea drying, but of saturated air [29]. The heat and mass transfer theory of tea drying had been reported with development of one leaf temperature moisture content model to describe the drying process of rolled tealeaves. The average difference between the predicted and experimental moisture contents of output leaves was 2.43% (w.b.) for rolled tealeaves in the primary drying process under various conditions. Leaf layer thickness: (3-4) cm, hot air temperature: (91-116) °C, rotary speed: (2.0-5.1) rev min^{-1}) respectively had been considered [30]. At constant temperature drying conditions, the moisture diffusion coefficient of tea leaves and stems (Yabukita variety, second cut) had increased from (1.24×10^{-9} and 2.07×10^{-8}) to (1.14×10^{-8} and 1.17×10^{-7} m^2 h^{-1}). The drying constants increased from (0.288, 0.155) to (2.089, and 1.273 h^{-1}) respectively as drying temperature increased from (30 to 70) °C. Under crude drying conditions, drying time significantly affected the diffusion coefficient and drying constants of stems in particular. Agitation was reported to have no significant effect on diffusion coefficient, but it was clearly at least partly responsible for the drying rate of stems that was greater than leaves drying rate under these conditions [31].

Similarly, quality of black tea that is dried to variable moisture assessed by spreading tealeavcs on troughs (25.75 kg m^{-2}) and withered by a combination of hot and cold air for 12-18 hours. The withered leaves were macerated in a spiral rotor-vane followed by a triplex CTC (cutting, tearing, and curling) to achieve fine cuts. The green *dhool* was fed into trolleys and fermented for (90 ± 2) minutes. The temperatures were controlled by manual forking and air volume adjustment from (30.8 ± 1.4) °C at the start to (23.1 ± 0.8) °C at the end of fermentation. The fermented *dhool* was dried in a 3-stage fluidized bed dryer with temperatures set at the standard firing regime of (145 ± 2) °C (wet end), (135 ± 2) °C (mid chamber) and (105 ± 2) °C (dry end). The dryer was set to fire teas to three different moisture content levels of (3.1-3.3) percentage (low), (3.4-3.6) percentage (medium), and (3.7-3.9) percentage (high). The results showed that optimum quality of black tea fired in a fluidized bed dryer was achieved at a moisture content of (3.0-3.4) percentage However, tea fired to high moisture content level of (3.5-3.9) percentage was also found to be of acceptable quality and with a higher throughput. This study demonstrates that the keeping quality of tea fired to high moisture content is similar to the tea fired to low moisture content for a period of up to 2 years [32]. Another study reported drying durations and quality parameters for orthodox and CTC tea in hot air, radio frequency, and hybrid hot air-radio frequency (RF) dryers. Drying duration was the shortest for RF drying at 60 min for orthodox tea whereas for CTC tea it was 90 min. Hybrid drying for CTC tea took total of 55 minutes and the same for orthodox at 20 kW power was 85 minutes. Aroma index of made liquor increased at 16 kW compared to 20 kW RF power applied [33].

1.6 Energy efficiency in processing industries

Different research, development and application based works are available regarding energy conservation, efficiency and renewable energy application in processing industries. Prospect of low-grade energy heat recovery had been reported in United Kingdom food processing industries. An estimated 11.4 TWh of recoverable heat was wasted each year, a quarter of that was from the food and drinks processing sectors. The most economical recuperation of the waste heat was by heat exchange/direct re-use to a nearby heat sink. This might be preferably from within the same process; numbers of different heat exchange systems were well developed and economically available for such projects. They observed that increasing energy costs and the drive towards energy efficiency and associated carbon reductions should increase motivation for such projects. Additional government funding towards demonstration of novel waste-heat recovery project highlighting successful cases were major factor in reducing the perceived risk and uncertainty of such projects amongst UK engineers [34]. The authors beautifully represent different type of possible combination of heat exchanger for waste heat recovery and low temperature thermodynamic cycle. However, authors fail to conclude about the most appropriate technology solution for food processing industry with waste-heat recovery. Another studies revealed possible Organic Rankine Cycle to generate power with waste heat in a crisps processing industry with five options. The first two options (A and B) made use of the waste heat from the foul gas and exhaust to stack respectively for power generation using a single ORC system each while the third option (option C) made use of a novel dual heat source single ORC system. Here the low temperature waste heat from the foul gas was used to provide preheating. The high temperature waste from the exhaust to the stack was used to provide the evaporation. Option D also showed a dual heat source ORC system where the high temperature waste heat to the exhaust stack was used to provide the preheating the lower temperature foul gas for the evaporation (reverse of option C in terms of waste heat usage). Option E made use of a reheat cycle where the waste heat from the foul gas was used to provide the reheating of the working fluid exiting the turbine [35]. It is really an appreciable work for waste heat utilization. However, the authors have not highlighted details technical specification and appropriate hardware for such an energy system. Energy requirement in cashew (*Anacardium occidentale L.*) nut processing operation had been reported and results of application test of the equations showed thermal energy intensity varied from (0.085 to 1.064) MJ kg^{-1}. Cashew nut drying and cashew nut roasting are two energy intensive operations. Both altogether accounted for over 85%

of the total energy consumption in all the three mill categories. They developed appropriate correlation for different unit operations of cashew nut processing is a commendable work. Diesel fired burner thermal energy represented about 90 % of the unit energy cost for cashew nut processing [36]. However, the analysis assumed the data provided by cashew nut processing milling that was not directly measured by the authors and it is only limitation of the work.

It has been seen that conventional thermal energy requirement for black tea drying is non-renewable fossil fuel (Coal, Tea Drying Oil, and Natural Gas) in the tea factories located in Assam, India. The variation of fossil fuels uses range from inefficient indirectly heated old coal fired furnace air heater to improved coal fired steam generator, furnace oil and natural gas fired furnace, etc. However, site specific improved solar air heater and locally available fuel specific gasifer performance study for black tea drying in Assam is necessary for sustainable development. The application of renewable sources of energy and technologies such as biomass gasification, solar thermal air heating have not been explored individually or hybrid mode yet for black tea processing in Assam. It was noticed that knowledge of material characteristics related to tea drying kinetics is essential for understanding and assessing drying performance using the existing theory of drying by incorporation of renewable thermal energy (producer gas combustion products mixed with air) as drying medium. However, there exists knowledge gaps, with reference to biomass gasification and solar air heating technology applied for black tea drying kinetics, for local varieties grown in Assam (India). Innovation in renewable energy resources and technologies based tea drying should be conceptualized and experimented to generate appropriate knowledge for selecting and characterization of appropriate local biomass samples, low cost and energy efficient solar air heater development, hybridization analysis, drying kinetics, conventional energy substitution potential and overall performance of the system. The above discussion is summarized with the following observations.

Tea is an important beverage product manufactured in Assam (India) and drying is a significant processing step that requires (85 to 90) % conventional thermal energy. This necessitates urgent research attention with reference to locally available renewable energy technology intervention for tea drying. The characterization of some locally available biomass as potential gasification feedstock for tea drying is necessary to study suitability for black tea drying. The existing theory of drying implies the requirement of information on fundamental material characteristics pertaining to drying and drying kinetics that are material and system dependent. Such information is not available for local variety of tea with intervention of renewable energy. Therefore, this is important to determine local variety tea drying kinetics through precise experimentation in producer gas fired dryer. Therefore, hybridization studies of biomass gasification technology and solar air heater for partial substitution tea drying thermal energy is necessary for optimal and assured utilization and reliable supply of above mentioned renewable energy sources in local tea industries.

1.7 Objectives of research work

Considering the discussion made in this Chapter, the focus of the present study has been to investigate the prospect of a new tea drying technique based on biomass gasification and solar thermal (Air heater) technology for supplying hot air. Therefore, this research work has been undertaken through a systematic procedure with the following objectives:

- Fuel characterization of some locally available biomass samples through proximate, ultimate analysis and calorific value determination to access potential feedstock for gasification in a downdraft woody biomass gasifier.
- Investigation of the best-fit tea-drying model and activation energy with producer gas fired tea-drying setup.
- To study an improved solar air heater to assist biomass gasification in hybrid energy based tea drying to substitute thermal energy partially in tea drying.
- Economic analysis of solar air heater assisted producer gas fired tea dryer over conventional inefficient coal fired furnace cum air heater.

1.8 Organization of report

- Chapter 1

  This chapter discusses importance of tea industry in Assam, different tea drying unit operations, thermal energy consumption pattern, and different type of industrial tea dryer performance, and energy efficiency. The problem statement and objectives of the research work have been defined.

- Chapter 2

  This chapter is consisted of literatures pertaining to renewable energy applications for different process industries with its potential for tea drying. Reason for selection biomass gasification cum improved solar air heater technology over other renewable energy system for tea drying, biomass gasification, drying kinetics, solar air heater technologies, and hybridization of biomass and solar energy for drying and a critical review have been presented.

- Chapter 3

  This chapter covers methodology adopted for characterization of some locally available biomass samples. The results of gasification studies of a selected biomass sample and gasifier performance have been presented in this chapter.

- Chapter 4

  This chapter covers detailed methodology of thin layer tea drying kinetics with producer gas as a fuel. The results of best thin layer drying kinetics model and activation energy from experimental data of tea drying had been presented.

  Chapter 5

  This chapter discusses detailed methodology of analysis of improved solar air heater. An analysis of improved low cost air heater and hybrid (solar assisted biomass gasifier performance) had been presented.

  Chapter 6

  This chapter enlists the summary of the results obtained to achieve the objectives of the thesis and concluding remarks. It also discusses the limitations and possible future extensions of the present work.

2.1 Renewable and non-renewable energy application for process industries

Solar and biomass are two renewable energy resources considered for present black tea drying studies for local tea industries. Therefore, the different relevant literature are presented in the following sections. Solar air preheating for Longan drying had been reported in North Thailand and liquefied petroleum gas (LPG) was used conventionally for its drying purpose. It was observed that solar collectors could replace up to 19.6% of the thermal energy demand during the drying season. Bigger collectors and smaller air channels resulted in more useful heat, but attention was paid to both costs and pressure drop in air channels. Moreover, they observed that monetary savings varied greatly among different facilities. A higher solar fraction did not mean higher absolute savings. Therefore, maximizing use of the equipment was more important than the size. Some facilities could save significant amounts of money by substituting part of the fossil fuel requirement with solar energy. Longan drying lasted less than two months each year. Appropriate utilization of solar energy necessitated more feasibility of the system. Therefore, the drying facilities should operate a longer period over the year. The use of these facilities for drying alternative crops during other seasons might be a feasible solution [37]. Another study revealed the potential of solar industrial process heat application with five solar collectors, varying from the simple stationary flat-plate to movable parabolic trough ones. An estimation of the system efficiency of solar process heat plants operating in the Mediterranean climate were given for the different collector technologies. The annual energy gains of such systems were from (550 to 1100) kWh m^{-2}. The resulting energy costs obtained for solar heat were from (0.015 to 0.028) C£ kWh^{-1} depending on the collector type applied [38]. Energy demand and supply options for primary processing of rice in India had been reported and feasibility of using rice husk for meeting mechanical energy demand through gasification in dual fuel engine-generation route was explored. Moreover, the solar water heater for soaking of parboiled rice was accessed. For meeting the thermal energy demand, husk would continue as energy source until it was available as a free resource [39]. Another study reported technical and economic evolution of solar dryer. They observed resources saving with such system by avoiding environmental pollution, product quality improvement, and increased energy effectiveness [40].

Wine industry wastes through thermal processing had been reported by proximate, ultimate, and calorimetric analysis (LHV 19.73 kJ kg^{-1}) of grape marc. It improved its fuel properties and revealed that their characteristics was similar to wood biomass, even higher energy impending. The product activation energy was 111.5 kJ mol^{-1}, and this was experimentally determined for industrial pyrolysis process conditions to provide a reliable value for real scale applications. The product equivalent chemical formula was established as $C_4H_7O_3$ and it could be used for thermal-chemical processes simulations. The pyrolysis solid, liquid, and gas products were investigated along with their formation mechanisms. For all treatment temperatures, the process energy balance was positive, and the process was self-sustained by the pyrolysis gas energy alone. The maximum net energy content found in pyrolysis products were achieved at 550 °C [41].

2.1.1 Energy conservation and efficiency

Energy use and energy efficiency in the European dairy industry had been reported and changes in energy efficiency were monitored in two different ways. One way was to look at the energy use by tonne of milk processed by dairies. Another way was by comparing the actual energy use with the energy that would have been used if no changes in energy efficiency had taken place. German, British, and Dutch dairy industries had achieved considerable improvements in energy efficiency, contrary to the developments showed by the French industry. Furthermore, by the end of the 1990s, Germany, Netherlands, and the United Kingdom were converging in their energy efficiency values [42]. Desiccated coconut industry of Sri Lanka for opportunities, energy efficiency, and environmental protection has been reported and it was estimated that the desiccated coconut sector in Sri Lanka consumed about 21,660 tons of firewood, 16.5 million liters of furnace oil and 10 GWh of electricity annually. This constituted about 0.16 % of the total energy consumption of 0.3 PJ of

Sri Lanka and about 0.2 % of the annual national electricity production. The implementation of energy saving devices and better energy management might lead to a reduction of CO_2 emission and reduced the cost of environmental cleanup [43]. Another study reported energy management method for the food industry by top-down modelling approach. This method was especially appropriate for non-energy intensive industry where the resources for energy management were often limited. The top-down approach had permitted to model the energy consumptions with multi-linear regression models [44]. Thermal energy management in the bread baking industry was reported using a system modelling approach. It quantified the energy required to bake the dough, and conducted a detailed analysis of the breakdown of losses from the oven. A computational fluid dynamics (CFD) optimization study was undertaken, resulting in improved operating conditions for bread baking with reduced energy usage and baking time. Overall, by combining the two approaches, the analyses suggested that bake time may be reduced by up to 10% and the specific energy required for baking each loaf reduced by approximately 2%. For UK industry, these savings equate to more than £0.5 million cost and carbon reduction of more than 5000 tonnes CO_2 per year [45].

A framework for estimation of specific energy consumption and carbon dioxide mitigation with solar drying was reported considering fossil fuels as coal, diesel, natural gas, and LPG. The results of investigation indicated that for all drying test conditions, the given dryer was capable to mitigate the maximum CO_2 emissions with the replacement of coal by solar energy. Larger values of absorbed energy and load density caused increased specific energy consumption and CO_2 mitigation potential whereas reverse trend was observed for sample thickness. However, the influence of airflow rate on these parameters was found to be quite different. In order to establish functional relationship between specific energy consumption and process variables, a correlation was developed using Levenberge Marquart algorithm. The statistical error analysis revealed that the proposed correlation was capable of satisfactory prediction of experimental results [46].

Food industry in Taiwan was labour intensive, cost of raw materials was high, and there was much product diversification. Although this industry was primarily small and medium scale, it was a large user of electricity in Taiwan's manufacturing sector. The concentration of greenhouse gases (GHGs) from manufacturing activities had increased remarkably. Energy audits were a basic and direct means by which energy efficiency could be improved, energy consumption reduced, and carbon dioxide emissions inhibited. This work summarized the energy saving potential of 76 firms and the energy savings implemented by 23 firms as determined by energy audit tracking and from the on-line energy declaration system in Taiwan's food industry. The results of this study can serve as a benchmark for developing a quantified list in terms of potential energy savings and opportunities for improving the efficiency of the food industry [47]. Another study observed that industrial sector used more energy than any other end-use sectors and currently this sector was consuming about 37 % of the world's total delivered energy. Energy was consumed in the industrial sector by a diverse group of industries including manufacturing, agriculture, mining, and construction and for a wide range of activities, such as processing and assembly, space conditioning, and lighting. Energy saving technologies, such as use of high efficiency motors (HEMs), variable speed drives (VSDs), economizers, leak prevention and reducing pressure drop has been reviewed. Based on energy saving technologies results, it has been found that in the industrial sectors, a sizeable amount of electric energy, emissions and utility bill can be saved using these technologies. Payback periods for different energy savings measures had been identified, and it was found economically viable in most cases [48].

Environmental policies are largely devoted to nurturing the development and implementation of renewable energy technologies. One important aspect of this transition was the increased use of biomass to generate renewable energy. Agricultural residues were produced in huge amounts worldwide, and most of this residue was composed of biomass that could be used for energy generation. As a result, converting this residue into energy could increase the value of waste materials and reduced the environmental impact of waste disposal. Studies analysed the situation of biomass energy resources in Andalusia, an autonomous community in the south of Spain. More specifically, biomass is a renewable source that prominently contributes to Andalusian energy infrastructure. The residual biomass produced in the olive sector is the result of the large quantity of olive groves and olive oil manufacturers that generate byproducts with a potentially high-energy content. The generation of agricultural and industrial residues from the olive sector produced in Andalusia was an important source of different types of residual biomass. They were suitable for thermal and electric energy since it reduced the negative environmental effects of emissions from fossil fuels, such as the production of carbon dioxide [49].

Thermal energy loss in the process industry was reported as a significant issue due to the high temperatures and multiple heat intensive processes involved. High-grade thermal energy was typically recovered within processes. However, lower grade heat was often rejected to the environment. The temperature of the low-grade heat stream was the most important parameter, as the effective use of the residual heat or the efficiency of energy recovery from the low-grade heat sources would mainly depend on the temperature difference between the source and a suitable sink. High and low-grade heat sources were defined according to the viability of recovery within the processes. Finally, different aspects that influenced the decision making for low-grade heat recovery in the process industry were discussed. It was concluded that organizational, financial, and economic barriers might be overcome and benefits from a holistic vision could be gained with stronger governmental policy and regulation incentives [50].

Fluid-milk processing industry around the world processes approximately 60 % of total unprocessed milk production to create various fresh fluid-milk products. Fluid-milk processing data across number of countries and regions were compiled and analysed. The study had found that the average final energy intensity of individual plants exhibited significant large variations, ranging from 0.2 to 12.6 MJ kg^{-1} fluid-milk products across various plants in different countries and regions. In addition, it was observed that while the majority of larger plants tended to exhibit higher energy efficiency, some exceptions existed for smaller plants with higher efficiency. These significant differences had indicated large potential energy-savings opportunities in the sector across many countries. Furthermore, this study illustrated a positive correlation between implementing energy-monitoring programs and curbing the increasing trend in energy demand per equivalent fluid- milk product over time in the fluid-milk sector. It was opined that developing an energy-benchmarking framework, along with promulgating new policy options should be pursued for improving energy efficiency in global fluid-milk processing industry [51].

Energy saving opportunities in the food-processing industry through a combination of top-down and bottom-up approaches was reported. On the one hand, the top-down modelling method aimed at correlating the measured energy consumptions with the final products and auxiliaries as well as at allocating the energy bills among major consumers. This approach might set priorities for energy saving actions. On the other hand, the bottom-up approach, which was based on the thermodynamic requirements of the process operations, was used to define the energy requirements of these consumers. A comparison of the measured consumptions and the energy requirements enabled the identification of energy saving opportunities. In the case study presented in this article, these opportunities had been evaluated using thermo-economic modelling tools and range from good housekeeping measured and optimized process operations to energy saving investments [52].

An indicator to monitor energy efficiency developments in the food and tobacco industry based on physical production data at the firm level provided by the statistics office of the Netherlands in a confidential basis was reported. They measured energy efficiency by using an energy efficiency indicator that was the aggregate specific energy consumption. The results showed that the food and tobacco industry had improved their energy efficiency indicator in primary terms by about 1 % per year (uncertainty range between 0.9 and 1.3). In terms of final energy, there had been a decrease on the indicator for final demand of fuels of about 1.8% per annum while there had been no improvement in the indicator for final demand of electricity. The development in energy efficiency was coherent with the reported implementation rate of energy conservation projects. They concluded that the type and the quality of the data compiled by Statistics Netherlands for the food sector was sufficient to develop indicators as required by energy and climate policy [53].

Global cheese-making industry was reported to process approximately one quarter of total raw milk production to create a variety of consumer cheeses. Characterizing energy usage in existing cheese markets and plants might provide baseline information to allow comparisons of energy performance of individual plants and systems. The study had found that the magnitudes of average final energy intensity exhibited significant variations, ranging from 4.9 to 8.9 MJ kg^{-1} cheese across the few countries. Energy intensity variation ranged from 1.8 to 68.2 MJ kg^{-1} of cheese from the countries in this study. These significant differences had indicated large potential energy savings opportunities in the sector. Development and dissemination of an energy-benchmarking framework including a process step approach and efficiency measures might be recommended for evaluating energy performance and improving energy efficiency in cheese-making industry [54].

Tea processing is energy intensive operation i.e., withering, drying, grading, and packing tea requires 4 to 18 kWh kg^{-1} of made tea, which compares to 6.3 kWh for a kilogram of steel. Energy cost is about 30 % of total cost therefore less importance is put for energy efficiency and conservation in tea manufacturing sectors. Total specific thermal energy consumption varies between 4.45–6.84 kWh kg^{-1} processed teas. Environment and climate impact show that total fuel consumption by the tea sector in India contributes annual CO_2 emissions of 1,352,000 tons [55].

2.1.2 Justification for renewable energy resources for tea industries

Energy in general and thermal energy in particular has been a critical input to the tea processing sector which is one of the important food industries in Assam (India). Renewable energy has been identified as the alternative to the conventional fossil based energy system mostly for electrical generation as well as thermal application all over the world. The attempts to use renewable energy sources for tea processing have been limited almost to research and development. The application of solar air heater to save about 25 % of the conventional energy in tea processing has been reported for a specific case in Tamil Nadu (India) [56]. There are also similar reports on prospects of solar thermal energy to preheat combustion air that saved (25-34) % conventional fuel. Computer model was developed to evaluate the performance of a solar-powered drying system in relation to sunshine hours and air relative humidity and temperature [57, 58]. Biomass generated producer gas in tea processing based on analytical study and experiment concerning a specific case in Sri Lanka has been reported [59]. Principles and field experience on the open top biomass gasification technology developed at Indian Institute of Science has reported diesel savings in the range of 80% for dual fuel mode of operation in the entire power range. Thermal applications for low and high temperature uses in the range of (0.2 to 5) $MW_{thermal}$ for drying and heat treatment applications were in operation. Cumulative experience of 80, 000 h over a dozen systems has resulted in a fossil fuel saving of 350 tonnes; typical daily saving was approximately 18 m^3 of fossil fuels. This replacement had resulted in a net reduction of approximately 1120 tonnes of CO_2 and this was a promising candidate for clean development mechanism [60].

The present studies consider prospect of biomass gasifier and solar thermal hybrid renewable thermal energy based tea-drying system in Assam. Biomass gasification is considered because tea industry is an agro based unit with own generation of waste biomass. Moreover, solar thermal energy is available except the a few summer and winter months (about 30-35% time over the year). Generation of electrical power from biomass gasifier and then use it for electric dryer is not recommended for higher overall cost and low overall efficiency. Cogeneration system with fluidized bed boiler or combined heat and power system are not consider because of complexity of technology for local tea industry to convince even though overall efficiency of the system is higher. Moreover, biomass preparation for fluidized bed boiler would increase fuel preparation cost. Therefore, a simple downdraft biomass gasifier and improved solar air heater technologies are considered for present studies.

2.2 Biomass gasification

Biomass gasification is a thermo chemical energy conversion technology that converts especially solid, liquid, and gaseous fuel (both fossil and non-fossil) into combustible gaseous products and useful chemicals. The primary objectives of gasification are to increase heating value of product fuel by rejecting non-combustible components like nitrogen, water, etc. As a result, it does not release these products to atmosphere. Moreover, gasification reduces carbon to hydrogen mass ratio in the fuel. Carbon to hydrogen ratio for anthracite coal is about 44, whereas for synthetic gas (CO: H_2) this value is 02 only. Normally gasification takes place in limited supply of air (sub-stoichiometric, ϕ = 0.20-0.35). Four overlapping biochemical processes take place inside a gasifier (reactor). They are namely drying, pyrolysis, combustion, and reduction reactions. The principal attraction of gasification is evident from following discussion. A gasified fuel is useful in wide range of energy applications. Downstream cleaning in gasification is less expensive than coal fired plant, with flue gas desulphurization, selective catalytic reducers, and electrostatic precipitator, etc. Poly-generation is effectively possible with a gasification plant. It can supply steam for process heat generation, electricity to grid and gas for synthesis of chemicals. If the gasification feedstock has high sulphur, elemental sulphur is produced as byproduct, for high ash fuel slag or fly ash is recovered that may be used for cement manufacturing. Integrated gasification combined cycle plant achieve higher overall efficiency (38-41) percentage and therefore gasification provides lower power production cost. Moreover, transportation of synthetic fuel or liquid produced from it is less expensive than that solid fuel. Carbon dioxide capture and sequestration cost for integrated gasification combined cycle (IGCC) plant is half to that of pulverized coal fired system. The total water consumption in gasification-based power plant is much lower than coal fired plants. Moreover, the same water may be recycled for gasification both in thermal and electrical generation. Gasification plant produces lower amount of sulphur dioxide, oxides of nitrogen, and particulate matter. Its emission is similar to a natural gas fired plant [61, 62].

2.2.1 Drying

Gasification comprises of four energy conversion processes namely drying, pyrolysis, char gasification, and combustion. However, there is no separate boundary for each reaction and they are mostly overlapping with each other. Drying of biomass is utmost important for subsequent appropriate gasification reaction. For production of producer gas with reasonable calorific value, the moisture of the feedstock must be within the range (10 – 20) percentage. The complete drying of biomass takes place when it enters into the gasifier. The heat available from combustion zone is utilized for drying purposes. Above 100 °C temperature, the loosely bound water removes irreversibly. As the temperature rises, low molecular weight extractives start to volatilize and the process continues until temperature reaches 200 °C [61].

2.2.2 Pyrolysis

After drying, next thermo chemical process is pyrolysis that takes place in absence of air. It involves thermal breakdown of large hydrocarbon molecules of large biomass into smaller gas molecules (condensable and non-condensable). There is no major chemical reaction with air, gas or any gasifying medium. Tar forms by condensation of vapour produced by pyrolysis. Tar is a sticky liquid that must be combusted for production of producer gas in subsequent process. The products of pyrolysis are solid, liquid and gas as given by following reaction [61].

$$CxHyO_z + Heat \rightarrow \sum_{liquid} C_a H_b O_c + \sum_{gas} C_m H_n O_p + \sum_{solid} C \qquad (2.1)$$

2.2.3 Gasification reactions

The following chemical reactions take place inside a gasifier when it is operated at appropriate condition [61].

Reaction Type	Reactions
Carbon reaction	
R1 (Boudouard)	$C + O_2 \leftrightarrow 2CO + 172\ kJ\ mol^{-1}$
R2 (Water gas or steam)	$C + H_2O \leftrightarrow CO + H_2 + 131\ kJ\ mol^{-1}$
R3 (Hydro gasification)	$C + 2H_2 \leftrightarrow CH_4\ -74.8\ kJ\ mol^{-1}$
R4	$C + ½O_2 \rightarrow CO\ -111\ kJ\ mol^{-1}$
Oxidation reaction	
R5	$C + O_2 \rightarrow CO_2 - 394\ kJ\ mol^{-1}$
R6	$CO + ½O_2 \rightarrow CO_2\ -284\ kJ\ mol^{-1}$
R7	$CH_4 + 2O_2 \leftrightarrow CO_2 + H_2O\ -803\ kJ\ mol^{-1}$
R8	$H_2 + ½\ O_2 \leftrightarrow H_2O\ -242\ kJ\ mol^{-1}$
Shift Reaction	
R9	$CO + H_2O \leftrightarrow CO_2 + H_2\ -41.2\ kJ\ mol^{-1}$
Methanation Reaction	
R10	$2CO + 2H_2 \rightarrow CH_4 + CO_2\ -247\ kJ\ mol^{-1}$
R11	$CO + 3H_2 \rightarrow CH_4 + H_2O\ -206\ kJ\ mol^{-1}$
R14	$CO_2 + 4H_2 \rightarrow CH_4 + 2H_2O\ -165\ kJ\ mol^{-1}$
Steam Reforming Reaction	
R12	$CH_4 + H_2O \rightarrow CO + 3H_2 + 206\ kJ\ mol^{-1}$
R13	$CH_4 + ½O_2 \rightarrow CO + 2H_2\ -36\ kJ\ mol^{-1}$

Charcoal gasification

Charcoal produced by pyrolysis of biomass is not necessarily a pure carbon. It may contain certain amount of hydrocarbon, hydrogen, and oxygen. Biomass char is normally more porous and reactive than coke. Gasification of biomass charcoal involves several reactions with carbon, carbon dioxide, steam, hydrogen, methane, etc., as discussed below.

$$Charcoal + CO_2 \rightarrow CO_2 + CO \quad (2.2a)$$

$$Charcoal + CO_2 \rightarrow 2CO \quad (2.2b)$$

$$Charcoal + H_2O \rightarrow CH_4 + CO \quad (2.2c)$$

$Charcoal + H_2 \rightarrow CH_4$ (2.2d)

Gasification reactions are generally endothermic, but some of them are exothermic also. Reactions R3, R4 and R5 are exothermic and reaction R1 and R2 are endothermic. The rate of gasification depends on its reactivity and reaction potential of gasifying medium. The rate of charcoal oxygen reaction is fastest among (R1 – R4) and it consumes oxygen immediately. The Boudouard reaction or char carbon dioxide reaction is six to seven orders slower [62]. The rate of water gas or water-steam gasification reaction (R2) is about two to five times faster than the Boudouard reaction [63]. The charcoal hydrogen that forms methane is slowest of all reactions. Walker estimated relative rate of four reactions at 800 °C and 10 kPa pressure, as 10^5 for oxygen, 10^3 for steam, 10^1 for carbon dioxide, 3×10^{-3} for hydrogen [64].

Boudouard reaction

According to Blasi [63], CO_2 dissociates at a carbon free active site. It releases carbon monoxide and forms a carbon-oxygen surface complex. This reaction can move in the opposite direction as well forming carbon active site and CO_2 in second step. In the third stage, carbon-oxygen molecules produce molecules of CO.

Water gas shift reaction

The gasification of charcoal in steam is known as water gas reaction. The first step involves the dissociation of water on free active site of carbon. It releases hydrogen and forms a surface oxide form of carbon. In second and third step, surface oxide complex produces a free new active site and a molecule of carbon monoxide. Balsi [63] suggested the possibility of hydrogen inhibition by C (H) or C (H_2) complexes. The presence of hydrogen has a strong inhibition effect on charcoal gasification rate in water.

Shift reaction

The shift reaction is an important gas phase reaction. It increases hydrogen content of gasification product at the expense of carbon monoxide. Reaction (R9) represents the syngas production downstream of gasifier, where ratio of hydrogen and carbon monoxide in the product gas is critical. The shift reaction is slightly exothermic, and its equilibrium yield decreases slowly with temperature. Depending on the temperature, it may proceed in either direction of product or reactant. However, it is not sensitive to change in pressure [65]. Above 1000 °C, the shift reaction (R9) rapidly reaches equilibrium. Probestien and Hicks [66] showed that this reaction had a higher equilibrium constant at a lower temperature that is high yield of hydrogen at lower temperature. With increase in temperature, yield decreases, but reaction rate increases. Optimal yield takes place at 225 °C.

Hydrogasification reaction

This reaction takes place with gasification of charcoal in a hydrogen environment that leads to production of methane. The rate of this reaction is much slower than that of other reaction.

Charcoal combustion reaction

Most of the gasification reactions are endothermic. To provide the required heat of reaction as well as required drying, heating and pyrolysis, a certain amount of exothermic combustion reactions are allowed inside gasifier. Reaction (R5) yields highest amount of heat (394 kJ) per kilo-mole of carbon consumed. The reaction (R4) takes place with production CO (111 kJ) per kilo-mole carbon. Combustion reactions rates are about one order magnitude faster than gasification reaction. Fine charcoal particles react faster due to its high pore diffusion rate.

2.3 Characterization of biomass

Biomass refers to any organic materials that are derived from plants or animal [67]. The United Nations Framework Convention on Climate Change defines biomass as a non-fossilized and biodegradable organic material originating from plant, animal, and microorganisms. This shall also include product, byproducts, residues, and waste from agriculture, forestry, and related industries as well as non-fossilized biodegradable organic fraction of industrial and municipality waste [68]. This includes both primary biomass and derived biomass. Primary biomass directly comes from plants and elements. Primary biomass includes woods, plants, and leaves (ligno-cellulose), crops, and vegetables (carbohydrates). Derived biomass includes solid and liquid waste, sewage human, and animals waste, gas derived from landfilling and agricultural waste.

Ligno-cellulosic biomass is non-starch fibrous part of the plant materials. Cellulose, hemicellulose, and lignin are its three principal constituents. Woody plants are lingo-cellulosic biomass and they may be of two types namely herbaceous and non-herbaceous. An herbaceous plant is one with leaves and stems that die annually at the end of the growing season. These plants do not have bark. Non-herbaceous perennials like wood plants have stem above the ground. The trunk and leaves of tree plants form the biggest group of biomass. Energy crops such as miscanthus, willow, switch grass, and poplar may be considered as very effective lingo-cellulosic woody biomass.

2.3.1 Constituents of biomass cell

The polymeric composition of the cell wall and other constituents of a biomass vary widely [69]. However, they are composed of three polymers hemicellulose, cellulose, and lignin. Cellulose is primary structural component of biomass and it varies from 90% in cotton to 33% in most other plants. The generic formula of cellulose is $(C_6\ H_{10}\ O_5)_n$ that has long polymeric chain with high degree of polymerization (≈10000) and a molecular weight (≈500000). It has crystalline structure of thousand units that are made of many glucose molecules. This gives cellulose high strength, permitting it skeletal structure of most terrestrial biomass [70].

Hemicellulose is another constituent of cell wall of the plant. The structure of hemicellulose is amorphous, random, and with little strength. It is a group of carbohydrates with branched chain structure and lower degree of polymerization (≈100-200). It may be represented by empirical formula $(C_5\ H_8\ O_4)_n$ [70]. Hemicellulose tends to yield more gases and less tar than cellulose. It constitutes about (20-30) percentage of the dry weight of wood [71].

Lignin is a complex highly branched polymer of phenyl-propane and it is an integral part of secondary cell wall of plants. This is a three dimensional polymer of 4 propenyl phenol, 4-propenyl-2- methoxy phenol, and 4 propenyl-2.5- dimethoxyl phenol [72]. Lignin is cementing agent for cellulose fibers holding adjacent cells together. Lignin is insoluble even in sulphuric acid. An average lignin content of hardwood is (18-25) percentage and that soft wood is (25-35) percentage of dry weight.

2.3.2 Physical properties of biomass

True density

True density is weight per unit volume occupied by the solid constituents of biomass. True density of most of the woody biomass cell wall is 1530 kg m^{-3} [73]. True density of selected biomass was determined with ultimate analysis data.

Apparent density

Apparent density of biomass is measured with volume displacement method. It includes the internal pores of biomass particles but not the interstitial volume of biomass particles packed together.

Bulk density

Computation of space occupied by a defined weight of biomass gives its bulk density. Bulk density may be measured as per ASTM (E-873-06). This involves pouring biomass samples into a standard size box (305 mm × 305 mm × 305 mm) from a height of 610 mm. The box is then dropped from a height of 150 mm three times for settlement. These three densities may be related by following two equations where ϵ_p is porosity of biomass and ϵ_b is bulk porosity.

$$\rho_{apparent} = \rho_{true}\,(1 - \epsilon_p) \tag{2.3}$$

$$\rho_{bulk} = \rho_{apparent}\,(1 - \epsilon_b) \tag{2.4}$$

2.3.3 Thermodynamic property

Thermal conductivity

Thermal conductivity of biomass changes with its moisture and density. Based on large number of samples the following correlation was proposed by MacLean, Kitani and Hall [74, 75], where S.G. is specific gravity of biomass.

$$k_{eff}\left(\frac{W}{mK}\right) = S.G.(0.2 + 0.004m_d) + 0.0238 \qquad \text{for } m_d > 40\% \qquad (2.5)$$

$$k_{eff}\left(\frac{W}{mK}\right) = S.G.(0.2 + 0.0055m_d) + 0.0238 \qquad \text{for } m_d < 40\% \qquad (2.6)$$

Specific heat

Specific heat is an indication of heat capacity of a substance. Both moisture and temperature affect the specific heat of biomass. Specific heat of large number of wood species (dry) may be expressed as following expression within temperature range of (0- 106) °C [76]. T is temperature in degree Celsius.

$$C_{pT} = 0.266 + 0.00116T \qquad (2.7)$$

The effect of moisture on specific heat is expressed as follows.

$$C_{pT} = M_{wet}\,C_w + (1 - M_{wet})T \qquad (2.8)$$

Heat of formation

Heat of formation or enthalpy of formation is enthalpy change when one mole of compound is formed at 25 °C and one atmosphere pressure from its constituent's elements in their standard state. One mole water is formed by combining one mole of hydrogen and half mole of oxygen, one mole of water is formed with release of (-421 kJ mol^{-1}) thermal energy.

Heat of combustion

Heat of combustion is defined as amount of heat released or absorbed in a chemical reaction without change in temperature. The following table gives heat formation for different compounds [77].

Table.2.1 Heat of formation of different compounds

Compounds	H_2O	CO_2	CO	CH_4	O_2	$CaCO_3$	NH_3
Heat of formation at 25°C (kJ mole $^{-1}$)	-241.5	-393.5	-110.6	-74.8	0	-1211.8	-82.5

Heat of reaction may be calculated from following relationship with heat of formation.

Heat of reaction = [Sum of heat of reaction of all products] – [Sum of heat of formation of all reactant] (2.9)

2.4 Biomass gasification for process heat generation

Dutta and Baruah [78], observed that biomass gasification derived producer gas applications for process heat generation and purely electrical generation are now established technologies although there is sufficient deration in former mode of operation. However, it has been observed that optimum application of biomass gasification technology as a source of thermal energy for tea drying is on research and development stage until now. Tea manufacturing industry is a plantation product based unit. Thus, biomass is generated by shading trees, uprooted tea shrubs, etc., itself within tea estate. Thus, uprooted tea shrubs gasification had been considered an appropriate conversion technology for gaseous fuel production and substitution of conventional fuel in black tea industries in Assam, India. Singh et al. [79], observed that combustion of cashew nut shells in furnace, semi open pit and other open burning was poor with lower combustion efficiency, high smoke emission, therefore efficient process control was not convenient in such situation. Jayah et al. [80] investigated the prospect of using producer gas for processing heat generation in tea drying. Rubber wood feedstock was used for an 80 kW thermal output downdraft gasifier. The moisture content of rubber wood was considered as an important parameter that in turn affected gasifier performance through reactor temperature and heat loss. Bhoi et al. [81] observed that optimum gasification zones length was a governing factor for maximum output in a given range of operating parameters. The principal gasification reactions were pyrolysis, oxidation, and reduction and they produced combustible gases like CO, H_2, CH_4, etc., with average calorific values of (4.18-4.62) MJ m^{-3} as reported by researchers. The use of producer gas for other industrial process heat generation was also reported. The generation of combustible producer gas from solid biomass makes gasification most suitable for diversified thermal energy applications [82]. Woody biomass gasifier energy balance was also performed for 454 kW gasifier and average cold gasification efficiency of 70 % was recorded using waste wood with moisture content (<20 %) [83].

Masek et al., [84] studied pyrolytic gasification of coffee grounds and its implication to allothermal gasification kinetics. They observed a high conversion rate (88 %) of coffee grounds into gaseous and volatile matter by fast pyrolysis at a temperature of 1073, K. Tar separation in allothermal gasification was done by combustion to produce additional process heat. Wilson et al., [85] reported coffee husk gasification using high temperature air steam in a batch facility that was maintained at three different gasification temperatures 900 °C, 800 °C, and 700 °C respectively. They observed that increased gasification temperatures led to a linear increment of CO concentration in syngas for all gasification conditions. They reported that kinetic parameters established the reaction mechanism of zero order with apparent activation energy of 161 kJ mol^{-1} and frequency factor of 6.48×10^2 s^{-1}.

Zainal, et al., [86] made an experimental investigation of a downdraft biomass gasifier using furniture wood chip as feedstock to measure equivalence ratio, gas composition, calorific value, and gas production rate. A peak was seen at about 0.38 equivalence ratios for optimum CO and CH_4 yields; it showed first increasing then decreasing trends of these constituents. At equivalence ratio 0.38, they observed best performance of the downdraft biomass gasifier. They also observed that gas production per unit weight of fuel increased linearly with equivalence ratio and a maximum cold gas efficiency of 80 % was achievable. Tippayawong et al., [87] performed an experimental study on gasification of cashew nut shells for hot water generation in a local food-processing factory. They found that cashew nut shells were excellent feedstock for gasification and it had high-energy content and similar composition as fuel wood. An economic analysis with the incorporation available literatures suitable to prospective renewable energy system was performed. Most of such studies estimated the probable saving in resources over existing technology as well as payback period for additional investment made in plant and machinery. Dasappa et al., [88] developed an open top gasifier that could replace 2,000-liter diesel per day completely. This system operated over 140 h per week on a nearly nonstop mode and over 4,000 h of operation for complete replacement of fossil fuel. Therefore, biomass fuels have important role in domestic and agricultural sectors in India. The substitution of fossil fuel with biomass for useful energy production results in reduction of greenhouse gas emission [89]. Patel et al., [90], studied on *Sardar Patel Renewable Energy Research Institute*, India (SPRERI's) open core gasifier (1.25 GJ h^{-1}) for steam generation in a dual fuel burner. Duel fuel burner was used with 60 % light diesel oil and 40 % producer gas. They observed that wood consumption was (70 – 80) kg h^{-1} that replaced 40 % (20 l h^{-1}) light diesel oil. The system was tested for a cumulative period of 600 h using sawmill woody waste as feedstock in test runs of 15–18 h. Panwer et al., [91], studied low temperature food processing industrial thermal application through an open core biomass gasifier. The gasification system was essentially consisted of an open top down draft reactor lined with ceramic. The experiment reveals that 6.5 kg of liquefied petroleum gas (LPG) was fully replaced by 38 kg of sized wood on hourly basis. The maximum temperature attained was 367°C in 130 min at 100.7 Nm^3h^{-1} flow rates. Singh et al., [92] evaluated performance of a biomass gasifier as solar dryer back up heater.

2.5 Drying modelling

The hot drying air removes moisture from the core of the fermented tealeaves by diffusion process. The products colour change from coppery red to black to arrest the fermentation process. The final moisture content of black tea (3 % w.b.) is a crucial aspect to get the stable product quality for preservation. Botheju et al., [93] observed wide variation of the critical moisture content of the black tea that promoted reactivation of hydrolytic enzymes such as peroxidase, catechol oxidase, etc. These hydrolyse lipids and heat might accelerate biochemical reactions. On the other hand, deactivation of catechol oxidase occurs during the drying of fermented *dhool.* Therefore, tea drying is not a simple moisture removal operation. Many associated quality parameters are involved during drying process. Incorrect selection of drying conditions and equipment might adversely affect dryer performance, predominantly in quality of made tea.

It has been observed that many theoretical and empirical models are available in literatures for various foods and agro based materials [94-96]. The design and control of a tea dryer fired with producer gas necessitated modelling of the actual drying process in term of mathematical relationships. It helped to define optimum tea drying process's parameters. Therefore, black tea drying kinetics data were obtained by operating a producer gas fired tea dryer. The process state parameters such as drying air temperature, moisture content, etc., were derived from heat and mass balance of the drying process. It was reported by thin layer drying and modelling of Assam variety black tea especially by combustion of producer gas as a source of thermal energy [97].

It was reported that vapour diffusion mechanism controls drying of hygroscopic material like fermented tea during falling rate period. Thin layer drying models describing the drying phenomenon of bio-hygroscopic material like fermented tea falls under three categories namely, theoretical, semi-theoretical and empirical models. The first one takes into account only internal resistance to moisture transfer while the other two consider external resistance to moisture transfer [98-99].

It is assumed that resistance to moisture migration distributes uniformly throughout the interior of the homogeneous isotropic fermented tea material. Therefore, diffusion coefficient D is independent of the local moisture content. The corresponding volume shrinkage is considered negligible, and then Fick's second law may be derived as Eq. (2.10).

$$\frac{\partial M}{\partial t} = D\frac{\partial^2 M}{\partial t^2} \tag{2.10}$$

Crank [100] gave the analytical solution of Eq. (2.10) for various regularly shaped bodies such as rectangular, cylinder, and sphere, etc. Drying characteristics of many food products such as rice, hazelnut, and rapeseed were predicted successfully using Fick's second law with Arrhenius type temperature dependent diffusivity coefficient [101-103].

Simplification of general series solutions of Fick's second law gives different semi theoretical models. They are valid within the specific temperature, relative humidity, airflow velocity and moisture content ranges of development of the models. These models require little time compared to theoretical thin layer models. They do not need assumptions of the geometry, mass diffusivity and conductivity of a typical food. Among the semi-theoretical thin layer drying models, the two terms model, the Henderson and Pabis model, the Page model and modified Page model are widely used [104-106].

Sharaf-Eldeen et al., [105] presented a two term model to predict the drying rate of shelled corn fully exposed to air. This model is the first two terms of general series solution to the Eq. (2.10). However, it requires a constant product temperature and assumes constant diffusivity. The two term exponential model has the form as:

$$MR = \frac{M - M_e}{M_0 - M_e} = A_0 exp(-k_0 t) + A_1\ exp(-k_1 t) \tag{2.11}$$

Where M, M_0 and M_e are the material, initial and equilibrium moisture contents respectively in dry basis, and A_0, k_0, A_1 and k_1 are the empirical coefficient. Since M_e is relatively small compared to M and M_o, therefore it may be neglected for computation of moisture ratio.

The Henderson and Pabis model is the first term of a general series solution of Fick's second law [106].

$$MR = \frac{M - M_e}{M_0 - M_e} = A_0 exp(-k_0 t) \tag{2.12}$$

This model was used successfully to predict drying characteristics of corn, wheat and peanut [106-108]. The slope of the model coefficient k_0, relates to effective diffusivity, when drying process takes place only in falling rate period. The liquid diffusion phenomenon controls this process [109]. The Lewis model is a special case of Henderson and Pabis model with intercept unity [110]. He described that moisture transfer from the food products and agricultural materials was analogous to the flow of heat from a body immersed in a cool fluid. Therefore, the drying rate is proportional to the difference between the drying material and equilibrium moisture contents analogous to Newton's law of cooling:

$$\frac{dM}{dt} = k_0(M - M_e) \tag{2.13}$$

After integrating we have,

$$MR = \frac{M-M_e}{M_0 - M_e} = A_0 exp(-k_0 t) \tag{2.14}$$

Bruce [111] studied drying behaviour of Barely with Lewis model. At the other hand, Page model is a modification of Lewis model to overcome its shortcomings. This model had produced good fits in predicting drying of rice [112], white bean [113], and short grain rice [114].

$$MR = \frac{M-M_e}{M_0 - M_e} = exp\ (-k_0 t^n) \tag{2.15}$$

Overhults et.al [115] also modified the Page model to describe the drying of Soybean as given in Eq. (2.16).

$$MR = \frac{M-M_e}{M_0 - M_e} = exp(-k_0 t)^n \tag{2.16}$$

The empirical models develop a direct correlation between average moisture content and drying time. They neglect the fundamentals of the drying process. Therefore, it is difficult to give a clear precise view of the essential processes occurring during drying. However, they may describe the drying curve for the conditions of experiment. Among them, the Thompson model (Eq. (2.17)) was used to describe the shelled corn drying and Eq. (2.18) was applied to study the intermittent drying of the rough rice [115, 116].

$$T = a \times ln(MR) + b \times (ln(MR))^2 \tag{2.17}$$

And

$$MR = 1+at+bt^2 \tag{2.18}$$

It has been observed from above literature that there are number of good examples for application of biomass gasification in food processing industries as well as food drying process modelling. Next we will discuss on different literature on improved solar air heater for process heat generation to assist tea drying process with gasification.

2.6 Introduction to Solar Air Heater

Solar air heater is a distinct type of solar thermal energy conversion device where air is heated over a metallic collector by absorption of incoming solar radiations. This is a modest and economically viable heat exchanger to convert the incoming solar radiations into relatively higher thermal energy. The elevated temperature solar thermal energy is extracted by air flowing over a black coated metallic surface. A conventional solar air heater is essentially a flat plate collector with an absorber plate, a transparent cover system at the top and insulation at the bottom and four sides. The whole assembly is enclosed in a sheet metal container to protect the unit from any thermal and mechanical damage. The working fluid is air with different combination of passages according to the type of air heater.

2.6.1 Types and application of solar air heaters

Depending on the type of the absorber plate, the solar air heater can be porous and non-porous. A porous type solar air heater uses porous absorber that may include slit and expanded metal, overlapped glass plate absorber and transpired honeycomb. Wire mesh, porous bed formed by broken bottles and overlapped glass plates are examples of porous type of absorbers. In non-porous type, air stream does not flow through the absorber plate but air may flow above and/or behind the plate. Depending on the number of passes for air flow, they may be classified as single pass solar air heater, double pass solar air heater or triple pass solar air heater, etc.

The main applications of solar air heaters are space heating, drying agricultural products such as fruits, seeds, and vegetables, seasoning of timber, curing of industrial products, crop drying, greenhouse heating, etc.

2.6.2 Advantages and limitations of solar air heaters

The solar air heaters have certain advantages such as necessity to transfer heat from the working fluid to another fluid is eliminated because; air is used directly as the working fluid. Moreover, the system is compact and less complicated. Corrosion, that may cause serious problems in solar water heaters, is completely eliminated. Leakage of air from the duct does not pose any major problem and freezing of working fluid virtually does not exist. The pressure inside the collector does not become very high.

Thus, air heater may be designed using cheaper as well as lesser amount of material and is simpler to use than the solar water heaters. The main disadvantages of solar air heaters are the poor heat transfer capacity of air. Moreover, it needs to handle large volumes of air due to its low density. Since the thermal capacity of air being low, it cannot be used as a storage fluid. The applicability of a solar air heater depends on various factors such as high efficiency, low fabrication, installation and operational costs and other practical aspects regarding the specific use.

2.7 Losses in solar air heaters

The thermal loss to the surroundings is an important factor in the study of the performance of a solar air heater. Heat is lost to the surroundings from the plate through the glass cover (referred as top loss) and through the insulations (referred as bottom loss and edge loss, etc.) These losses take place by conduction, convection, and radiation.

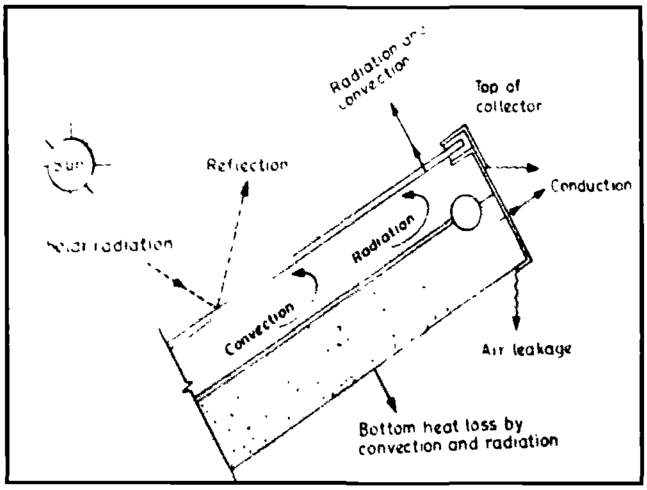

Fig. 2.1 Solar air heater showing different losses

2.7.1 Top Loss:

Top loss is a combination of convective heat losses and radiation heat losses and it is given by Eq. (2.19). Convective heat loss occurs from absorber plate to cover and from cover to ambient. Radiation heat losses take place from absorber plate to cover and from glazing cover to ambient [117].

$$U_t = \left[\frac{N}{\left(\frac{C}{T_m}\right)\left(\frac{T_m - T_a}{N+F}\right)^{0.33}} + \frac{1}{h_w}\right]^{-1} + \frac{\sigma(T_p^2 + T_a^2)(T_p+T_a)}{\frac{1}{\epsilon_p+0.05N(1-\epsilon_p)} + \frac{2N f-1}{\epsilon_g} - N} \tag{2.19}$$

$$f = (1 - 0.04h_w + 0.0005h_w^2)(1 + 0.091N) \tag{2.19a}$$

$$C = 365.9(1 - 0.00883\beta + 0.0001298\beta^2) \tag{2.19b}$$

$$h_w = \frac{8.6V^{0.6}}{L^{0.4}} \tag{2.19c}$$

The minimum value of wind heat transfer co-efficient for still air is 5 W m^{-2} °C

2.7.2 Bottom Loss:

Heat loss from the plate to the ambient takes place by conduction through the insulation and then subsequently by convection and radiation from the bottom surface casing, and is given by Eq. (2.20). The general acceptable value of back loss coefficient varies (0.3-0.6) W m^{-2} °C.

$$U_b = \frac{1}{\frac{t_e}{k_e}+\frac{1}{h_{cb}}} \tag{2.20}$$

2.7.3 Edge Loss:

It is the energy lost from the side of the collector casing and is exactly same as the back loss if the thickness of the edge insulation is the same as that of the back insulation. Edge loss coefficient varies from (1.5-2) W m^{-2} °C.

$$U_e = \frac{1}{\frac{t_e}{k_e}+\frac{1}{h_{ce}}} \tag{2.21}$$

2.7.4. Overall Heat Loss:

It is the sum of top, bottom and edge losses of a solar air heater. There is about (33-50) % heat loss in most commercial flat plate collectors, the breakup of which can be given as (22-30) % convective and (5-7) % radiation loss from the back surface. In order to improve the collector efficiency, the heat losses should be minimized. To minimize the heat loss from the back surface, a highly reflective coating may be used on the back surface of the collector. Mainly convective and radiation losses take place from the front space of the absorbing plate. These two losses are minimized by altering the spacing between cover and plate, and using absorbing surface of different emissivity. The optimum gap width is different for different absorbing surfaces.

2.8 Improving heat transfer coefficient between absorber plate and air

Conventional solar air heaters have low thermal efficiencies primarily due to the low convective heat transfer coefficient between the absorber plate and the flowing air stream over it. There are two basic methods for improving the heat transfer coefficient between the absorber plate and air. (1) Increasing convective heat transfer by creating turbulence at the artificially roughened heat-transferring surface and (2) by increasing the area of heat transfer by using corrugated surfaces or extended surfaces called fins.

There are various methods of increasing convective heat transfer by creating turbulence. They are artificial roughening by ribs, wire meshes, and geometric protrusions. To improve heat transfer in solar air heaters, artificial roughness, in the form of repeated ribs, is used to disturb the laminar sub-layer. The ribs are one of the most desirable methods because of their ability to combine enhanced heat transfer coefficient with limited frictional losses. The most important effect produced by the presence of a rib on the flow pattern, is that generation of two flow separation regions, one on each side of the rib. The vortices so generated are responsible for the turbulence and hence the enhancement in heat transfers as well as in the friction losses takes place. Another way to provide artificial roughness on the surface of absorber plate is by forming dimple/protrusion shape geometry. Formation of dimples/protrusions on absorber plate can be considered an innovative technique as dimples/protrusions are easy to fabricate and do not add extra weight to the absorbing plate.

To improve the heat transfer from the plate to air stream, and hence the efficiency of the heater, fins are added to the rear side of the absorber. This, however, introduces some extra pressure drop. In addition, the number of fins and their depth cannot increase beyond a limit because then compressor power requirement will also increase. The heat transfer model of such an air heater may be easily developed since heat transfer from finned surfaces is very common in convective heat transfer problems. However, the limitation of this model is that there are hardly any appropriate correlations for heat transfer coefficients corresponding to situations encountered in air heaters. Test results of air heaters with staggered galvanized fins and U-shaped staggered aluminum fins attached to the rear side of the absorber plate have been reported. The efficiencies with fins are substantially higher than conventional air heaters [115-118].

2.8.1 Double pass solar air heater

The double pass solar air heater consists of two passages; first passage is formed between the two glass covers and the second passage, where air flows in the reverse direction, is formed between the bottom glass cover and the absorber plate. Both the passages normally have identical length. The application of double pass arrangement reduces the top heat loss coefficient considerably that improves the thermal efficiency. Additionally, this kind of solar air collectors may be fabricated with a little additional expenditure over the conventional air collectors.

Ramadan et al., [119] studied thermal performance of a packed bed double pass solar air heater. Sopain et al., [120] carried out the simulation study and thermal performance of double pass solar air heater with and without porous media. The double passes counter flow arrangement with porous material in the second air passage was one of the effective alternatives to improve its thermal performance. The major reason of interest in porous material includes high effective heat transfer area per unit volume resulting in high heat transfer capability. Moreover, solar radiation was absorbed gradually by layers of porous matrix, resulting in effective heat transfer between the porous material and the flowing air. Different investigators had proposed use of porous packing material for improving the performance of solar air collector [121-125]. Some pioneering research work regarding heat transfer on wire mesh screens as packing elements may be considered. These researches have led to the conclusion that double pass counter flow solar air collector with porous material in the second pass gives higher thermal efficiency in comparison to double pass counter flow solar air collector without absorber matrix and conventional single pass solar collector. This is because the porous material provides a very large surface area for heat transfer and therefore, the volumetric heat transfer coefficient is very high. Further, in the double pass solar air heater, the air flowing in the first passage picks up heat from the glass covers reducing their temperatures and then flows over the absorber plate/matrix. The heat energy extracted by the flowing air in the first pass from the glass covers is used to preheat incoming air. This decreases the temperature of glass covers which in turn reduces the heat losses to the surroundings and hence the performance of such collectors have been found to be superior compared to conventional solar air collector where air flows in one pass either above or below the absorber plate [126 – 128].

2.8.2 Solar air heater with artificially roughened absorber plate

In order to make a solar air heater more effective solar energy utilization system, thermal performance needs to be improved by enhancing the heat transfer rate from the absorber plate to the air flowing in the duct of the solar air heater. One of the methods for enhancement of convective heat transfer is by creating turbulence at heat transfer surface with the help of artificial roughness on absorber plate. Ribs are provided by artificial roughness to break laminar sub-layer. This creates local wall turbulence due to flow separation and reattachment between consecutive ribs. As a result, thermal resistance decreases and heat transfer rate is greatly enhanced. However, simultaneous increase in friction loss also takes place in the duct with application of artificial roughness. In order to reduce friction loss with application of artificial roughness, turbulence should be created in the region very close to the heat-transferring surface i.e. in laminar sub-layer only. Therefore, height of roughness element should be kept small in comparison with duct dimensions.

Artificial roughness on the surface of the absorber plate may be provided by fixing small diameter wires, ribs formed by machining process, wire mesh, or expanded metal mesh and by forming dimple/protrusion shape geometry. However, it has been observed that creating artificial roughness on absorber plate is a tedious task and may not be economically feasible for large-scale production of solar air heaters. Therefore, a suitable geometry of roughness element needs to be selected, which should be easy to fabricate on the surface of absorber plate [129-132]. Saini and Verma [133] reported an experimental investigation for fully developed turbulent flow in rectangular duct having dimpled absorber plate. Experimental data of heat transfer and friction in the roughened duct as a function of system and operating parameters have been reported. They have observed that under a given set of operating conditions, Nusselt number was a strong function of relative short way length, relative long way length, and relative print diameter. For given value of roughness parameters, Nusselt number increases monotonously with an increase of Reynolds number.

Various researches have proved that Nusselt numbers for protruded absorber plate is considerably higher as compared to those obtained for smooth absorber plate. Protrusions on absorber plate result in enhancement in heat transfer coefficient. Enhanced heat transfer occurs due to main flow impingement, vortex generation on both sides of the protrusions and flow separation. Because, decelerating motion is accompanied by adverse pressure gradient that promotes separation, instability, eddy formation, and large energy dissipation [134, 135].

2.8.3 Solar air heater duct artificially roughened with V-ribs

In order to improve heat transfer in solar air heaters, artificial roughness, in the form of repeated ribs, is used to disturb the laminar sub-layer. The ribs are one of the most desirable methods because of their ability to combine heat transfer-coefficient enhancement with limited friction losses. Protruded wires for improving the plate efficiency factor of solar air heaters from 0.63 to 0.72 resulted in 14% improvement in the performance. Multiple v-ribs along the width of heat exchanging surface of a solar air heater to create artificial roughness enhanced heat transfer. They reported Nusselt number and friction factor enhancement of 6 and 5 times respectively, compared to a smooth duct [129, 132, 136, 137]. An enhancement in Nusselt number and friction factor over smooth duct of the order of 2.38 and 4.25 times, respectively, corresponding to relative roughness height value of 0.033 and relative roughness pitch value of 10 has been reported. An arc shaped ribs reported to enhance Nusselt number and friction factor of order 3.6 and 1.75 times, respectively, in comparison with the smooth duct [136-138].

Various researchers had reported enhanced heat transfer-coefficient between the hot metallic surface and fluid flowing over it with artificial roughness of defined geometries [139-143]. Several research works are available on augmentation of heat transfer coefficient by using different geometries in solar air heaters [144-153]. Khattab evaluated performance study of a perforated solar air heater. He concluded that optimal perforation geometry had great role on thermal and hydraulic efficiency of said solar heater [154]. Languri et al., [155], studied energy, and exergy analysis of double pass solar air heater with and without porous medium. They concluded that the porous medium embedded inside the lower channel led to an increase in the thermal efficiency of the collector of more than 30% compared with the case without porous medium. Therefore, studies showed the importance of employing porous medium in thermal solar collectors. On the other hand, the pressure drop in the air caused by friction with porous medium was not negligible and this was studied with second law analysis. Imbriale et al., [156] investigated the effect of periodic patterns of protrusions (ribs) on the free-convection heat transfer of a vertical plate, with a uniform heat-flux rate boundary condition. The convective fluid was considered as air. Two-dimensional, high-resolution heat transfer measurements were performed by using infrared thermograph and the heated thin foil technique. Experiments were performed on two types of ribs pattern topology: single or two staggered rows of ribs inclined at different angles and single or two-staggered rows of V-ribs. Bharadwaj et al., [157] experimented to determine the effect on the heat transfer and friction characteristics of an equilateral triangular solar air heater duct using inclined continuous ribs as roughness element on the absorber plate. The experimental study encompassed the range of Reynolds numbers from 5600 to 28,000, relative roughness height ($\frac{e}{D}$) 0.021–0.043, relative roughness pitch ($\frac{p}{e}$) 8–16, and angle of attack (α) 30–60°. The duct had an aspect ratio ($\frac{W}{H}$) of 1.15. The effect of flow parameters and roughness parameters on heat transfer and friction factor was discussed. The thermo-hydraulic performance parameter had been determined for the given range of flow parameters and roughness geometries. Rallabandi et al., [158], studied heat transfer, and pressure drop correlation on 45° ribs at high Reylonds number ranged from 30,000 to 400,000. The rib height (e) to hydraulic diameter (D) ratio ranged from 0.1 to 0.18 for experimentation. The rib spacing (p) to height ratio ($\frac{p}{e}$) ranged from 5 to 10. Results showed higher heat transfer coefficients at smaller values of ($\frac{p}{e}$) and larger values of ($\frac{e}{D}$), though at the cost of higher friction losses. Saha and Dutta [159] studied thermo-hydraulic of laminar swirl flow through a circular tube fitted with twisted tape. Thermo-hydraulic performance showed that twisted-tapes with multiple twists in the tape module were not much different from that with single twist in the tape module. Friction factor and Nusselt number were approximately 15 percent lower for twisted-tapes with smooth swirl having the average pitch same as that of the uniform pitch (throughout) twisted-tape. The twisted-tapes with gradually decreasing pitch performed worst compared to uniform pitch counterpart. Saha [160] made another study on thermo-hydraulics of laminar flow through rectangular and square ducts with axial corrugation. He observed that based on constant pumping power, up to 45% heat duty increase occurred for the combined axial corrugation and twisted-tape insert case compared with the individual axial corrugation and twisted-tape insert cases in the measured experimental parameters space. On the constant heat duty basis, the pumping power had been reduced up to 30% for the combined enhancement geometry than the individual enhancement geometries. Sebaii et al., [161] investigated thermal performance of a double pass solar air heater. They observed that that the double pass V-corrugated plate solar air heater was (9.3–11.9) percentage more efficient compared to the double pass-finned plate solar air heater. It was also indicated that the peak values of the thermo-hydraulic efficiencies of the double pass-finned and V-corrugated plate solar air heaters were obtained when the mass flow rates of the flowing air equaled to 0.0125 and 0.0225 kg s^{-1}, respectively. Aharwal et al., [162] experimented on heat-transfer enhancement due to a gap in an inclined continuous rib arrangement in a rectangular duct of solar air heater. The duct had a width to height ratio (W/H) of 5.84, relative roughness pitch ($\frac{p}{e}$) of 10, relative roughness height ($\frac{e}{D}$) of 0.0377, and angle of attack (α) of 60°. The gap width, ($\frac{g}{e}$) and gap position ($\frac{d}{W}$) were varied in the range of (0.5–2.0) and (0.1667–0.667), respectively. The heat transfer and friction characteristics of this roughened duct had been compared with those of the smooth duct under similar flow condition. The effect of gap position and gap width had been investigated for the range of flow Reynolds numbers from 3,000 to 18,000. The maximum enhancement in Nusselt number and friction factor was observed 2.59 and 2.87 times that of a smooth duct. The thermo-hydraulic performance parameter was found maximum for the relative gap width of

1.0 and the relative gap position of 0.25. Mohammed et al., [163] studied effects of geometrical parameters of a corrugated channel within out of phase arrangement. The corrugated channel with three different corrugated tilt angles of 20°, 40°, and 60° with different channel heights of 12.5, 15, and 17.5 mm and different wavy, heights of 2.5, 3.5, and 4.5 mm were tested. This investigation covered Reynolds number and heat flux in the range of 8,000–20,000 and 0.4–6 kWm^{-2}, respectively. The numerical results indicated that the wavy angle of 60° and wavy height of 2.5 mm with channel height of 17.5 mm were the optimum parameters and they had a significant effect on the heat transfer enhancement. It was observed that wavy channel was a suitable method to increase the thermal performance. Moreover, it gave higher compactness of the heat exchanger [164].

Since air is a bad conductor of heat, therefore rate of heat transfer from conventional solar air heater absorber to air flowing over it is not significant. It has been observed that different researchers put effort for performance evaluation of solar air heater by incorporation by enhancing turbulence of air [165, 166]. The evaluation of thermo-hydraulic efficiency of roughened solar air heater had been performed. They observed that system operated optimally with a specified set of Reynolds number [167].

2.9 Biomass energy and solar air heater hybridization

Solar thermal energy based air heater or dryer frequently encounters with natural variation of solar radiation over the day as well as over season. This gives rise to an unsteady and varied quality of hot air in terms of temperature and relative humidity to a given thermal load. Therefore, solar dryers alone continue to struggle for its independency in industrial drying applications over fossil fuel fired or electric dryer. Since specific heat capacity of air is much lower than water and air is a bad conductor of heat, it is almost impossible to raise air temperature around 100 °C in conventional solar air heater. However, specific geometry of black coated aluminum absorber such as protruded one gives rise overall higher thermal efficiency and air temperature in the range of (60 -65) °C in summer at Tezpur University campus. At the other hand, black tea drying process needs average hot air temperature (100 ± 10) °C for continuous operation and quality. As it has been already stated thermal energy requirement for black tea manufacturing in tea industries are provided by coal, natural gas, tea drying oil, or diesel. There is hardly any scope for only solar thermal energy based dryer application in black tea manufacturing. Therefore, an effort has been directed to study the possibility of solar thermal and biomass gasification as the renewable sources of energy for tea drying application in hybrid mode.

Different research works are available on hybrid drying of different agricultural produces for reliability and enhanced efficiency. Leon and Kumar [168] designed and studied performance of solar assisted biomass drying system with a thermal storage. They observed that solar assisted biomass air heating system with rock bed thermal storage could supply load fraction of hot air exceeding 90% for 24 hours. Application of biomass gasifer and an unglazed transpired solar collector were supposed to deliver hot air at (55-60) °C at the flow rate of hot air in (70-100) $m^3 h^{-1}$ continuously for drying of chilli. The system could reduce the drying time of chilli by 66 % compared to open sun drying with superior quality product. It was concluded that almost 100% of the drying energy demand was met from renewable sources of energy. Hirunlabh et al., [169] studied a new type of modular dryer powered with solar energy and producer gas. An updraft charcoal gasifier was considered for the study. They used a 0.6 m^3 modular cabinet that supported a solar collector of 2.5 m^2 surface area. Producer gas at 60 °C for four hours and solar energy at 40 °C for six hours to dry beef were used. The energy consumed for drying of 16 kg beef was 7.5 MJ kg^{-1} of water removed. The fraction energy contributed from solar, producer gas and blower were 8.72%, 31.44% and 59.84% respectively. The initial moisture of beef was 75% (w.b.) and final moisture was 25% (w.b.). Since two renewable energies solar and biomass may be used most effectively from morning to evening in appropriate combination, therefore such a hybrid drying energy system produced better quality product at lesser time uninterruptedly. Gupta et al., [170] studied energetic utilization of solar energy for feed water preheating in a thermal power plant. They observed that solar thermal energy was an added utility source for feed water preheating. It helped to reduce exergy loss in feed water heater of Rankine cycle and developed more work that could have been produced in a solar thermal power plant. They computed the work output from a 50 kW solar thermal power plant as 59.312 kW and that from a 220 MW fuel fired thermal power plant with 50 kW solar thermal power plants as solar feed water heating was 90.27 kW. Lokeswaran and Eswaramoorthy [171] performed and experimental study on a solar drying system with a biomass backup heater. They had dried coconut in four different drying systems namely a solar greenhouse dryer with a biomass back up heater, a biomass heater, a solar greenhouse dryer and open sun drying. It was observed that hybrid-drying system took 26 hours, whereas open sundering took 88 hours to reduce moisture of coconut from 53.4 % to 9.2% on wet basis. The drying efficiency of solar greenhouse dryer was about 19% in average. Prasad et al., [172] evaluated performance of hybrid drying of turmeric (*Curcuma longa* L.) at village scale. They developed a direct type natural convection solar cum biomass dryer. The system was capable of generating an adequate and continuous flow of hot air temperature between 55 and 60 °C. Turmeric rhizomes were successfully dried in developed system. Dried turmeric rhizomes obtained under solar biomass drying by two different treatments that is water boiling and slicing were similar in respect to physical appearance, texture, and colour with significance variation in volatile oil. They observed that eight-kilogram fuel wood was burned and 12.6 kg of water was removed to dry fifteen kilogram of fresh rhizome to 9% moisture. The dryer overall thermal efficiency was (28.5%). Bena and Fuller [173] studied on a natural convection solar dryer with a biomass back up heater. It demonstrated the drying technology suitable for small scale processing of fruits and vegetables in non-electrified areas of developing country. The dryer capacity was (20 – 22) kg of fresh pineapple arranged in a single layer of 0.01 m thickness and overall drying efficiency of the unit was 9 % only. However, drying efficiency of solar component was 22% and 27% for burner that produced useful heat in other experiments. Installation of an internal baffle lengthened the exhaust gas exit-path with a variable air inlet valve. It was observed that for same load of dryer, energy used only by solar component was 112 MJ and that by biomass alone is 463 MJ.

Almost four times more energy requirement for biomass furnace is because of indirect heating of drum over combustion chamber. They suggested for necessity of further investigation to improve the combustion and heat transfer efficiencies for biomass burner. Khairiddinov et al., [174] studied heat balance of cotton dryer with combined fuel solar recuperative heat supply. They performed general material balance and heat flux in the drying system. They computed the drying agent heat loss as (47-51) % and a portion of this heat was utilized in recuperative process. This was returned to the dryer together with solar radiation. This amount of heat is designated by substitution coefficient typically varied from (10 – 21) % and thermal efficiency of dryer was (36.8 – 43.7) % and solar recuperation was (39.4 – 50.2) % respectively. There was an efficiency increment of (7.1 – 15.7) % due to utilization of heat of solar recuperative natural gas fired cotton dryer. Srinivas and Reddy [175] performed a study on hybrid solar-biomass power plant without thermal energy storage. They observed that both solar thermal and biomass had limitation. Solar radiation is uncertain and high initial investment of solar technology (parabolic collector system). Biomass power plant demands a huge amount of feedstock that may not be radially available. The feed control of biomass fuel saves the cost of thermal energy storage. They observed that plant fuel efficiency increased with an increase in solar support, boiler pressure, and temperature but hybrid plant thermal efficiency decreased with an increase in steam temperature. The optimum boiler pressure decreased (50-40) bar with an increase in solar sharing (10-50) %. They designed the solar collector for 350 °C steam temperature compared to 450 °C for biomass combustion. Therefore, more quantity of water (60%) was supplied to solar collector and rest 40% was supplied to biomass furnace. The specific output of the plant was 0.8 MW kg^{-1} of steam with total heat of 3 MW supplied. The cycle thermal efficiency under the specified condition was 27% and fuel efficiency increased to (27-32) % with participation of solar energy. During the day, hybrid thermal efficiency drop from 15% to 11% with solar collector because of low collector efficiency.

Lopez-Vidana, et al., [176] evaluated efficiency of a hybrid solar-gas dryer. Hossain and Bala [177] performed drying experiment of hot chilli using solar tunnel dryer. They considered a mixed mode type forced convection solar tunnel dryer. Flat plate collector absorber with transparent plastic cover constituted the solar air heater in series with tunnel dryer. The moisture content of red chilli was reduced from 2.85 to 0.05 kg kg^{-1} (db) in 20 h and it took 32 h to reduce moisture content to 0.09 and 0.40 kg kg^{-1} (db) in improved and conventional sun drying method. The corresponding values for green chilli were 7.6 to 0.06 kg kg^{-1} (db) in 22 h and 35 h to reach moisture content to 0.1 and 0.7 kg kg^{1} (db) in improved and conventional sun drying. Sreekumar [178] studied techno-economic aspect of a roof-integrated solar air heating system for drying fruits and vegetables. The initial moisture contents of 82% were reduced to the desired level (< 10%) within 10 hours. The drying cost of 1 kg pineapple was computed as Rs.11, that was about 20% of an electric dryer and payback period was worked out as 0.54 year. Palaniappan and Subramanian [179] performed economics of solar air preheating in South Indian tea factories. They observed that requirement of hot air temperature (100 – 130) °C for tea drying and withering was obtained by burning firewood or coal in those factories. Roof integrated solar air heater system was introduced in some of these south India tea factories. The solar air heater was fabricated from galvanized iron sheet. This was painted with commercial, heat resistant dull black paint. The collector transparent cover was 4 mm thickness transparent tampered glass. They performed an economic analysis of a 212 m^2 solar air heater collector area operated for 2.75 years. The system was reported to reduce specific energy consumption from 0.932 to 0.71 kg/kg of dry matter. This saving was approximately 25% of conventional fuel energy. They computed the payback period as two to four year depending on whether the company is profit making or not profit making. Modhlopa and Ngwalo [180] designed and studied a solar dryer with thermal storage and biomass backup heater. The major components of the dryer were biomass burner with a rectangular duct flue-gas chimney, collector storage thermal mass and drying chamber. The dryer was fabricated with simple material, skill, and tools. This was tested in three modes namely, solar, biomass and solar biomass combined by drying twelve batches of pine apple weighing 20 kg each. They observed that thermal mass was capable of storing a part of solar energy. In solar biomass hybrid mode, the dryer reduced moisture content of sliced pineapple from 66.9 % to 11 % (db). The average values of dry moisture pick up efficiencies were 15 %, 11 % and 13 % respectively for solar, biomass and solar biomass hybrid drying. Khanna [181] studied design data for solar heating of air using a heat exchanger. Heat transfer took place both natural and forced convection. This design data assisted the final design of a shell and tube heat exchanger used in drying application. Ayensu [182] developed a solar dryer with rock bed storage. He observed that rock bed storage could hold enough energy to enhance nocturnal drying. Aboul- Enein et al., [183] had developed a solar air heater and experimented this with and without thermal storage for drying of agricultural products. They observed that drying process could be continued during night by using thermal mass. Prasad and Vijay [184] developed a direct solar and biomass powered dryer. The biomass burner had a rock slab on the top that helped in moderating the temperature of the drying air. The dryer designs had a backup heater without thermal storage of captured solar energy. As a result, the air temperature in the drying chamber dropped down to ambient level immediately after sunset. This necessitated backup heating even when the preceding day was sunny. Hossian et al., [185] developed a prototype solar dryer to dry good quality tomato. It consists of a flat-plate concentrating collector, heat storage with auxiliary heating unit, and drying unit. The dryer had a loading capacity of 20 kg of fresh half-cut tomato. The dryer was tested in different weather and operating conditions. The performance of the dryer was compared with an open sun-drying method. Drying performance was evaluated in terms of drying rate, color, ascorbic acid, lycopene, and total flavonoids. Tomato halves were pre-treated with UV radiation, acetic acid, citric acid, ascorbic acid, sodium metabisulphite, and sodium chloride. Sodium metabisulphite (8 g L^{-1}) was found to be effective to prevent the microbial growth at lower temperature (45 °C). Chavan et al., [186] studied mathematical modelling of drying characteristics of Indian Mackerel (*Rastrilliger kangurta*) in solar-biomass hybrid cabinet dryer. The temperature of hot air in solar biomass hybrid dryer could be controlled automatically. The hybrid dryer was constructed of bricks and mortar. This had been found to be more efficient than a conventional solar cabinet dryer made of steel and aluminum. The hot flume gases from the biomass gasifier stove was used to heat the process air inside the drying chamber, with a pipe heat exchanger. The temperature of air inside the drying cabinet was maintained in the range (55–60) °C. The gasifier stove consists of four main parts: fuel chamber, reaction chamber, primary air inlet, and combustion chamber. Thus, the solar-biomass dryer allows the continuous drying of the product. They conducted eight trials for drying mackerel by a solar biomass hybrid cabinet dryer (S-BHCD) and open sun drying (OSD) at air temperatures of (32.39–57.69) °C, relative humidity (23.9–85.8) %, and air flow rate of 0.20–0.60 m s^{-1} . The solar radiation ranged between 287 and 898 W m^{-2} during the time of experimentation. At nighttime, drying was carried out by combusting biomass. The initial moisture content of the processed mackerel was 72.50 ± 0.44 % (w.b.) and was reduced to the final moisture content of 16.67 ± 0.52 % (w.b.) in S-BHCD and 16.92 ± 0.54% (w.b.) in OSD. Eleven drying models were used and the coefficients of determination (R^2) and constants were evaluated by nonlinear regression to estimate the drying curves of dried mackerels. The Midilli model was found to more satisfactorily describe the drying process of mackerel in S-BHCD with R^2 of 0.9999, $\chi 2$ of 0.0000374, and RMSE of 0.0057. In the OSD, a two-term drying model satisfactorily described the drying process with R^2 of 0.9996, $\chi 2$ of 0.0000519, and RMSE of 0.0072. The variation of Free Fatty acid (FFA), Peroxide value (PV), Thiobarbituric acid (TBA), Total volatile bases nitrogen (TVB-N), Trimethylamine nitrogen (TMA-N), and Histamine contents of dried Mackerel by using S-BHCD showed very high corresponding coefficients of determination, where all R^2 were greater than 0.90, except TBA value. There was no discoloration of the product during 4 months of storage. Contour plots of S-BHCD and OSD dried mackerel also showed that for all sensory attributes examined, panellists preferred fish dried with S-BHCD. The organoleptic analysis showed that the S-BHCD drying methods have a highly significant effect ($P<0.01$) on texture and overall acceptability. Biochemical, microbial analysis, and sensory evaluation showed that the product was in prime acceptable form for 4 months of storage at ambient temperature. Kumar and

Bhattacharya [187] studied on technology packages with solar, biomass and hybrid dryer. Gunasekaran et al., [188] performed modelling and analytical study of hybrid solar dryer integrated with biomass dryer for drying *Coleus Forskohlii* stems. They observed that by using solar biomass hybrid dryer, the moisture content of the stems had been 12.3%, whereas solar dryer produced 33% and biomass produced 19.6% respectively. Sopain et al., [189] had developed four solar assisted drying systems namely (a) the V-groove solar collector, (b) the double-pass solar collector with integrated storage system, (c) the solar assisted dehumidification system for medicinal herbs and (d) the photovoltaic thermal (PVT) collector system. The common problems associated with the intermittent nature of solar radiation and the low intensities of solar radiation in solar thermal systems could be remedied using these types of solar drying systems. These drying systems have the advantages of heat storage, auxiliary energy source, integrated structure control system and could be used for a wide range of agricultural produce. Reyes et al., [190] dehydrated Mushrooms (Paris variety) in a hybrid solar dryer (HSD) provided with a 3 m^2 solar panel and electric heaters. Mushrooms were chipped into 8mm or 4mm thickness slices. At the outlet of the tray dryer (80–90) % air was recycled and the air temperature was adjusted to the pre-defined levels (50 or 60) °C). At the outlet of the solar panel the air temperature raised between (2 and 20) °C above the ambient temperature, subjected to the variation of solar radiation level. They observed that temperature, slices thickness and air recycle level had statistically significant effects on critical moisture content (X_c), as well as on the time necessary to attain a moisture content of 0.1 (wb). The color parameters of dehydrated mushroom indicate a disreputable darkening, in all runs. Rehydration assays at 35 °C showed that in less than 30 min rehydrated mushrooms reached a moisture content of 0.8 (wb). The simplified *Constant Diffusivity Model* (SCDM) estimated effective diffusivity (D_{eff}), and it ranged between 6E-10 and 40E-10 m^2 s^{-1}, with R^2 higher than 0.98, complying with literature. The adjustment of experimental drying kinetics with the empirical Page's model resulted in R^2 higher than 0.997. The input of solar energy resulted in (3.5–12.5) % conventional energy saving. These values could even be improved by very small compared to the life of the dryer 15 years. Farkas [192] studied an integrated use of solar drying system. Factors such as energy efficiency, the quality of products, and environmental aspects were necessary to account during the drying of agricultural produce.

2.10 Dryer and factors affecting its performance

The drying capacity of a dryer varies with the type of product and the amount of moisture to be removed. Tray area indirectly refers to the loading or drying capacity of the dryer. Since the products need to be spread in a single layer for efficient drying, total tray area available in the dryer for spreading the product is important. In the case of cabinet type dryers, that have more than one layer of trays, number of layers will be an additional parameter that needs to be indicated. The conditions of drying air, flow rate and the product loaded will determine the number of tray layers for a particular dryer. Dryer capacity also depends on the aperture area or collector area and the size of the drying chamber. Loading density determines the capacity of a dryer (together with total tray area and drying time) for a particular product. Placing products one above the other rather than a single layer tends to limit the area of exposure of product surfaces to drying air, resulting in poor drying [193, 194]. Loading density depends on the type of product, its moisture content, and airflow rate, and may be assessed by rules of thumb, as average dryer loading is 4 kg of fresh produce per square meter of tray area. The solar collector size is 0.75 times total tray area and airflow rate is 0.75 $m^3\ min^{-1}\ m^{-2}$ of tray area [195- 198].

Higher drying air temperature will increase the drying rate in two ways. (1) This increases the ability of drying air to hold moisture. (2) The heated air will heat the product, increasing its vapour pressure. This will diffuse the moisture to the surface faster [196]. Operation of dryers at high temperatures is normally constrained by the thermal sensitivity of most fruits and vegetables. If the temperature is too high in the beginning, a hard shell known as case hardening may develop on the outside trapping moisture inside the shell [199]. Temperatures that are too high at the end of the drying period may cause food to blacken. Irreversible changes of colloidal components of fruit and vegetable tissue occur if the product is held for prolonged periods at high temperature, even if the exposure is insufficient to produce browning or scorching[194]. A high drying air temperature could also result in more heat loss by conduction and radiation from both the collector and drying cabinet, resulting in overall reduction in system efficiency. Mahapatra and Imre [200] had summarized the maximum allowable drying temperatures for a variety of agricultural food products.

Relative humidity of drying air is a crucial parameter to the drying process. If the exit air from the drying chamber still has considerable drying potential, mixing a fraction of the warm, humid exit air with fresh air and recirculating it in the dryer will help to utilize part of the thermal energy in the exit air. Thus, the thermal efficiency of the system is thus improved [201, 202]. Crapiste and Rotstein [203] observed that the fraction of air recirculate can often be high, in the range of about (80–95) %. Soponronnarit et al., [204] reported that there is a 50% drop in drying energy consumption of banana, when a fraction of 95 % air was recycled.

2.11 Critical review of literature

This chapter initially discusses different renewable and non-renewable thermal energy applications for different process industries. We try to present a critical appreciation and summery of cited works briefly. It was reported that improved solar air heater could save 19.60% thermal energy (LPG) for Logan drying in Thailand. Similar energy saving result has been reported in Mediterranean climate for different flat as well as parabolic trough type collectors. Desiccated coconut industry in Sri lank reported to have great potential for solar thermal application to mitigate carbon di-oxide emission. These works are impressive however; authors did not consider thermo-hydraulic efficiency of solar air heater. Energy efficiency of diary industries in German, British, and Dutch had improved compare to France (30% energy saving potential). A systematic energy audit reported in 76 food processing farm in Taiwan revealed fair potential for improving energy efficiency. Energy intensity has been reported ranged from 0.2 to 12.60 MJ kg^{-1} fluid milk products across various countries. Global cheese making industries got energy intensity 4.9 to 8.9 MJ kg^{-1} of cheese across the few countries. These are appreciable reviews on energy conservation and efficiency for food processing industries even though details experimental technological intervention was not recommended.

India tea processing industries annually emit 1.35 M t CO_2 with energy cost is 30% of total cost. There is a scope for application of renewable thermal energy in tea industries. The few tea factories in Tamilnadu reported to use solar air heater that saved 25% conventional energy. Rubber wood waste is reported to use as gasification feedstock for both analytical and experimental study for black tea drying in Sri lanka. However, it is clear from the reviews that hybrid biomass gasification cum solar thermal is not experimented for black tea drying as of today. It has been reported that gasification plant produces less sulphur, carbon di-oxide, oxides of nitrogen and particulate matter. Gasification of waste biomass may be used for process heat generation conveniently. Up rooted tea shrubs has been reported to gasify for black tea drying process heat generation by us. Since tea industry is an agro based unit, therefore other surplus biomass from its own generation may be utilized and therefore other combination of renewable energy have not been considered at present.

Thin layer drying model for different agricultural produces have been reported. However, thin layer drying model of black tea with producer gas fired dryer has not been reported so far. Different designs artificially roughen improved solar air heaters have been reported. Our design considers hemi-spherically protruded improved solar air heater on aluminum plate where a correlation was developed for Nusselt number. Hybridization of biomass and solar thermal energy for drying chili, pineapple, coconut, turmeric, etc., are available. However, none of them refers to black tea processing in hybrid energy mode that is addressed by our present study.

Therefore, we conduct experimental study of characterization of ten biomass samples, gasifier performance, black tea drying experimentation, and modelling, improved solar air heater development, testing and possible hybridization of solar thermal and biomass gasification technology for black tea drying in Assam (India).

3. Introduction

There are adequate works on biomass gasification for different thermal and power applications. However, literature pertaining to gasification of biomass for process heat generation in tea processing industry is very much limited. As mentioned in Chapter:1 (Introduction) that with the crisis of conventional fossil fuel both in terms of environment and economy, substitute renewable fuels in tea industries need to be searched. It is realized that application of gasification technology in tea drying using locally available biomasses would require a systematic investigation. Keeping in view of above, the present works have been undertaken to investigate the efficacy of application of locally available some biomasses as fuel for gasification and to examine the feasibility of using such biomass derived producer gas for tea drying.

The brief description of selected biomass samples [207], the procedure of characterization of biomass samples, the thermal performance of downdraft gasifier using selected biomass fuel, have been presented in this chapter as below.

3.1 Woody biomass samples and their characterization

3.1.1 Selection and description of biomass samples

Ten locally available biomass samples had been considered for characterization. The brief descriptions of these biomass plants are presented below.

1. *Psidium guajava*: It is an evergreen shrub, small tree native to the Caribbean, Central America, South America and India. It is widely cultivated in tropical and subtropical regions around the world. This tree is generally (2.7- 6.0) m in height, with wide-spreading branches and square. The wood of *Psidium guajava* may be used to make pole, fencepost, hand tool handle, handicraft, and charcoal and fire wood production. The average life of this plant is (30 to 40) years (Fig.3.1a). The fruits of the tree are used for preparation of jam and jelly.

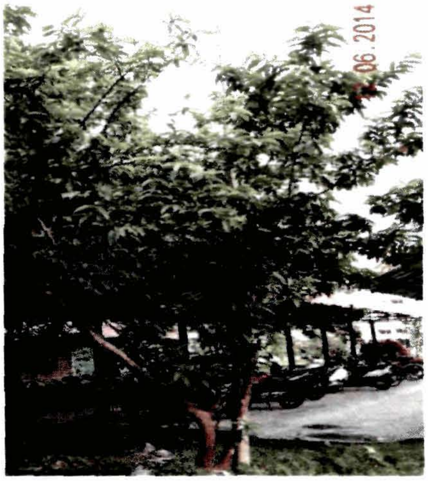

Fig. 3.1a. *Psidium guajava*

2. *Bambusa tulda*: This plant is found in the Southeast Asian rainforest. It grows as undergrowth scattered or in patches. *Bambusa tulda* (Fig.3.1.b) may grow anywhere between (12 – 24) m height. It has multifaceted uses including fuel wood, different handicraft material, fencing, erection of shed particularly in village, paper making industries, etc. The bamboo is a fast growing plant, matures normally 3 to 4 years. However, life of bamboo may be as high as 25 to 40 years and it dies after profound flowering.

Fig. 3.1b. *Bambusa tulda*

3. *Camellia sinensis*: An ever green bushy plant. The young leaf of this plant is used for production of different tea. It is prominently grown in Assam, India. As a plantation woody plant in tea estate, its average height is (1.0- 1.5) m. The productive average life of *Camellia sinensis* (Fig.3.1c) is about 50 years. Since tea estates in Assam generate biomass in the form of uprooted tea branches, pruning litter and branches of shading trees, etc. The uprooting is done at certain intervals of plantation to replant, so as to maintain optimum level of tea productivity. Such uprooted tea branches are generally used as cooking fuel through direct combustion in low efficiency traditional cook stoves. The introduction of improved cook stoves with higher conversion efficiency may lead to a substantial saving of uprooted biomass and this saved biomass may be used for tea manufacturing process heat generation. It has multifaceted uses including fuel wood, and structural material for decorative furniture making. The present gasification study is considering the uprooted tea shrubs as a feedstock for gasifier.

Fig.3.1c. *Camellia sinensis*

4. *Samanea saman*: It is generally used as shading trees in tea estates. This is a tropical tree grows (25-35) m, with rough wrinkled bark (Fig.3.1d). The average life

of *Samanea saman* is about 80 to 100 years. Average growth rate 1.0 m per year and timber yield of a five year old plant is 10 to 25 $m^3\ ha^{-1}y^{-1}$.

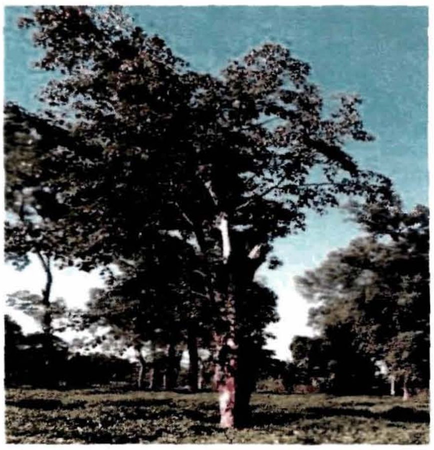

Fig.3.1d. *Samanea saman*

5. *Moringa oleifera* – The tree is slender, with drooping branches that grows to approximately 10 m in height. It is native to the southern foothills of the Himalayas in north-western India and widely cultivated in tropical and sub-tropical areas. It is also known as drumstick tree (Fig.3.1e), and the fruits (drumstick) are consumed as vegetable. The average life span of this plant varies between 30 to 40 years.

Fig.3.1e. *Moringa oleifera*

6. *Polyalthia longifolia* –The tree may grow over 09 to 12 m in height. Found natively in India and Sri Lanka. It is introduced in gardens in many tropical countries. Its bark and trunk are used to manufacture fibre. Timber is used to make pencil, boxes and long masts. The average maturity age of the tree (Fig.3.1f) is around 10 to 15 years.

Fig.3.1f. *Polyalthia longifolia*

7. *Delonix regia* – It usually grows to a modest height of mostly 10 m and can reach a maximum height of 20 m. It spreads widely and its dense foliage provides full shade. It is fast growing tree and mostly used for fire wood and sometime planks are used for supporting reinforced concrete slab casting. About 07 to 10 years, this plant (Fig.3.1g) becomes matured and red colour flowers come out.

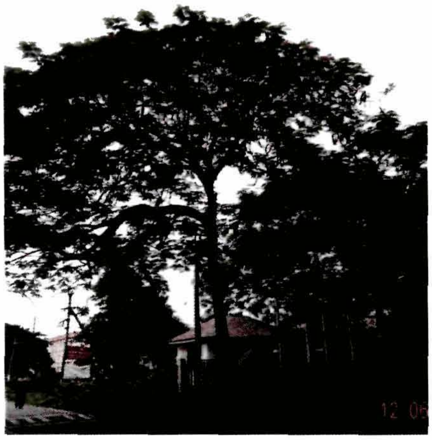

Fig.3.1g. *Delonix regia*

8. *Azadirachta indica*: It is native to India and the Indian subcontinent including Nepal, Pakistan, Bangladesh and Sri Lanka. It grows in tropical and semi-tropical regions (Fig.3.1h). A fast-growing tree can reach a height of (15–20) m and rarely grows to (35–40) m. Its maximum life may be as high as 200 years. This plant's oil is used for preparation soap, etc. Generally matured branches are used for fire wood in rural area.

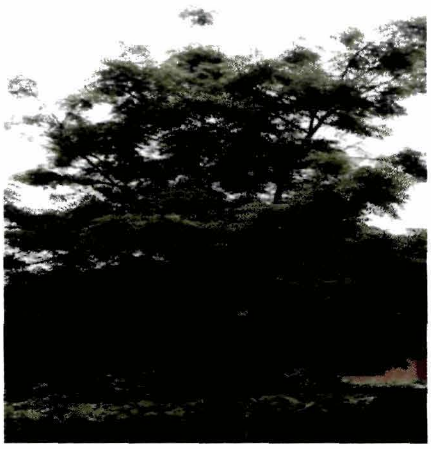

Fig.3.1h. *Azadirachta indica*

9. *Ficus lepidosa*: It is a deciduous tree and grows to heights up to 6 m (Fig.3.1i). It is widespread in tropical and subtropical areas. Its seed has white latex and trunk and branches are mostly used for fire wood in rural area. It becomes mature around 10 to 15 years.

Fig. 3.1i. *Ficus lepidosa*

Fig.3.1j. *Dalbargia sissoo*

10. *Dalbergia sissoo* – It is primarily found growing along riverbanks with 900 m elevation, but may naturally grow up to 1,300 m above sea level. The height of the tree is (10-20) m. This plant (Fig.3.j) gives premier timber for shade and shelter. It is an excellent fuel wood. As a fuel wood it grows in 10 to 15 years rotation. The charcoal produced from this wood is excellent. Moreover, the timber obtained from matured plant is used for different furniture making and building fittings.

Ten locally available woody plants have been briefly described above. *Camellia sinensis* plant is a plantation shrub in tea estate. Uprooted tea shrubs have been proposed for gasification studies in a downdraft gasifier. Gasification performance of *Camellia sinensis* shrub is not found in literature for process heat generation. Even though *Camellia sinensis* is not fast growing for woody biomass production compared to other discussed woody plant. Its specific selection for gasification is that the plant is directly related with tea manufacturing industries for which the investigation is made.

3.1.2 Collection and preparation of biomass samples

Above mentioned ten locally grown biomass samples had been considered for characterization studies. All the woody biomass samples were collected from matured branches of respective plants. The maximum age of *Camellia sinensis* (up rooted tea shrub) and *Samanea saman* (Siris) was around 50 years and they were collected from a tea estate nearby to Tezpur University. Other eight biomass plants, age varied from (10-20) years. These eight biomass samples were collected from Tezpur University (latitude 26° 42′ 03″ N and longitude 92° 49′ 49″ E) campus. Saw dusts of all ten biomass samples obtained through wood chipping machine were collected for characterization. It was followed by sieving the saw dust of all ten woody biomass samples (<475 micron).

3.1.3 Parameters and procedures of fuel characterization of biomass

Experiments were conducted in the month of April 2012 at Sophisticated Instrumentation Facilities Centre (SIFC), Tezpur Uinversity, Assam, India. The ten biomass samples had been characterized by using a CHN Analyser (PerkinElmer, Series II, CHNS/O Analyser, 2400), (Fig.3.2). The higher heating value of biomass, (HHV), also called gross calorific value (GCV), had been determined by the oxygen bomb calorimeter (Make: 5E-1AC/ML, Changsha Kaiyuan Instruments Co., LTD, China), (Fig. 3.3). The detailed procedure for characterization of biomass samples has been presented below.

3.1.3.1 Ultimate analysis

Composition of hydrocarbon fuel is expressed in terms of its basic elements except for its moisture and inorganic components. Ultimate analysis shows the ratio of combustible elements (Carbon, Hydrogen, Nitrogen, Sulphur and Oxygen) to non-combustible fraction like inorganic ash residue. A typical ultimate analysis relationship is given by following expression [61].

$$C + H + O + N + S + ASH = 100\ \% \qquad (3.1)$$

where, C, H, O, N, and S are weight percentage of carbon, hydrogen, nitrogen, and sulphur respectively. Ultimate analysis refers to the following ASTM standards for measurements such as Carbon, Hydrogen and Nitrogen (ASTM E-777, and ASTM E-778), Oxygen (By difference), Ash (ASTM D-1102) respectively.

Carbon, Hydrogen and Nitrogen

These three combustible elements may be measured concurrently on dry and ash free basis. Carbon, Nitrogen and Hydrogen in sample are combusted to for their corresponding gases (CO_2, H_2O and N_2) in Oxygen environment. The carbon di-oxide, water vapour and elemental Nitrogen are detected by appropriate detector TCD (Thermal Conductivity Detector) and result is given in percentage mass basis.

Ash

Ash measurement calculates the % by mass of the initial total sample that consists of ash, after the hydrocarbons are burnt and consumed in a 575 °C temperature for 3 hours.

Oxygen

Oxygen estimated from difference of initial weight of dry sample and summation of all other constituents of biomass sample (CHNO and ash). Since the samples for CHN analysis of were on dry basis, therefore moisture fraction was zero. Moreover, sulphur in biomass sample is generally negligible, therefore it was assumed as zero.

3.1.3.2 Proximate analysis

Proximate analysis of woody biomass gives gross constituents such as moisture (M), volatile matter (VM), ash (ASH), and fixed carbon (FC) [205]. The procedure for determination of different biomass samples constituents have been presented below.

Volatile matter

Volatile matter of woody biomass fuel refers to condensable and non-condensable vapour released as the fuel is heated. As per E-872 standard, about 50 g test sample woody biomass should be collected from not less than 10 kg representative sample with ASTM D-346 protocol. The sample is ground to less than 1 mm in size; 1g is taken from it, is dried and put in a crucible. The covered crucible is placed in a furnace at 950 °C and is heated for seven minutes. The volatiles released are detected by luminous flame. After seven minutes, the crucible is taken out, cooled in a desiccator, and is weighed to determine loss in weight.

Ash

The principal constituents of ash are silica, iron, aluminium, calcium, and small amount of sodium, potassium, magnesium, titanium may also be present. As per standard D-1102, specifies 2 g samples of woody biomass (< 475 micron) was dried in standard condition and placed in a muffle furnace with the lid of crucible removed. Temperature of the furnace was raised slowly (580 - 600) °C to avoid flaming. As all carbon is burnt, sample was cooled and weighed for determination of ash. It may be mentioned that ash plays an important role in biomass combustion and gasification if potassium and halides (Chlorine, etc.) are available. These components may lead to serious agglomeration, fouling, corrosion in boiler and gasifier [206].

Moisture

The moisture in woody biomass may be in free (external) and inherent (equilibrium) forms. It is determined by ASTM standards (D – 871- 82) for woody biomass. As per this standard, 50 g wood sample was dried at 130 °C for 30 minutes. Then the sample was left at that temperature of 16 hours and was weighed. The weight loss was recorded to determine moisture content of the woody sample.

Fixed carbon

A sample of biomass constitutes moisture, volatile matter, ash and fixed carbon. As per the standard procedure, fixed carbon was estimated by deducting the amount of remaining three constituents from the initial amount of sample. Fixed carbon determination is an important parameter for gasification because conversion of fixed carbon into gaseous products determines rate of gasification and gas yield.

3.1.4 Expression of biomass composition

The woody biomass composition may be expressed as received basis, air dry, total dry, dry, and ash free basis. "As received basis" may be expressed with total sum of either proximate analysis of constituents or ultimate analysis data on 100%

exactly. However, for present study, total dry and dry and ash free basis is considered.

Total dry basis

Total dry basis consider both surface and internal moisture of woody biomass. As a result, numerical value of total dry representation is less than air dry basis. Chipped woody biomass sample for gasification is considered on total dry basis.

Dry and ash free basis

Dry and ash free basis considers subtraction of ash along with total moisture from the gross mass of woody fuel. Woody biomass sample for determination of calorific value is considered dry and ash free basis in automatic bomb calorimeter.

3.1.5 Heating values of biomass

The experimental determination of higher heating value of a biomass is important from gasification or combustion point of view. The present study deals with experimental determination of higher calorific values of ten woody biomass samples in automatic bomb calorimeter (Fig.3.2).

Higher heating value of biomass

It is defined as the amount of combustion heat released by unit mass of fuel (25 °C initially) after combustion when products come to initial temperature (25 °C). Bomb calorimeter is used to measure higher heating value as per ASTM standard D 2015 [Fig.3.2].

Fig.3.2 Automatic Bomb Calorimeter

Fig.3.3 CHN Analyzer

Lower heating value of biomass

Lower heating value is also known as net calorific value (NCV). It is defined as amount of heat released by combustion of specified quantity of fuel excluding the heat of vaporization of water in combustion products. The relation between higher heating value and lower heating value is given by Eq. (3.2) [61].

$$LHV = HHV - h_g\left(\frac{9H}{100} + \frac{M}{100}\right) \tag{3.2}$$

where *LHV*, *HHV*, h_g , *H*, *M* are lower heating value, higher heating value of biomass sample, latent heat of steam (2260 kJ kg^{-1}), hydrogen and moisture percentage of biomass respectively. Heating value of woody biomass may be represented as dry basis (db) or moisture free basis (mf), dry and ash free basis (daf) or moisture ash free basis (maf). For M_f kg of fuel with Q kJ of heat, M_w kg of moisture and M_{ash} kg of ash, different higher heating value may be written as following equations [61]. However, determination of higher heating value [Eq. (3.3)] by adiabatic bomb calorimeter is considered on dry and ash free basis.

$$HHV_{daf} = \frac{Q}{(M_f - M_w - M_{ash})}\ kJkg^{-1} \tag{3.3}$$

Density

Apparent density of biomass is measured with volume displacement method. Bulk density may be measured as per ASTM (E-873-06). This involves pouring biomass samples into a standard size box (305 mm × 305 mm × 305 mm) from a height of 610 mm. The box is then dropped from a height of 150 mm three times for settlement.

3.2 Biomass gasification

Based on calorific value and ultimate analyis data of the ten selected biomass, an experimental study was carried out to gasify uprooted tea shrubs (*Camellia sinensis*) at Tezpur University, Assam (India). The appropriate moisture content and sizing (feed stock preparation procedure) of these three biomass samples for gasification in a 30 $kW_{thermal}$ biomass gasifier is as follows. Further, based on characterization results and availability in tea estate, *Camellia sinenesis* uprooted shrubs were considered for gasification. All the biomass samples used for gasification were chipped [(35 ± 5) mm in length, (20 ± 5) mm in diameter] by wood chipping machine. Chipped biomass samples were sun dried until moisture was (15 ± 5) % (w.b.). It was then stored in gunny bags in store-room, adjacent to the laboratory to use for gasification experiments. A laboratory scale biomass gasification unit was operated for process heat generation.

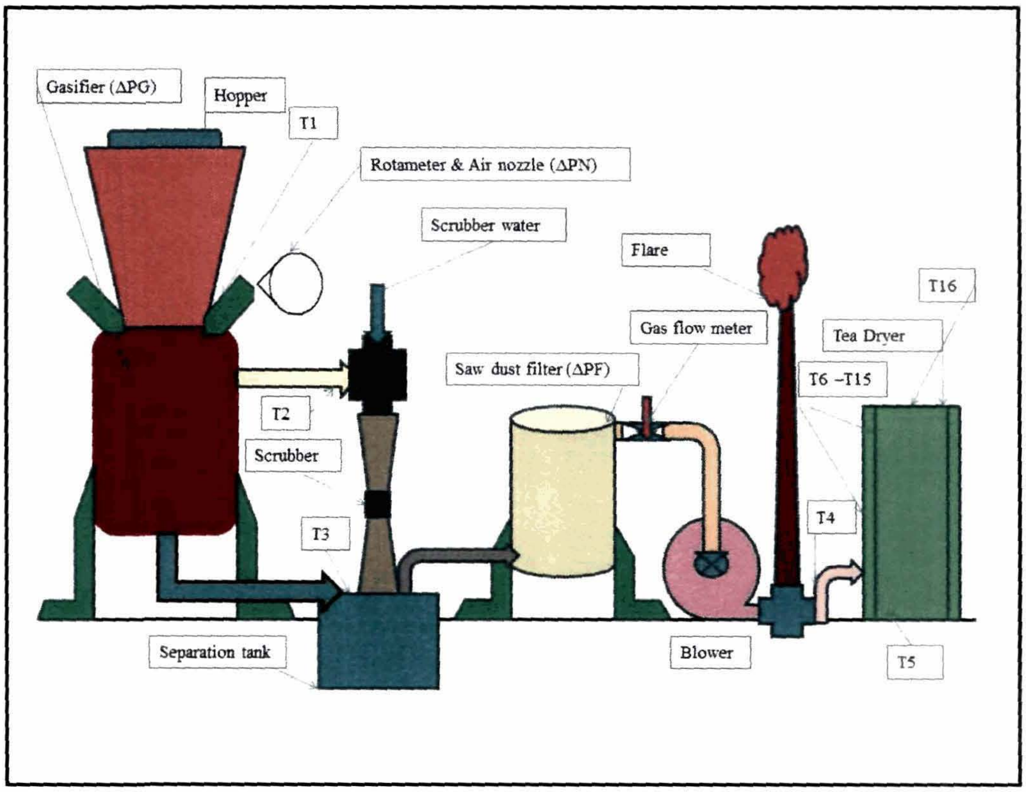

Fig. 3.4a: Experimental setup of producer gas based tea drying using uprooted tea shrubs layout diagram

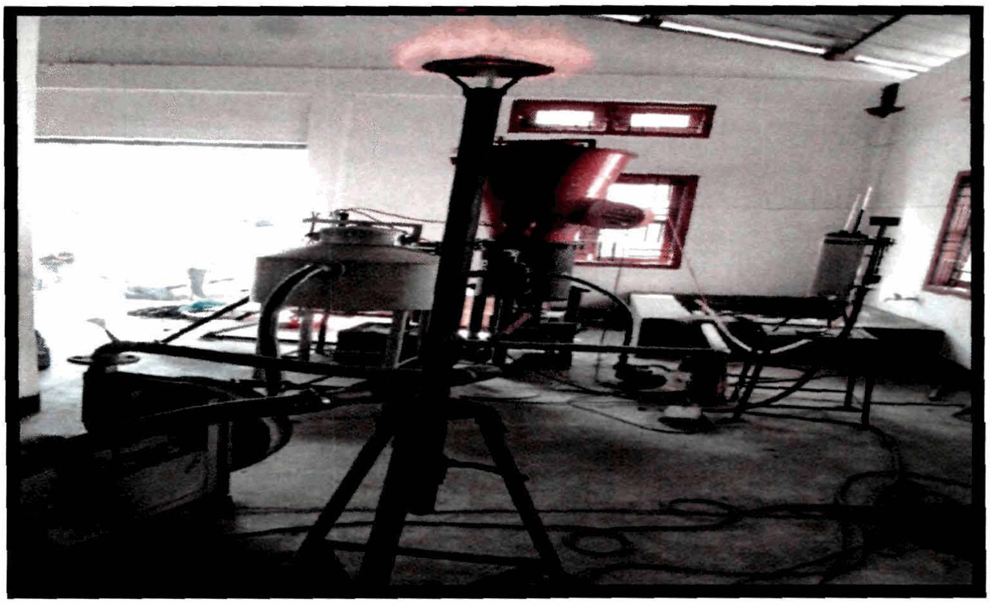

Fig.3.4b: Experimental setup of 10 kW thermal output downdraft gasifer

3.2.1 Details of experimental set up for thermal performance evaluation of gasifier

A detail of the experimental setup (Fig. 3.4a, Fig. 3.4b) and instrumentations used for evaluation of the gasifier performance using uprooted tea shrubs (*Camellia sinensis*) is presented in Table 3.1. Description of different subassemblies and measuring instruments are briefly highlighted as follows. An experimental setup for gasification of uprooted tea branches (*Camellia sinensis*) has number of components as summarized as below.

Gasifier

An Ankur make downdraft type woody biomass gasifier (Model-WBG-10, 10 kg h^{-1}) was used for the present study. The gasifier was consisted of (i) hopper, (ii) a double walled air insulated cylindrical reactor, (iii) air nozzles (iv) a rotatable grate controlled by a comb-rotor, (v) ash pit and (vi) some auxiliaries *viz.*, scrubber and water pump assembly, vibrator, blower and saw dust filter. The controls of auxiliary operations were done with the help of a control panel. The total electrical energy requirement to run the supplementary equipment of the gasifier was 0.8 kW. Air was supplied by two air nozzles circumferentially at 180° apart. The nozzle ends pointed into the combustion zone and they were extended up to the minimum constriction of V throat inside reactor. The gasifier setup was also provided with water filled U- tube manometers to observe the pressure drop at air entry nozzle and at reduction zone inside the reactive gasifier.

The gasifier was operated using uprooted tea shrubs for performance evaluation. The air and fuel ratio was varied and thermal output in terms of calorific value; gas composition and flow rate of producer gas were measured to find performance (best operating condition) of the gasifier. The ash and excess charcoal from the grate were rejected automatically into the ash pit to maintain a constant reduction zone height inside the gasifier. The gasification air discharge into the gasifier at various loads was measured with rotameter. A continuously running gasifier under study has been termed as reactive gasifier.

The cold gas efficiency of a biomass gasifier is defined as the ratio of energy content of producer gas against unit weight of biomass to lower heating value of unit weight of biomass as given by Eq.(3.4) [209]

$$\eta_{cold} = \frac{(CV\ of\ producer\ gas\ (MJ\ m^{-3}))\times(Gas\ production\ rate\ (m^3 kg^{-1}))}{Lower\ heating\ value\ of\ the\ biomass\ (MJ\ kg^{-1})} \quad (3.4)$$

Junker gas calorimeter for measurement of calorific value of producer gas

Junker gas calorimeter (INSURF, Make: Instrumentation and Refrigeration of India) was used for online measurement of calorific value of producer gas. Producer gas contains five principal components namely nitrogen, carbon dioxide, some hydrogen, carbon mono-oxide, and traces of methane out of which last three gases are combustible. Producer gas calorific value was measured by tapping a small amount of gas from the main gas stream to feed Junker gas calorimeter and then its calorific value was evaluated at an interval of 10 minutes. The higher heating value of producer gas thus generated from woody biomass sample was determined with Junker Gas Calorimeter using standard procedure.

$$HHV_{Producer\ gas} = \frac{m_w C_p (t_{ow} - t_{iw})}{m_f} \tag{3.5}$$

where, m_w is the mass of cooling water passed through the cooling jacket during the experimental period, C_p is specific heat capacity of water; m_f is the mass of producer gas burnt during the experimental period, t_{iw} is inlet water temperature and t_{ow} is outlet water temperature.

Measurement of gas flow using Master turbine flow meter

A master turbine flow meter was used in addition to a rotameter to measure producer gas discharge for combustion in the partially premixed gas burner as well as surplus flared gas. Flow straighteners of 10D and 5D were provided at upstream and downstream of flow meter installation for minimizing flow fluctuation. A magnetically coupling meter head directly gave producer gas discharge used for combustion in tray dryer burner.

Measurement of air flow using Rotameter

Rotameter was used to measure gasification air coming through air nozzles. A producer gas suction blower was used at the outlet of gasifer to adjust the output gas flow rate. The flow of input air was recorded using a Rotameter (Table 3.1) for all the test conditions. The measurement of this air was very important aspect to calculate the equivalence ratio for biomass gasification process and system efficiency.

Measurement of pressure drops by U tube water manometer

Pressure drop across the gasifier and nozzle were measured with U tube water manometer at varying output gas flow rates. With variation of air fuel equivalence ratio for gasification, these two important pressure drops were indicative parameter for optimum performance and health of a reacting gasifier. U tube manometer gives pressure drop inside gasifier and in air nozzle by difference of water column in millimetre with respect to atmospheric pressure. The pressure drop in millimetre of water column was further converted into Pascal.

Table 3.1 Experimental set up and details of instrumentations used for gasifier performance

No.	Items	Technical specification	Remarks
1.	V throat downdraft woody gasifier	WBG-10 (Thermal), Make: Ankur [210]	Used for generating producer gas
2.	Junker Gas Calorimeter	INSREF, Fuel type: Fuel gas/Petrol [211]	On line measurement of calorific value of producer gas
3.	Gas Turbine Flow meter	DN50-G65, (6-2500) $m^3 h^{-1}$ Rockwine India Ltd. [212]	To measure the producer gas flow rate.
4.	Temperature data logger	CDL-28, Shivaki, India, Accuracy: ± 0.15 % FS [213].	Online measurement of various temperatures.
5.	Rotameter	Acrylic Body, Range: (0.1-10) m^3h^{-1}, Accuracy: + 2% FSD	To measure gas flow of gasification air
6.	Wood moisture Meter	Moisture: (0 to 40) %, Resolution: 0.1 Accuracy: ± (0.5% n + 1), 190 g	To measure moisture content of biomass feedstock.
7.	U tube differential manometer	Acrylic Body, Range: (250-0-250) mm	To measure pressure drops
8.	Digital weighing balance	KERN: Read out 0.01 g, Range:1210 g, linearity ± 0.03	To measure moisture loss of fermented tea.
9.	Gas Chromatograph	Thermo-fisher Trace GC:600	To measure producer gas composition
10.	Multifunction gas analyser	Testo, Germany	To measure flue gas composition producer gas burner

Measurement of biomass moisture and consumption

The moisture of the woody biomass feedstock was measured with established method [214]. The gasifier hopper had a capacity of 100 kg dry wood and average fuel consumption ranged from (7 to 10 kg h^{-1}). Once filled, it may uninterruptedly run for average 8 hours depending upon the operating condition. However, refilling of wood on hourly basis was performed to calibrate hourly fuel consumption data. Besides, to nullify the effect of excess air because of refilling of wood, constant pressure drops across the nozzles and gasifer were maintained by controlling the blower outlet flap valve. During experiments, gasifier was filled once after every eight hours and normally tea drying experiments complete before eight hours average hourly fuel consumption was calculated accordingly. Moreover, any minor variation of excess air was controlled by suction blower flap valve adjustment. The hopper door was closed for entire period of experiments.

Temperature data logger with computer interface

A multi-channel (16 channel) online temperature data logger, (Model No: CDL-28, SHIVAKI, and India: accuracy ± 0.15 %) with K – type thermocouples (Chromel-Alumel) were used to measure temperatures at different locations such as gas outlet, scrubber water outlet, ambient air temperature, over the entire experimental periods. The temperature measurements were performed as per ASTM standard [217]. The temperature sensors were connected to computer using RS232 interface through 16 channel data logger which recorded online temperatures at the desired locations as shown in (Fig.3.4a).

Gas chromatograph

An off line Gas Chromatograph (Trace GC: 600, Make: Thermo Fisher, Italy) was used to measure producer gas quality at different air fuel equivalence ratio (Fig.3.5). Producer gas samples were collected in a bladder to inject it into the gas chromatograph and producer gas tapping point was fixed after fine filter of gasifier setup to get desired quality of gas.

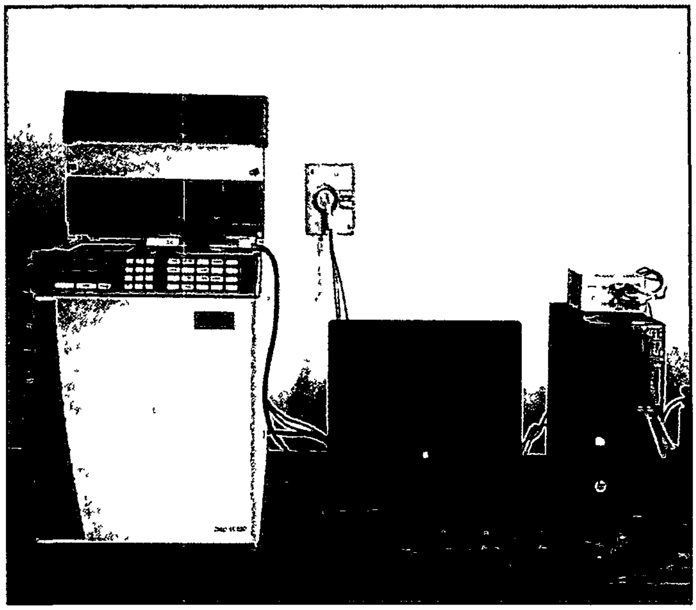

Fig.3.5- GC Trace 600 for producer gas composition analysis

3.3 Results of fuel characterization of selected biomass samples to examine suitability as gasification feed stocks

The proximate and ultimate analysis results of ten different locally available biomass samples, e.g. *Psidium guajava, Camellia sinensis, Moringa oleifera, Samanea saman, Polyalthia longifolia, Delonix regia, Azadirachta indica, Ficus lepidosa, Dalbargia sissoo* and, *Bambusa tulda* have been presented in Table 3.2 and Table 3.3, respectively [208]. The reported values are the average three replicates. It had been observed that *Dalbargia sissoo* has highest fixed carbon (15.60%). *Bambusa tulda* has second highest fixed carbon (15.2 %) and *Ficus lepidosa* had minimum fixed carbon (12.2 %). Ash value of *Dalbargia sissoo* was minimum 4.4% and *Ficus lepidosa* was maximum 5.8% respectively. More ash content of biomass adversely affects the performance of a gasifer because of slag formation at high temperature. It melts and fuses subsequently that may block the down draft gasifier throat. Volatile matter was minimum for *Dalbargia sissoo* (80.00%) and maximum for *Ficus lepidosa* (82%) respectively.

Table 3.2 Proximate analysis of ten locally available biomass samples

Biomass	Volatile matter % (db)	Ash % (db)	Fixed Carbon % (db)
Bambusa tulda	80.30	4.50	15.20
Delonix regia	81.25	5.50	13.25
Azadirachta indica	81.75	5.60	12.65
Ficus lepidosa	82.00	5.80	12.20
Dalbargia sissoo	80.00	4.40	15.60
Psidium guajava	80.25	4.64	14.87
Camellia sinensis	80.20	4.78	14.53
Moringa oleifera	80.15	4.93	14.20
Polyalthia longifolia	80.10	5.07	13.86
Samanea saman	80.05	5.22	13.53

Table 3.3 presents different ultimate analysis results of ten biomass samples. It was found that *Psidium guajava* had the highest calorific value (18.403 MJ kg^{-1}) and *Ficus lepidosa* had the lowest (15.96 MJ kg^{-1}) among the tested samples. Calorific value of *Bambusa tulda* was (18.40 MJ kg^{-1}). Moreover, calorific value of *Camellia sinensis* was (18.401 MJ kg^{-1}) in the (Table 3.3). Other eight woody samples had calorific value in between *Psidium guajava* and *Ficus lepidosa.* The approximate empirical bio-chemical formula for all ten biomasses has been obtained from CHN/O analysis of data. For each atom of C, the variation of H atoms ranges between 1.866 (*Delonix regia*) and 1.580 (*Ficus lepidosa*). Such variation for N is *Azadirachta indica* (0.051) to *Camellia sinensis* (0.03).

Table 3.3 Ultimate analysis of biomass samples

Biomass (By weight)	C %	H %	N %	O %	CV (MJ kg^{-1})	Empirical formula molecular formula
Bambusa tulda	50.19	6.76	2.94	40.11	18.401	$CH_{1.604}N_{0.050}O_{0.599}$
Delonix regia	46.78	7.33	2.82	43.07	16.202	$CH_{1.866}N_{0.050}O_{0.690}$
Azadirachta indica	47.38	7.14	2.84	42.64	16.603	$CH_{1.795}N_{0.051}O_{0.675}$
Dalbargia sissoo	48.45	7.10	2.90	41.55	17.154	$CH_{1.745}N_{0.051}O_{0.643}$
Psidium guajava	49.85	6.83	2.89	40.43	18.403	$CH_{1.632}N_{0.049}O_{0.608}$
Camellia sinensis	49.48	6.90	2.86	40.76	18.400	$CH_{1.65}N_{0.03}O_{0.642}$
Moringa oleifera	49.12	6.97	2.82	41.09	17.831	$CH_{1.690}N_{0.049}O_{0.628}$
Polyalthia longifolia	48.77	7.06	2.77	41.40	17.332	$CH_{1.724}N_{0.048}O_{0.637}$
Samanea saman	48.41	7.11	2.74	41.74	17.211	$CH_{1.750}N_{0.048}O_{0.647}$
Ficus lepidosa	47.13	7.12	2.78	42.97	15.952	$CH_{1.580}N_{0.050}O_{0.698}$

The variation of O atom is 0.698 (*Ficus lepidosa*) and 0.599 (*Bambusa tulda*). Now, all the samples seem to be potential feedstock for downdraft gasification and to generate combustible producer gas used for thermal applications.

Table 3.4 Average physical properties of biomass considered for gasification

Feed stock	Chip sizes (mm^3)	Apparent density ($kg\ m^{-3}$)	Bulk density ($kg\ m^{-3}$)	Porosity
Camellia sinensis	9425	1050	560	0.47

Table 3.4 presents average physical properties of *Camellia sinensis* measured in triplicate. The porosity was calculated from apparent density and bulk density.

3.4 Estimation of stoichiometric air fuel ratio

The ultimate analysis data of uprooted tea shrubs (*Camellia sinensis*) had been used to compute stoichiometric air fuel ratio and equivalence ratio for gasification. The molecular formula $[(CH_{1.65}N_{0.03}O_{0.71})_n]$ of feed stocks [*Camellia sinensis*] was calculated by taking mole ratios of hydrogen, oxygen and nitrogen to one mole of carbon. Stoichiometric oxygen requirement is the amount of oxidizer to completely form one mole of carbon dioxide and water. The stoichiometric oxygen requirement [61] may be computed from Eq. (3.6). Now, kilogram of oxygen per kilogram of fuel neglecting Nitrogen and Sulphur contents in biomass:

$$M_a = 2.68C + 8H - O \qquad (3.6)$$

By using ultimate analysis data (Table 3.4), the stoichiometric air and biomass (*Camellia sinensis*) ratio is calculated from, Eq. (3.6) as 5.44 kg kg^{-1} of dry fuel. This value of stoichiometric air fuel (*Camellia sinensis*) ratio will be useful for calculating different equivalence ratio during gasifier performance study.

3.5 Performance testing of biomass gasifier

3.5.1 Warm up and medium duration test

The gasifier was operated according to the standard procedure prescribed by the Ministry of New and Renewable Energy, Govt. of India [MNRE, 220]. Since the gasifier (producer gas generator) converts the solid biomass into gaseous fuel by a series of thermo-chemical reactions, therefore to initiate proper gasification, some minimum warm up period is necessary. The hopper of the gasifier was fully loaded with biomass (*Camellia sinensis* chips) through top lid and then the lid was tightly closed. A firing torch wrapped with cotton waste in support of kerosene oil was used to fire the gasifier through air nozzles. The blower was started immediately and combustion air was controlled by means of the flap valve such that oxidation zone inside the gasifier could be established. At the beginning, white opaque smoke was released that was not combustible. After about (15-20) minutes, the output gas was less opaque with more combustible constituents and continued with sustained flame in producer gas burners. Measuring parameters were rate of fuel consumption, pressure drop in gasifier and nozzles, calorific value of producer gas, producer gas compositions, gasification air requirement, and different fluid temperatures [221].

Normally gasifier performance is measured in terms of fuel consumption rate, cold gas efficiency, producer gas production rate, calorific value of producer gas and optimum air fuel equivalence ratio for gasification. The quality of producer gas depends on the various factors such as moisture content of the feed stock, air flow rate into the gasifier, the sizes of wood chips, position of air inlet nozzles and reduction zone volume, etc. [51]. The different variables effecting performance of the gasifier are presented as follows.

3.5.2 Pressure drop and gas flow rate

Pressure drop across a porous reactive gasifier bed, air nozzle, and filter are important controlling variables. The flow of ambient air into the gasifier was assumed to be isothermal and (Fig.3.6) shows the variation of gas flow rate with respect to gasifier pressure drop for both a newly charged gasifier and a reactive gasifier. It is clear that pressure drop is higher in a reactive gasifier compared to a newly charged gasifier for same output gas flow rate. This is because of less porosity and higher resistance to gas flow in a reactive gasifier. Therefore, it may be opined that optimum pressure drop in a reactive gasifier is an indication of good health and its efficient operation.

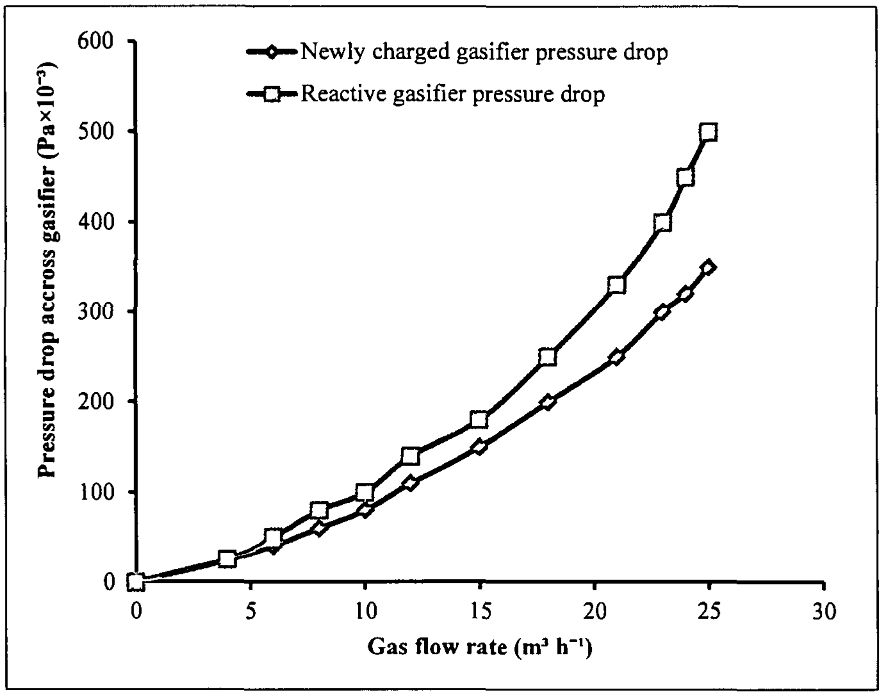

Fig. 3.6: Pressure drop across gasifier with gas flow rate

Pressure drop across air nozzle is plotted against the gas flow rate (Fig.3.7) which is again another indicator of proper gasification processes. If this pressure drop is increased beyond certain values for a newly charged gasifier and a reactive gasifier then the gasifier may go into combustion mode. The flow of output gas still increased but the quality of gas as measured by Junker gas calorimeter was poor due to combustion (at higher air fuel ratio) of a part of producer gas. It also increased corresponding pumping power of gasification process leading to losses of output energy and power from the gasifier.

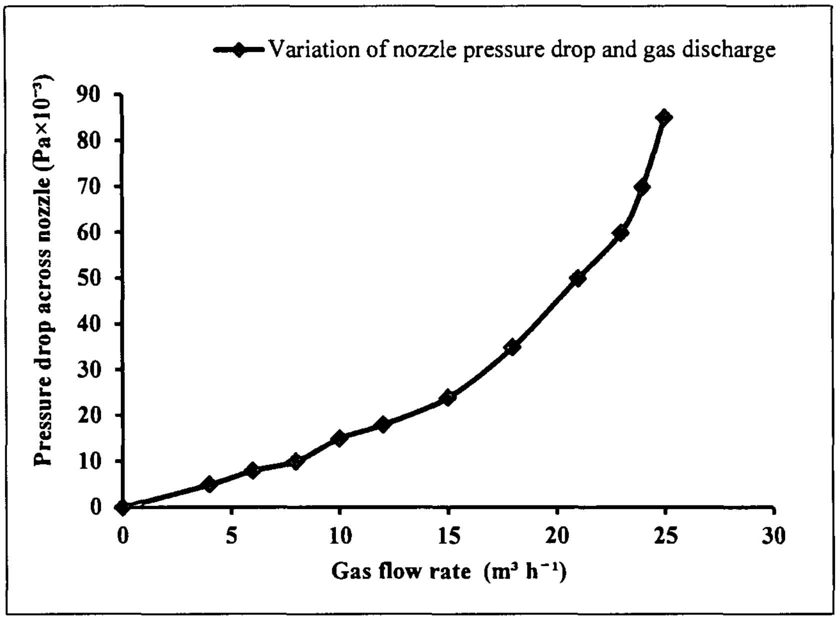

Fig. 3.7: Pressure drop across nozzle with gas flow rate

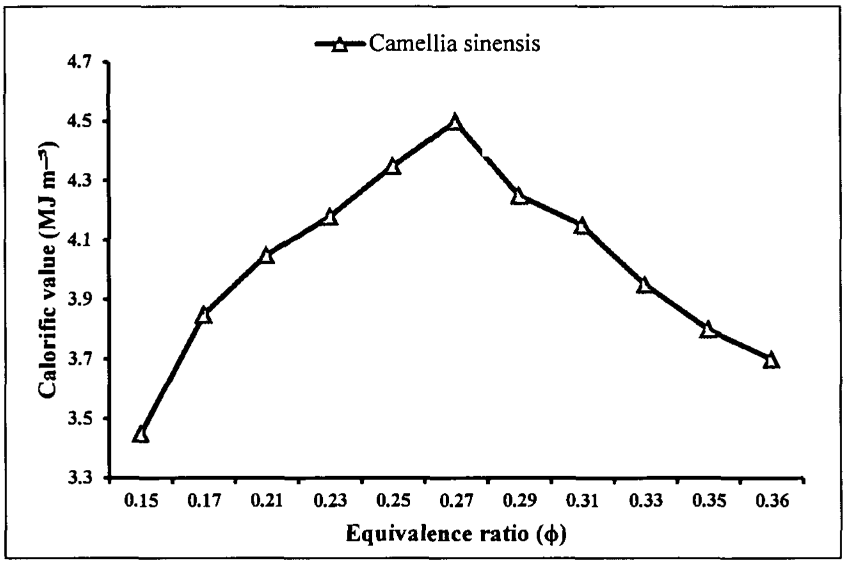

Fig. 3.8: Variation of calorific value with equivalence ratio for *Camellia sinensis* derived producer gas

3.5.3 Measurements of different temperatures

Temperature of scrubber water, producer gas had been measured during experiment at variable gas flow rate. As gas flow increases from (16 to 25) m^3h^{-1} average temperature gas outlet temperature changed (380 to 450) °C (Table 3.5)

Table 3.5 Average temperatures at different points in experimental setup

Gas flow rate ($m^3\ h^{-1}$)	Ambient (°C)	Gas outlet (°C)	Scrubber outlet (°C)
16	35	380	42
18	35	390	44
20	35	405	45
22	35	425	48
24	35	450	50

3.5.4 Equivalence ratio

The stoichiometric air fuel ratio for biomass combustion is 5.22:1 as reported by Zainal et al. [86]. The equivalence ratio is an important design controlling parameter of a gasifier. It is defined as the ratio of actual air fuel ratio to stoichiometric air fuel ratio. Gasification always takes place at an air deficient environment whereas pyrolysis takes place in absence of air. Different researchers found effective equivalence ratio for wood gasification in the range of 0.25-0.35 in their experimental down draft gasifer [61]. If equivalence ratio is below 0.20, it may give rise to incomplete gasification, excessive char formation and lower heating value of producer gas. For equivalence ratio above 0.4, it may result in excessive formation of complete combustion products in the expense of CO, CH_4 and H_2 of producer gas. The present experimental gasification studies of uprooted tea branches (*Camellia sinensis*) gave best overall performance at 0.27 equivalence ratio (Fig.3.8). Table 3.6 shows experimental variation stoichiometric air fuel ratio (SAFR) and actual air fuel ratio (AAFR) for a set of gasification air flow rate. It is clear from this table that at equivalence ratio 0.27, wood consumption was 8.5 kg h^{-1}.

Table 3.6 – Computation of equivalence ratio for gasification.

Air flow rate (m^3 h^{-1})	SAFR	Biomass (kg h^{-1})	AAFR	Equivalence ratio (ϕ)
7.5	5.44	8	0.94	0.17
8.5	5.44	8	1.06	0.20
9.5	5.44	7.5	1.27	0.23
10.5	5.44	8	1.31	0.24
11	5.44	8.20	1.34	0.25
11.5	5.44	8.20	1.40	0.26
12.5	5.44	8.50	1.47	0.27
13	5.44	8.50	1.53	0.28
14	5.44	9.00	1.56	0.29
14.5	5.44	9.00	1.61	0.30
16	5.44	9.50	1.68	0.31
16	5.44	9.00	1.78	0.33
17	5.44	9.00	1.89	0.35

3.5.5 Producer gas calorific value

The calorific value of producer gas obtained from gasification of uprooted tea branches was similar as reported by researchers in literatures [79, 81, 84, 89, 90, and 91]. With increase in equivalence ratio, the gas production rate continuously increased up to particular value because it gave rise to a higher air flow rate. After certain value of equivalence ratio, calorific value of producer gas declined probably because of higher concentration of CO_2.The maximum calorific value of producer gas was measured as 4.5 MJ m^{-3}) at 0.27 equivalence ratio (Fig.3.8) for gasification of, *Camellia sinensis*.

3.5.6 Gasifier efficiency and air fuel ratio

It.is evident that for a constant calorific value of biomass, cold gas efficiency depends on calorific value of producer gas and amount of gas produced per unit weight of input biomass. Maximum cold gas efficiency of 65 % was observed with uprooted tea shrubs as woody biomass feed at equivalence ratio of 0.27 and it gave rich yield of producer gas (Table 3.6). The cold gas efficiency was then falling gradually beyond this equivalence ratio (Fig.3.9) due to complete combustion of a part of producer gas. Equivalence ratio beyond 0.27, the bulk volume of producer gas mixture sharply increased because part of producer gas was converted into flue gas in presence excess oxygen. An optimum discharge of (20 to 22) m^3 h^{-1} was quite economic for overall efficiency of gasification process with *Camellia sinensis* as gasification feed stock.

3.5.7 Producer gas compositions

Fig.3.10 shows variation of producer gas composition and average calorific value with air fuel equivalence ratio for gasification reaction. Both H_2 and CO had increased with increase in gasification air fuel equivalence ratio (Φ = 0.27) and maximum values of these two components were reported as 18% and 24% respectively. Beyond this equivalence ratio, CO decreased and H_2 contents almost remained constant. The CH_4 content nearly remained constant at about 1.5% and maximum calorific value (4.5 MJ m^{-3}) of producer gas was reported at this air fuel equivalence ratio. The Gas Chromatograph setup used for analysis of producer gas has been presented in Fig.3.5. The producer gas composition was similar as reported in modelling and simulation study of a down draft gasifer with some locally available biomass samples [222].

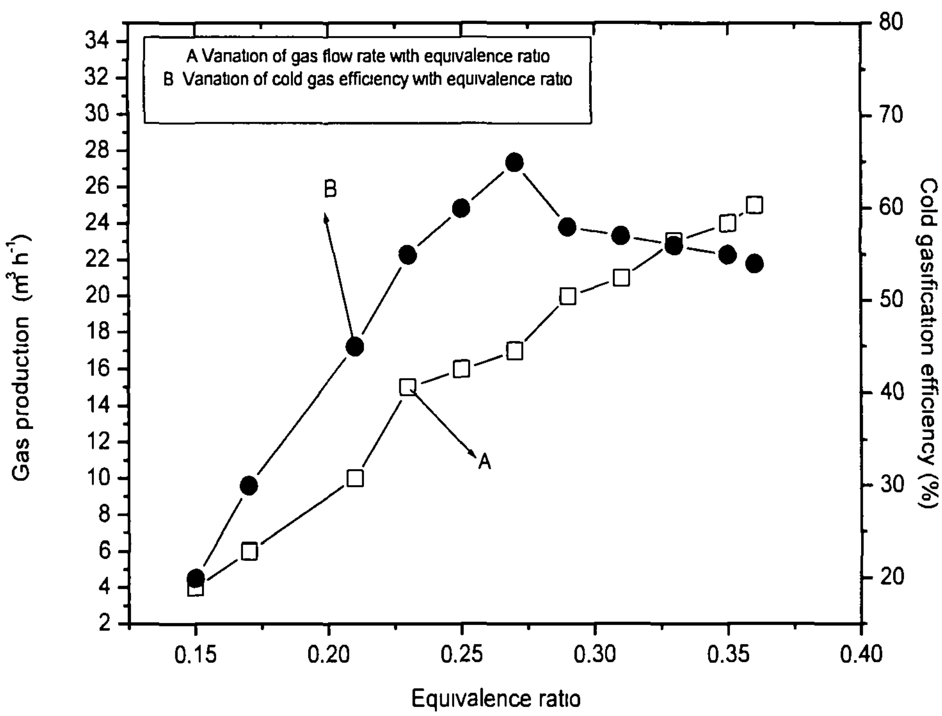

Fig. 3.9: Variation of gas production and cold gas efficiency with equivalence ratio

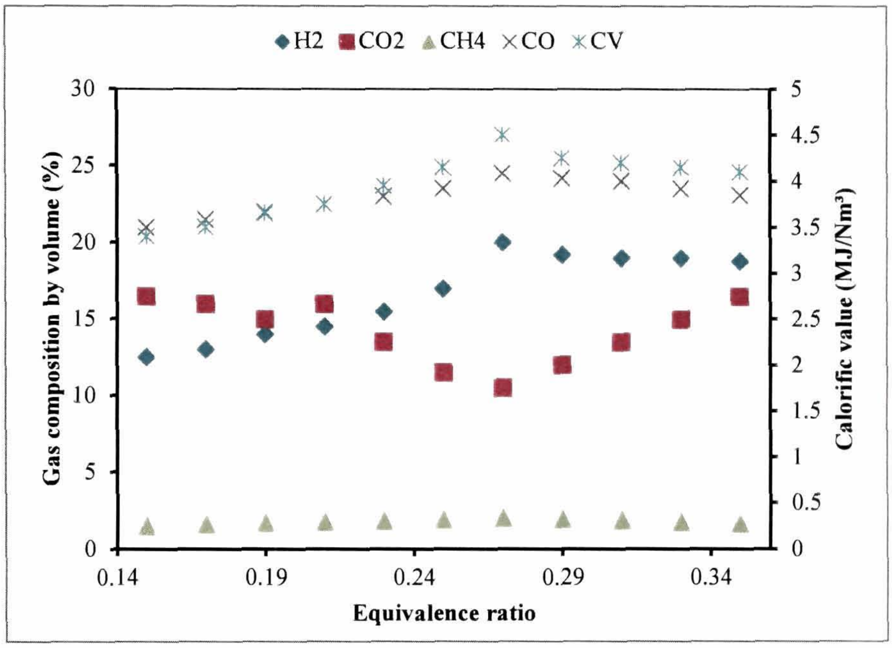

Fig. 3.10: Variation of gas composition and calorific value with air fuel equivalence ratio

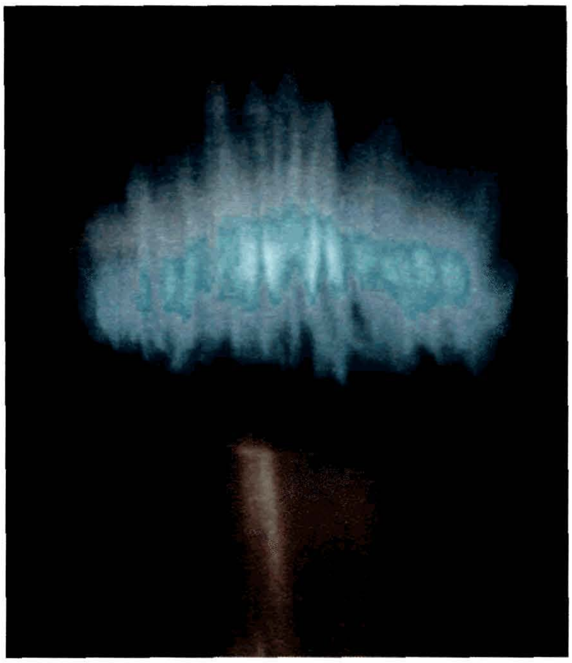

Fig. 3.11: Flame of producer gas combustion at equivalence ratio (ϕ =0.27)

3.5.8 Producer gas burner and conventional fixed bed coal fired burner

It has been observed from studies that there may be two distinct options for generation of tea drying process heat using surplus uprooted tea branches; viz. (1) Gasification (3.11) and (2) Direct combustion (Fig.3.12). Direct combustion of biomass in conventional inefficient coal fired furnace of some tea factories has socio-environment problem including greenhouse gas emission and accumulation of tars and shoots in nearby areas. Because the existing coal fired furnaces in the representative tea factories had been observed running with a very low overall efficiency. The reasons behind very low overall efficiency in existing coal fired air heating furnaces are inappropriate control of excess air for combustion, improper insulation in flue gas path, inconsistent quality of coal, inherently low flue gas to air heat exchanger heat transfer rate, frequent fouling of cast iron tube heat exchanger, and old conventional overall design of the system. Therefore, flue gases to air heat exchangers have very low effectiveness compared to shell and tube heat exchanger using steam as an intermediate heat transferring medium to heat tea drying air. Now, if these uprooted tea branches were utilized through efficient gasification technology, then lesser volume of greenhouse gases will be emitted compared to inefficient fixed bed coal combustion furnace cum air heater system. This will contribute to a substantial saving of scared fossil fuels such as coal or natural gas by application of renewable energy for tea drying and greenhouse gas emission balance, etc.

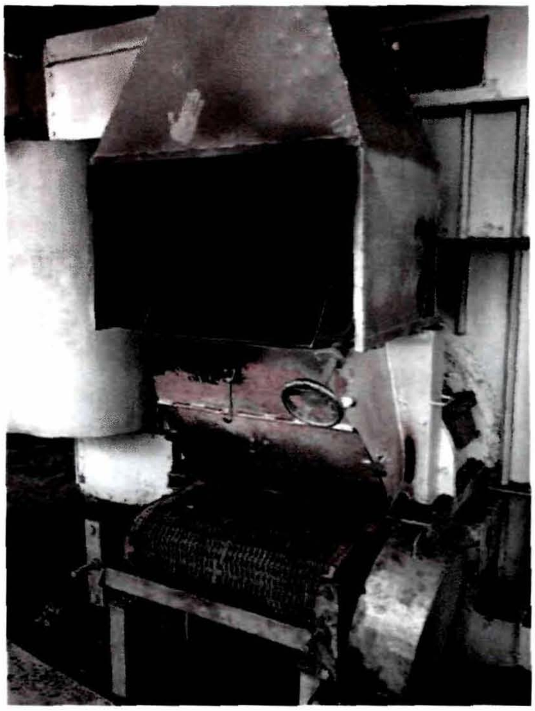

Fig. 3.12: A conventional inefficient fixed bed coal fire furnace for tea drying

3.5.9 Exhaust flue gas emission of producer gas fired burner

Producer gas fired tea dryer burner and conventional ID and FD coal fired tea dryer furnace have been presented in Fig.3.11 and Fig.3.12. The average temperature of flue gas in the combustion chamber of producer gas burner was 375 °C, at air fuel equivalence ratio (Φ =1.1). The average value of carbon monoxide was 8.5 ppm, carbon dioxide was 15.54% and NO_x emission was 150 ppm. The carbon monoxide emission was within acceptable level as per ASHRAE standard [223]. The NO_x emission in the flue gas was higher probably because presence of fuel bound nitrogen in the woody feedstock.

3.5.10 Maintenance of gas producer system

Various field studies and literature surveys revealed that normally after certain hours of operations, the gasifier system may give rise to certain operational problems. They are excessive pressure drop across the gasifier, less porosity of reduction bed, clogging of gas cleaning system, removal of excessive charcoal from the ash pit, bridging of V throat inside gasifier, congestion of scrubber pump nozzle, etc. It may be noted that regular health checking and appropriate preventive maintenance of gasifier as per operational manual is the healthiest practices. Hopper feed door rubber seal may be checked after every 150 hours. Similarly charcoal bed reconditioning should be done every after 400 h operations and checking for crack at cone may be maintained after elapse of 400 h as per manufacturers specifications [210].

It has been observed that all ten biomass samples may be considered for gasification studies in downdraft gasifier because their elemental compositions are similar and variation in calorific values do not differ much. They much have identically dried for gasification. Regarding gasifier performance with *Camellia sinensis* as feed stock, the maximum calorific value was (4.5 MJ m^{-3}) around air fuel gasification equivalence ratio (0.27). In the next chapter, we will discuss tea drying modelling and experimentation with three mixed biomass samples (*Camellia sinensis, Bambusa tulda, Psidium guajava*) fuelled gasifier. The producer gas thus generated will be used for tea drying experiment by its combustion product mixed with air for maintaining appropriate black tea drying temperature. These samples have been considered for further gasification experimentation based on their calorific value, carbon, hydrogen content, local availability and cost compared to the cost of coal in present market. However, cost of cultivation of biomass is not considered and that is a limitation of the present studies.

Thin layer tea drying experimentation with biomass fuelled producer gas

In the previous Chapter, we had discussed the details procedure of selection and characterization of biomass as prospective fuel for tea processing through gasification. We found that fuel properties of these three biomass samples (*Camellia sinensis, Psidium guajava,* and *Bambusa tulda*) were almost identical. It was observed that gasifier performed satisfactorily with uprooted tea shrubs (*Camellia sinensis*) as gasification feedstock. The maximum calorific value of producer gas thus generated from *Camellia sinensis* was 4.5 MJ $m,^{-3}$ at air-fuel equivalence ratio of 0.27. However, availability of *Camellia sinensis* sample is not sufficient for large-scale gasification and other renewables are not efficient. Therefore, a mixture of these three biomass samples was considered for further experimentation. A series of experiments were conducted with these biomass samples in an experimental downdraft biomass gasifier unit. Clean producer gas available from the output of the downdraft gasifier system was intended to use as a fuel for tea drying. In this process, we felt necessity of an appropriate gas burner to conduct our experiments with producer gas. Therefore, an improved burner (air fuel mixing chamber and gas nozzle) was developed through a systematic design for producer gas operation. The burner was used to control air fuel equivalence ratio appropriately for combustion of producer gas. This burner was used to conduct thin layer tea drying experiment. Further, experimental data of thin layer tea drying were used to fit and to identify best-fitted tea drying model. The details of the procedure and findings are presented below.

4.1 Producer gas fired burner

Development and performance testing of different gas burners such as liquefied petroleum gas, biogas, natural gas, producer gas, etc., are available in literatures [224-227]. The present work considered redesigning and development of air fuel mixing chamber of a commercially available gas burner. The redesigning and development of air fuel mixing chamber was performed to control producer gas and airflow appropriately to get best thermal efficiency of the gas burner.

As discussed in the previous Chapter, Producer gas generated from a 30 kW (maximum thermal output) woody biomass gasifier was used to test the burner as well as to conduct drying experiments. The burner heating capacity was 05 $kW_{thermal}$. Combustion air first entered perpendicularly into an annulus formed by outer diameter of nozzle and its housing (Fig. 4.1a-4.1c). The flows of air then become concurrent with producer gas flow direction up to entry of the mixing length of the burner. Both producer gas and airflows could be controlled for maintaining appropriate air and producer gas mixing ratio for combustion. The producer gas flow could be controlled by changing the opening of suction blower flap valve (connected to the gasifier). The combustion airflow for improved producer gas burner could be controlled with a variable speed blower and a rotameter was connected in series with the gas burner. The velocity of producer gas coming out from the nozzle was much higher than combustion air velocity (natural draft) inside the annulus and entry point of mixing chamber. This velocity difference between producer gas and air in mixing zone created swirls. A porous bluff body (Fig.4.1b) was used at the top of the burner housing for flame stabilization. The pressure difference between producer gas stream and air expected to enhance swirl mixing and combustion intensity, which would cause burner to operate in stable regime. As a result, this reduced the flame length without causing flame blowout. The relationship between length of the orifice and its diameter before the mixing tube is given by (Eq.4.1) [225].

$$\frac{l}{d} = 0.58 \qquad (4.1)$$

The angle of approach (45°) and coefficient of discharge (0.81) were selected. Considering a gas nozzle with minimum diameter (5 mm) the nozzle (orifice) length was estimated as ($l \approx 3$ mm). Length of the mixing tube and its diameter was selected as (L = 10D) [225]. The different dimensions of the burner have been presented in Fig.4.1a.

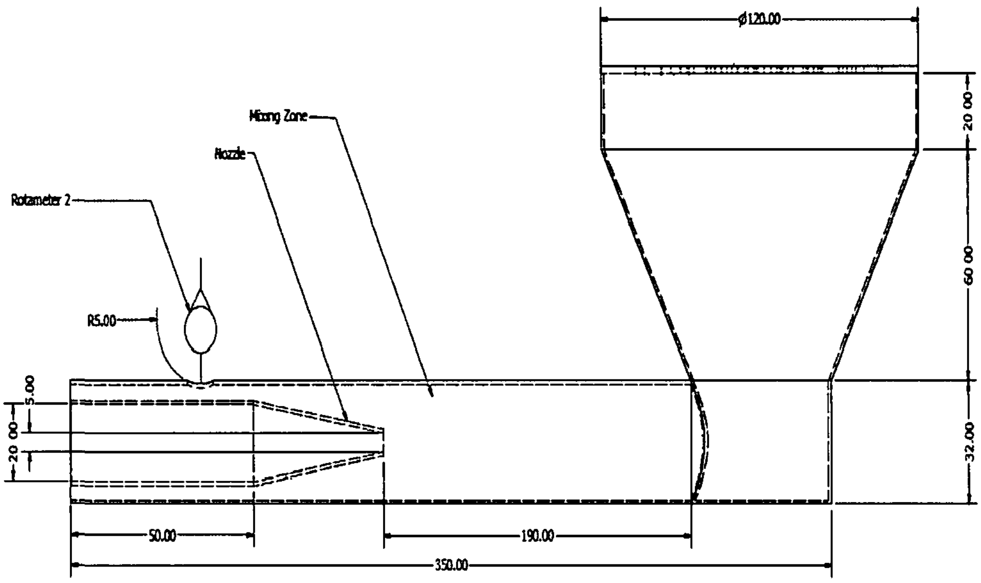

Fig. 4.1a Producer gas burner front view

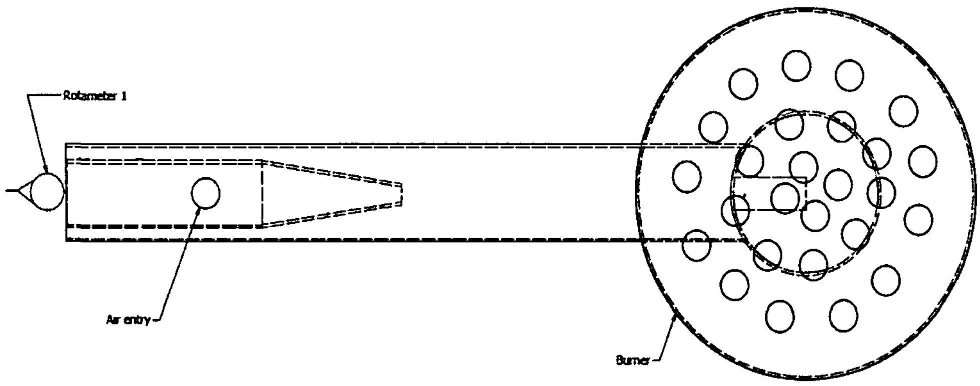

Fig.4.1b Top view of producer gas burner

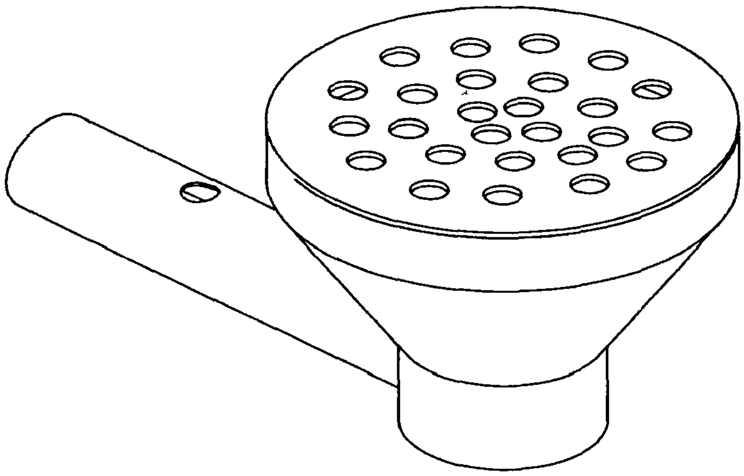

Fig.4.1c Isometric view of producer gas burner

4.2 Tea drying experiments with producer gas

Fresh macerated tea was collected inside airtight containers just after fermentation process from a tea factory nearby Tezpur University. Common name of fermented CTC tea undergoing drying is *dhool*. The fermented tea was refrigerated inside an airtight container for preservation. In normal practice of black tea processing, *dhool* is directly taken for drying. Preservation of the fermented tea samples was done considering the experimental convenience. This fermented tea was used for series of drying experiments.

4.2.1 Drying equipment and experimental setup

The tea drying experiments were conducted at Department of Energy, Tezpur University, India. The tea drying set up was consisted of the assemblies/subassemblies/equipment and instruments as discussed in Chapter 3. The (Table 4.1) gives the additional equipment and instruments required for tea drying experiment with technical specifications. The details experimental set up for WBG-10 woody biomass gasifer system for tea drying was presented in Fig.3.1 (Chapter: 3). A portion of producer gas thus obtained from this 30 $kW_{thermal}$ (Maximum output) downdraft gasifier was taken into the gas burner assembled in the tray type drying chamber. The details of the tray dryer have been presented in Appendix: A5.

Table 4.1 - Experimental set up and details of the instrumentations

Sl. No.	Items	Technical specification	Application
1.	Hot wire anemometer	Range: (0.00 – 20) ms^{-1}, Accuracy: ± 1% FSD, TESTO-425, Germany.	To measure drying medium velocity above the bed plate
2.	Tray dryer	10 kg h^{-1} Size: (0.620 × 0.533 × 0.38) m^3	To dry fermented tea
3.	Digital weighing balance	KERN: Read out 0.01 g, Range:1210 g, linearity ± 0.03	To measure moisture loss of fermented tea.

4.2.2 Experimental procedure and estimation of drying parameters from drying curve

As mentioned earlier, the gasification system was operated using a mixture of three biomass samples. The gas obtained was directed to producer gas burner of tray type dryer. The experiment was conducted one hour for attaining a near steady condition. Constant gas flow rate and gas quality (Calorific value) indicated the gasifier a near steady state realization. On stabilization of tea dryer, the tea samples were fed into the bedplates in thin layers. Experiments were performed to observe the effect of process variables such as drying medium (producer gas combustion product and air) temperature and velocity on thin layer drying kinetics of black tea. The change in absolute humidity of tea drying medium was expected to be insignificant. Therefore, it was considered constant over time of experimentation. Series of experiments were designed to cover these process variables effectively. The drying medium temperature was varied from (80-110) °C in steps of 10°C by controlling producer gas flow rate into the burner. The producer gas flow control was performed by changing the blower (suction blower of gasifier) flap valve position. For a particular opening of blower flap valve and corresponding dryer variable speed suction blower speed, specific drying medium average velocity at the bedplate was measured with hot wire anemometer before actual tea drying experiments. Three different drying medium velocities (0.50, 0.65, and 0.75) m s^{-1} were measured just above the bedplate had been considered for conducting tea dying experiments at a specific temperature (100 °C). Similarly, temperatures of drying medium were maintained at (80, 90, 100, and 110) °C with associated velocity of drying medium 0.65 m s^{-1}. The temperature and velocity of drying medium was measured by (PT-100) thermocouples with display units and a hotwire anemometer. Since the dryer was a cross flow type, therefore hot air was flowing perpendicular to the bedplate. Water loss from drying tea was determined by sampling periodically with a sample tray and an electronic balance. The samples weighing process performed within 15 seconds to minimize experimental errors. It was considered that no disturbance was made for drying process by sampling method adopted. During initial runs, weight was recorded every two minutes then after every three minutes until the end of the drying process. Insignificant change in weight of tea sample over time indicated completion of drying process. The initial and final moisture contents of the samples were measured using the oven method at 105 °C until fixed weight was obtained for verification of experimental tea drying data.

4.2.3 Experimental drying curve and mathematical modelling

The back tea drying curves (moisture ratio versus time) had been plotted from range of values of a given variable (temperature and drying medium velocity above bedplate) keeping the other variable constant.

Ficks's second law applies to describe moisture diffusion in the tea particles. The Eq. (4.2) gives general series solution of Fick's second law in the spherical coordinate. Assuming tea particle is spherical in geometry, the relationship of moisture ratio, diffusivity and drying time can be written as:

$$MR = \frac{M-M_e}{M_0-M_e} = \frac{6}{\pi^2}\sum_{n=1}^{n=\infty}\frac{1}{n^2}exp\left[\frac{-\pi^2 D_{eff} n^2}{R^2}\right]t \qquad (4.2)$$

where MR is moisture ratio of tea samples undergoing drying, D_{eff} is effective diffusivity (m^2 s^{-1}) and R is average radius (m) of the tea particle. For long drying period, the above equation simplifies only to first term of the series (Henderson and Pabis model). Thus, Eq. (4.2) can be simplified as below.

$$ln\, MR = ln\frac{6}{\pi^2} - \left[\frac{\pi^2 D_{eff}}{R^2}\right]t \qquad (4.3)$$

The Eq. (4.3) is linear in logarithmic scale. Experimental results could be used to determine the slope of the plot and hence the effective diffusivity.

Thus, Eq. (4.4) gives the effective moisture diffusivity estimated by using method of slope (coefficient [*k*] in Handerson and Pabis model).

$$\lfloor k \rfloor = \left[\frac{\pi^2 D_{eff}}{R^2}\right] \qquad (4.4)$$

The Eq. (4.5) describes the relationship between effective diffusivity (D_{eff}) and activation energy (E_a):

$$D_{eff} = D_o\, exp\left[-\frac{E_a}{RT_a}\right] \qquad (4.5)$$

where, Do is the diffusivity constant and R is the universal gas constant (8.314×10^{-3} kJ mol^{-1} K). A plot between ($ln\ D_{eff}$) and ($\frac{1}{T}$) shows a linear relationship similar to the Arrhenius type characteristics. The experimental data concerning the tea drying experiment using producer gas fired flue gas mixed with air was used to estimate effective diffusivity (D_{eff}) and activation energy (E_a).

4.2.4 Modelling and simulation

To examine the feasibility of application of drying medium (producer gas fired combustion products mixed with air), an attempt was made to observe black tea drying kinetics. Five drying models (Henderson and Pabis model, Lewis model, Page model, Modified Page model, Two term model) were used to fit the drying kinetics of fermented tea samples [112, 114-117, 229]. The non-linear regression analysis was performed using SPSS commercial software to fit the drying data with the available mathematical models. The coefficient of determination (R^2) is one of the principal criteria to estimate fit quality of the model. Its value ranges from (0 to 1) for worst, best fit situation, and it is given by Eq. (4.6):

$$R^2 = 1 - \frac{Residual\ sum\ square}{Total\ sum\ square} \tag{4.6}$$

$$\chi^2 = \frac{\sum_{i=1}^{N}(\mathrm{MR_{ei}} - \mathrm{MR_{pi}})2}{\mathrm{N-z}} \tag{4.7}$$

$$RMSE = [\frac{1}{\mathrm{N}}\sum_{i=1}^{N}(\mathrm{MR_{ei}} - \mathrm{MR_{pi}})^2]^{½} \tag{4.8}$$

where MR_{ei} and MR_{ep} are i^{th} experimental and predicted moisture ratio. Moreover, reduced chi-square (χ^2) and root mean square error ($RMSE$) were used to determine the suitability of fit. The reduced chi-square (χ^2) and $RMSE$ were calculated by using above relationships (Eq. (4.7) and Eq. (4.8)).

Higher the value of R^2, lower χ^2, and *RMSE* values, better are the integrity of fit [218]. The fit of the tested mathematical models to the experimental data were examined by taking the final moisture content approximately equal to 3% (w.b.) for all experiments.

4.2.5 Producer gas fired burner and its thermal efficiency

Average thermal efficiency of the burner is given by Eq. (4.9) and this was estimated from standard water boiling test [226].

$$\eta = \frac{[(m_1 \times C_{p1} + m_2 C_{p2})\Delta T + m \times L]}{Q \times CV} \quad (4.9)$$

Where m_1, m_2, m are the mass of water and container and water evaporated (kg), C_{p1}, C_{p2} are specific heat of water and container, ΔT (°C) is rise in temperature of water; L is latent heat (2660 kJ kg^{-1}) of vaporization of water Q and CV are producer gas volume (Nm^3) and calorific value (MJ Nm^{-3}). Initially, water-boiling experiment was conducted with varying air-fuel ratio to estimate burner thermal efficiency. The results of this series of experiments were used to decide the best air-fuel (producer gas) equivalence ratio to conduct the tea drying experiments. Moreover, producer gas combustion airflow was also controlled to get appropriate air fuel equivalence ratio. During the experiments, the product of producer gas combustion was mixed with fresh air to lower its temperature from (80 – 110) °C suitable for tea drying.

4.2.6 Specific energy consumption

Specific energy consumption in dryer depends on drying medium temperature as well drying medium velocity in the bed. Normally increased retention time of unsaturated hot air and corresponding elevated temperature of drying improve specific energy consumption. Specific energy consumption (J kg^{-1} of water removed) in producer gas fired dryer was computed by using Eq. (4.10) as suggested by Zhang [226]:

$$SFC = \frac{Q(C_{pa} + C_{pv}h_a)\times(t_{hot}-t_{amb})\times t}{60V_h m_v} \qquad (4.10)$$

where, Q = hot drying medium discharge (m^3 h^{-1}) that was measured from volume flow rate of producer gas and at a selected equivalence ratio and corresponding combustion air flow rate, C_{pa} = specific heat capacity of air (J kg^{-1} $°C^{-1}$), C_{pv} = specific heat capacity of vapour (J kg^{-1} $°C^{-1}$), [Both were taken from data book], t_{hot} = temperature of hot medium (°C), t_{amb} = temperature of ambient air (°C), t = Drying time (min), V_h = specific drying medium volume (m^3 kg^{-1}), that was computed for experimental data, and m_v = mass of water removed (kg) that was measured from initial weight of fermented tea and final weight of tea dried tea.

4.3 Results and discussions

4.3.1 Selection of burner operating condition

Performance analysis of producer gas fired premixed burner shows that fuel air equivalence ratio affects burner thermal efficiency. The appearance of flames with various equivalence ratios were recorded for examining the effect of equivalence ratio on quality of flame. The different producer gas flames obtained through this gas burner at equivalence ratios (0.7, 1, 1.1, and 1.5) have been presented in (Figs.4.1d to Fig.4.1g). It was clear that for air fuel equivalence ratio (ϕ =1), a short intense blue flame was obtained. At this point, thermal efficiency of producer gas burner was also recorded as maximum (57%). This might be due to complete combustion of producer gas in the premixed burner. In either side of this equivalence ratio, the burner efficiency decreases due inappropriate air fuel ratio (Fig.4.2) and diffusion flame dominates the premixed flame in these regions.

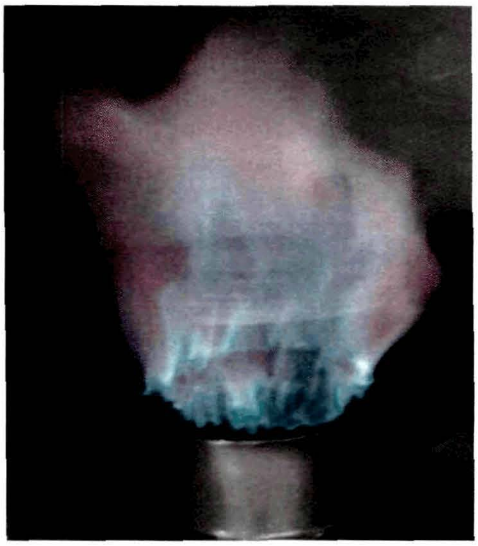

Fig.4.1d Producer gas flame ($\phi = 0.7$)

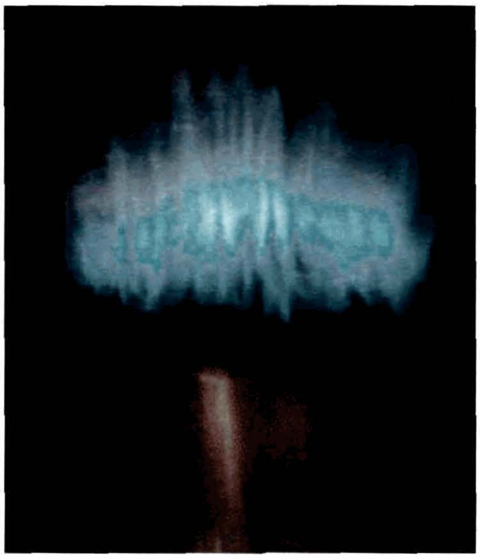

Fig.4.1e Producer gas flame ($\phi = 1.0$)

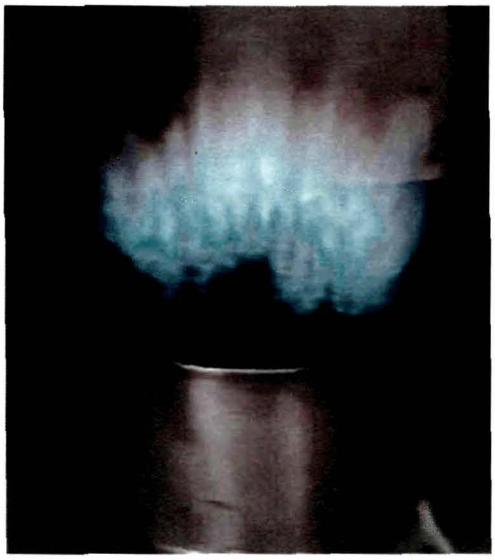

Fig.4.1f Producer gas flame (ϕ = 1.1)

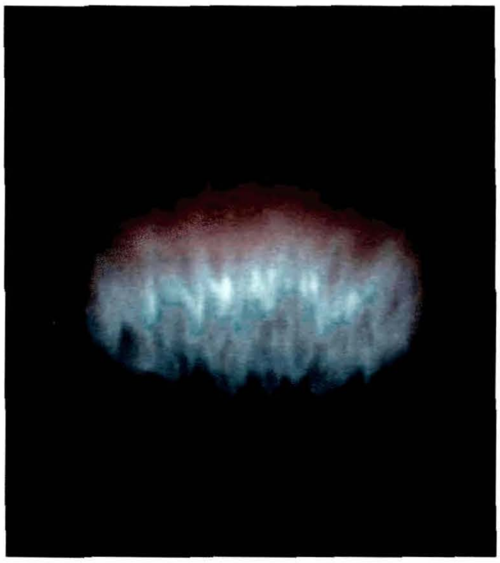

Fig.4.1g Producer gas flame (ϕ = 1.5)

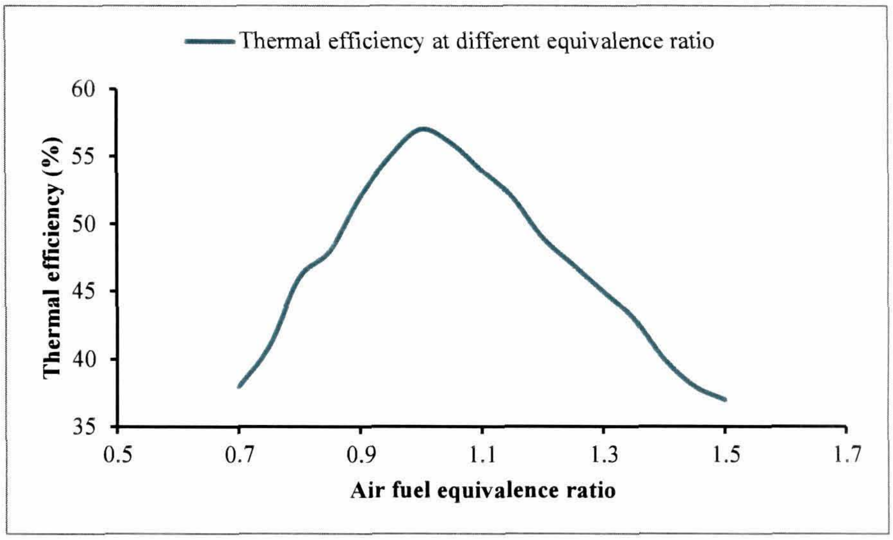

Fig.4.2 Variation of thermal efficiency with air fuel equivalence ratio

4.3.2 Tea drying kinetics

The experimental results of black tea dying kinetics data have been presented in (Figs.4.3- Fig.4.4) with mixture of producer gas combustion product and air as drying medium. Percentage wet basis moisture content were transformed into a dimensionless parameter called moisture ratio and plotted against the tea drying time as per standard practice. The drying curves [$MR = f(t)$] of black tea dried in a producer gas fired dryer for different drying medium temperatures, and velocities have been discussed below.

It is clear from the drying kinetics characteristics that with increase in drying medium temperatures (80, 90, 100, and 110) °C, at constant drying medium velocity (0.65 m s^{-1}), there was a reduction in tea drying time. Therefore, quicker drying at higher temperature has been characteristics of drying process. About 60 % drying time may be reduced while drying at 110 °C instead of 80 °C. However, quality of made tea is better for drying at lower temperature. Increased drying medium temperature gave higher slope of drying curve than that a low drying medium temperature one (Fig.4.3).

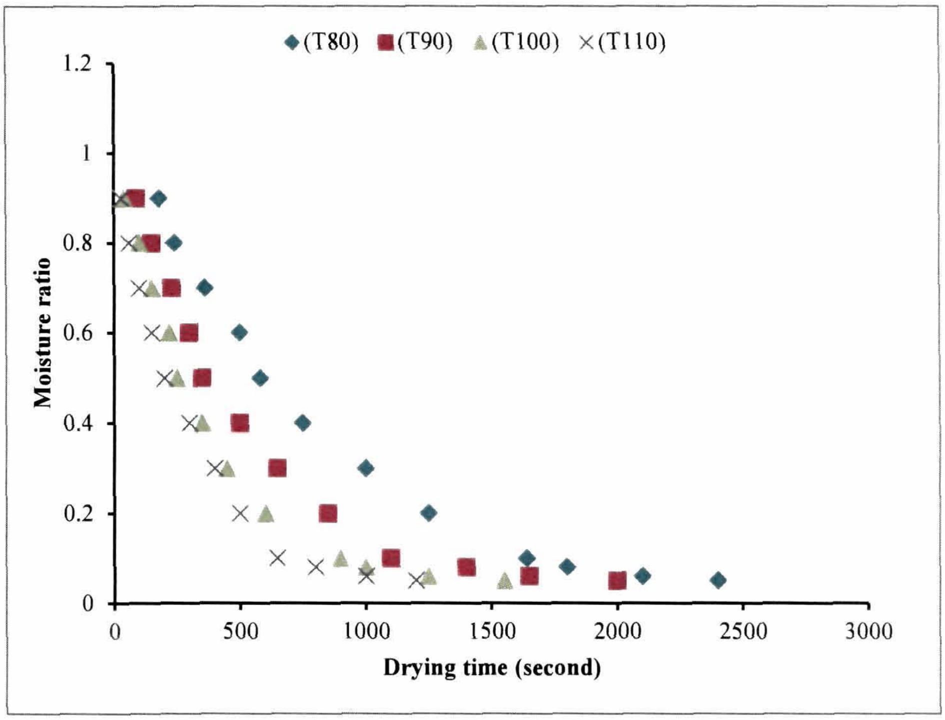

Fig.4.3 Variation of moisture ratio with drying time at different air temperatures.

Fig. 4.4 presents variation of moisture ratio with black tea drying time with variable drying medium (producer gas combustion products mixed with air) velocity (0.50, 0.65, 0.75) m s^{-1} just above bed plate and at constant temperature (100 °C). It is clear from this characteristics that increase in drying medium velocity at constant drying medium temperature also increases drying rate. However, below minimum fluidization velocity of drying medium, the increase in drying rate is not much prominent by increasing velocity compared to the drying medium temperature enhancement. Minimum fluidization velocity of tea particle undergoing drying varies from 0.95 to 1.1 m s^{-1} [231]. About 33% reduction in tea drying time is achievable for increase in tea drying medium velocity from (0.50-0.75) m s^{-1} at constant temperature of 100 °C.

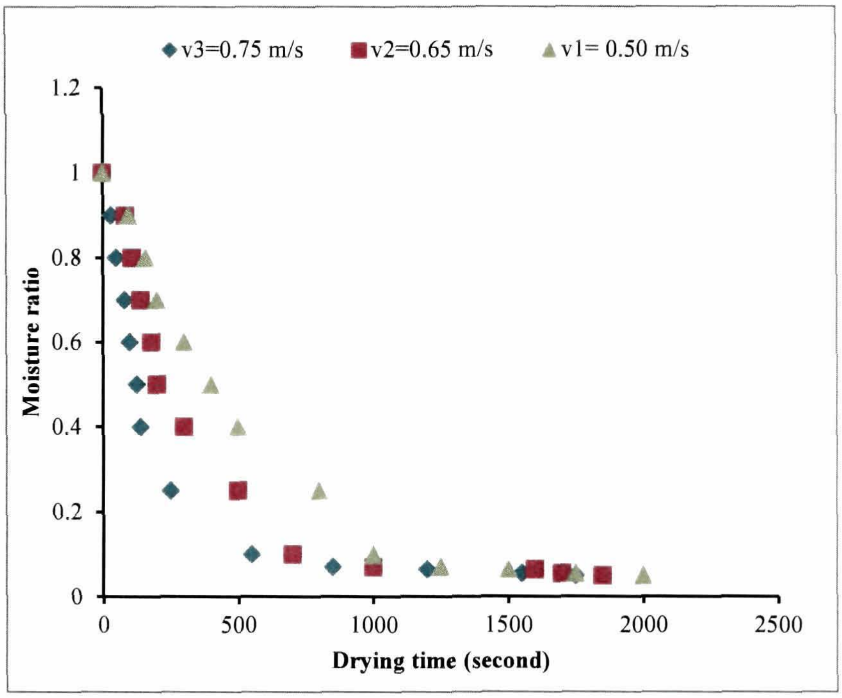

Fig.4.4 Variation of moisture ratio with drying time at different air velocities

4.3.3 Drying model

As discussed earlier, fitting of drying kinetics data into standard available drying Models have been a regular practice to ensure and to record the drying behaviour hygroscopic material with a set of operating conditions [93, 94, 97, 228, 229, 230, 231, and 232]. The black tea drying through thin layer drying model had been modelled earlier while using hot air as drying medium [229, 230, 231]. It has already been stated that, the feasibility of black tea drying with producer gas as a source of thermal energy has been the focus of the present investigation. With combustion of producer gas, and then mixing it with air, an appropriate temperature for black tea drying medium could be generated.

The experimental results enabled to record the drying behaviour of black tea and finally to fit the recorded data into the existing drying Models. The details of the all the drying Models tested are provided in Appendix: A2. Based on [the *RMSE*, coefficient of determination (R^2) and reduced chi-square ($\chi 2$)], the following two models are found fitted as best and second best for the present studies [Table 4.2]. It has been observed that the Henderson and Pabis, Page, Modified Page and Lewis models fetched R^2 greater than acceptable value (0.90) at all drying temperatures [228, 229]. The minimum values of *RMSE* (0.61×10^{-5}) and χ^2 (0.043×10^{-9}) were obtained for the Lewis model at 100 °C drying medium temperature. However, the Modified Page model yielded least average χ^2 (0.029×10^{-9}) values at 100 °C drying medium temperature. The coefficient of determination R^2 (0.969) and reduced chi-square χ^2 (0.029×10^{-9}) respectively were observed from experimental studies. Hatibaruah [230] observed that Midlli model conformed to black tea (Tea cultivars: T3E3) drying kinetics with hot air temperatures variation from (80 to 95) °C. Because air mixed with producer gas combustion product was used as drying medium at different range of drying temperature (80, 90, 100, and 110) °C for present study, therefore, the best fit might vary. Moreover, a heterogeneous tea cultivar was used for drying experiment in present case.

The experimental results revealed that tea drying in falling rate period was significantly important to reduce its moisture to the desired value. This indicated that diffusion was the prominent physical moisture transport mechanism in a tea particle undergoing drying with producer gas combustion product mixed with air as heating medium. Temple and Boxtel [231] also reported identical behaviour of black tea (African variety) drying with hot air from their experimental analysis.

Table 4.2 Statistical analysis of different thin layer models.

Model	Temp. (°C)	R^2	RMSE ($\times 10^{-5}$)	$\chi^2 (\times 10^{-9})$	$k(\times 10^{-4})$	n /A
Lewis model	80	0.956	1.25	0.185	12.76	
	90	0.967	0.66	0.052	18.29	
	100	0.968	0.61	0.043	25.91	
	110	0.970	0.35	0.023	33.91	
Modified Page model	80	0.956	0.84	0.083	15.95	0.8
	90	0.959	0.64	0.048	21.52	0.85
	100	0.967	0.49	0.029	25.91	1
	110	0.968	0.43	0.022	30.81	1.1

4.3.4 Significance of drying rate-controlling variables on drying behaviour of black tea

Different drying rate-controlling variables such as drying medium temperatures, and velocities were considered in the Arrhenius model. Arrhenius activation energy for the physical diffusion refers to temperature dependence of reaction rate. This Arrhenius equation may be used to model the temperature variation of diffusion coefficient. Therefore, it is a relationship between water diffusion rate and energy required for diffusion of water from core of the tea particle. The moisture ratio versus drying time characteristics presents for the variable hot drying medium temperatures and at constant velocity (0.65 m s^{-1}). The influence of temperature on black tea drying curve is evident from the Fig.4.3 above. It shows that an increase in drying medium temperature enhances the drying rate exponentially. Similarly, the Fig.4.4 shows effect of hot drying medium velocity on CTC tea drying rate over the bed at constant air temperature (100°C). With an increase in drying medium velocity (below fluidization) at constant temperature, there is an augmentation of drying rate so long as surface moisture prevails. This is probably because effective contact between hot drying medium and tea particles in fixed bed. As a result, enhancement of heat and mass transfer takes place. The Fig.4.5 shows the logarithmic variation of moisture ratio with drying time and these curves are useful for computation of the drying rate constant *(k)* at different drying medium temperature (80, 90, 100, 110) °C and constant velocity (0.65 m s^{-1}) . This drying constant (*k*) was derived from linear regression of *ln (MR)* and drying time.

The Fig. 4.6 shows variation of drying constant (*k*) with the hot air temperature at different air velocities. The values of drying constant *(k)* were derived from black tea drying kinetics data at different drying medium velocity and temperatures. It is clear from Fig. 4.6 that there is an increment of *k* (=0.0005) as velocity changes from 0.5 m s^{-1} to 0.75 m s^{-1}. The corresponding augmentation of the drying constant *k* is (0.0017) when drying medium temperature changes from (80 to 110) °C. Therefore, during diffusion dominated drying process, change in drying medium velocity below fluidization velocity does not have much effect on rate of drying compared to temperature rise of drying medium. Therefore, the rate of increase in drying constant (*k*) was more prominent with increase in drying medium temperature (at constant drying medium velocity) than that of velocity (at constant drying medium temperature) below fluidization. It is clear that with an increase in hot air velocity there is almost a linear increment in drying rate constant (*k*) as shown Fig.4.6 below.

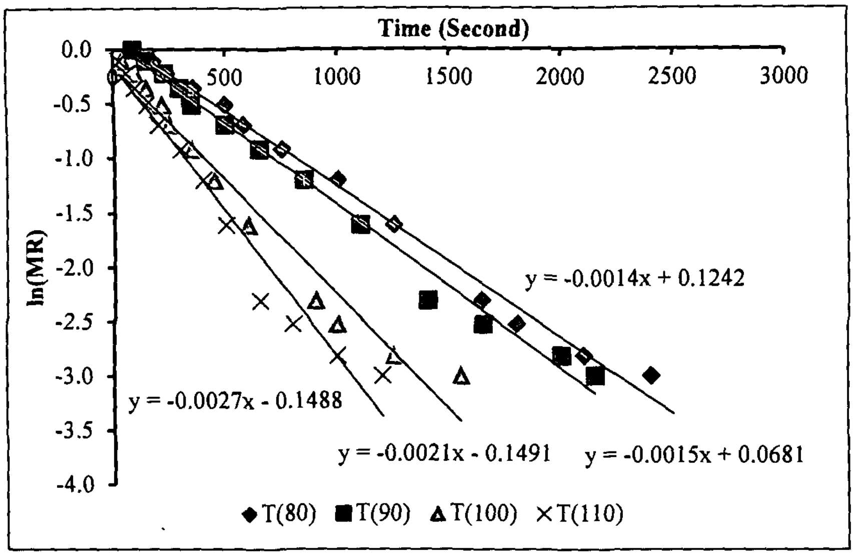

Fig.4.5 Experimental logarithmic moisture ratios at different drying times

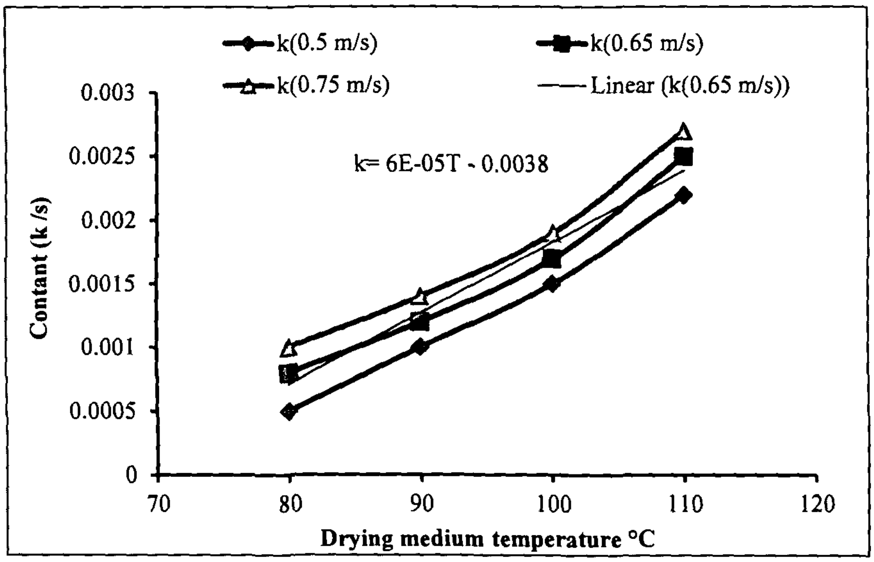

Fig.4.6 Variation of drying constant with temperature at different air velocities

4.3.5 Computation of effective diffusivity and activation energy

Drying of black tea mostly occurs during falling rate period and liquid diffusion plays a great role for process control. Therefore, Ficks's second law [Eq. (4.2)] applies to describe moisture diffusion in the tea particles. For the present case, the mean tea particle size is considered as 0.60 mm based on the results of sieve analysis. The effective diffusivity is calculated using the Eq. (4.4). The slope [*k*] was obtained from the linear regression of $ln\, MR$ against drying time (t) as in Fig. 4.5. The effective diffusivities of a tea particle varied from (3.644×10^{-11} to 7.287×10^{-11}) $m^2\, s^{-1}$ in the temperature range of (80-110) °C and at drying medium velocity 0.65 $m\, s^{-1}$ during producer gas combustion product mixed with air for black tea drying. The Arrhenius type relationship described the influence of temperature on effective diffusivity to obtain better agreement of predicted curve with experimental data [98, 73]. Crisp and Wood [103] opined that temperature was not a function of the radial position inside a grain with the normally experienced drying conditions. The diffusivity varies more with temperature than moisture content.

The diffusivity constant (D_o) and activation energy (E_a) were computed from the linear regression analysis of experimental data as ($0.746 \times 10^{-3}\, m^2\, s^{-1}$) and (52.104 $kJ\, mol^{-1}$), respectively. It is substantially lower than the activation energy (989 $kJ\, mol^{-1}$) of the garlic slice [184] and higher than the kiwi fruit (27 $kJ\, mol^{-1}$) as observed by Simal et al., [232]. Hati Baruah [230] computed effective diffusivity of thin layer CTC drying at air temperature of 80, 90 and 95 ◦ C, as 5.5162×10^{-9}, 7.1569×10^{-9} and $7.739\times10^{-9}\, m^2\, s^{-1}$.

The estimated value of activation energy of CTC tea is 24.88 $kJ\, mol^{-1}$ for hot air drying [232]. The lower activation energy compared to present study (52.104 $kJ\, mol^{-1}$) might be because of dissimilar fermented tea drying sample, drying medium and its temperature range used and drying medium velocity.

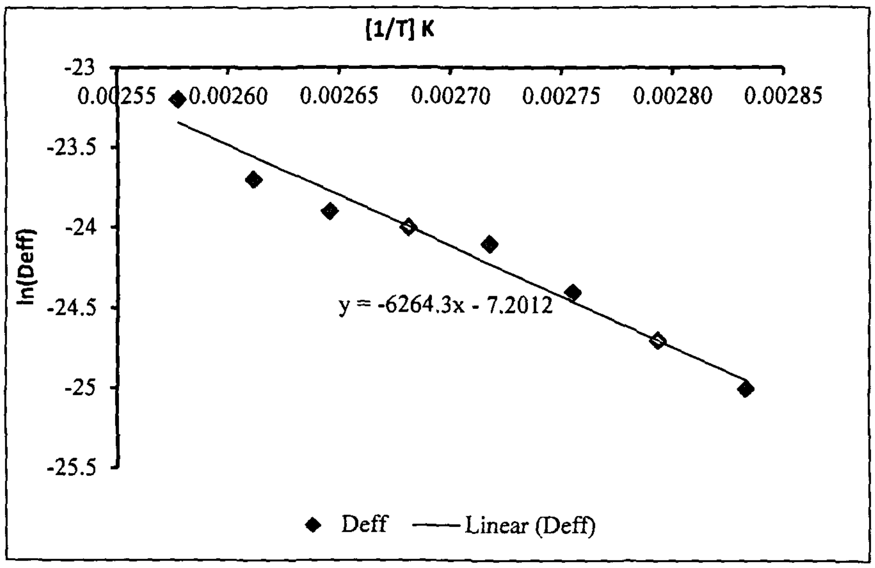

Fig.4.7 Arrhenius type relationship between logarithmic effective diffusivity and inverse temperature in Kelvin

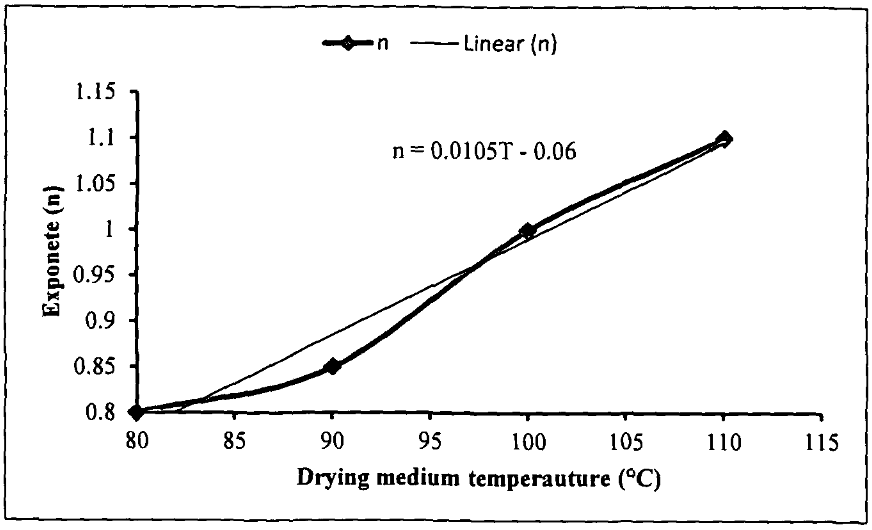

Fig.4.8 Variation of (n) with drying temperature at constant velocity (0.65) m s^{-1}

4.3.6 Variation of (n) with drying medium temperature at constant velocity

Fig.4.8 shows variation of drying exponent (n) with drying medium temperature at constant velocity 0.65 m s^{-1}. It is clear that with increase in temperature of drying medium, (n) increases almost linearly from (0.8 to 1.1). This was obtained from modelling of black tea drying kinetics experimental data.

4.3.7 Measurements of different temperatures

Temperature of scrubber water, producer gas, combustion products and mixed air temperature in mixing chamber of dryer, out let temperature of dryer had been measured during experiment. They are presented in Table 4.3 and dryer temperatures are useful for computation it efficiency in Chapter: 5.

Table 4.3 Average temperatures at different points in experimental setup

Gas flow rate (m^3 h^{-1})	Ambient (°C)	Gas outlet (°C)	Scrubber outlet (°C)	Dryer inlet (°C)	Mixing chamber (°C)	Average tray (°C)	Dryer outlet (°C)
16	35	380	42	45	100	95	67
18	35	390	44	45	105	95	67
20	35	405	45	48	110	100	70
22	35	425	48	52	120	105	70
24	35	450	50	55	130	110	70

4.3.8 Energy consumption for black tea manufacturing with producer gas as a source of thermal energy

As discussed earlier, the rate of producer gas consumption data was also recorded during the drying experiment. It was also mentioned earlier that experiments were conducted with varying temperature and flow rate of drying medium. Accordingly, it is expected that rate of drying and corresponding energy consumption would vary. The specific energy consumption has been estimated as 25.50 MJ kg^{-1} of the made tea (3 % w.b.) at drying medium temperature 100 °C and velocity 0.65 ms^{-1}. The corresponding specific energy consumption of this producer gas fired dryer was approximately 10.20 MJ kg^{-1} of water removed. The specific energy consumption per kg of made tea (25.50 MJ kg^{-1}) is smaller than a conventional coal-fired (43.72 MJ kg^{-1}) air heater dryer and a natural gas fired (27.49 MJ kg^{-1}) tea dryer as reported earlier [13]. However, the full capacity of dryer was not utilized and therefore specific energy consumption estimated from experimental result was somewhat higher.

Performance of producer gas fired tea drying system may be affected by different factors such as appropriate sized (length 35 ± 5, diameter 25 ± 5) mm of woody biomass feedstock, excessive moisture content (if > 20%) of feedstock. Moreover, bluish flame in the gas burner is required that is an indication of appropriate air fuel ratio and quality of producer gas produced. The temperature of producer gas combustion products mixed with air should be around 100 °C for best overall efficiency and quality of made tea. The velocity of drying medium should be well below 1 m s^{-1} to control drying process appropriately in fixed bed dryer.

It has been observed from this study that biomass gasification technology may partially substitute conventional coal fired furnace for tea drying. However, biomass availability in large scale for gasification and its conservation is another issue. Certain amount of biomass conservation would be achieved if we get another renewable energy technology. In the next Chapter, investigation for another renewable energy resource, i.e. solar air heating technology will be presented.

In Chapter: 3, we have discussed characterization (proximate, analysis, ultimate analysis and higher heating value) of ten locally available biomass samples and performance testing of a WBG - 10 downdraft biomass gasifier. It had been observed that *Dalbargia sissoo* has highest fixed carbon (15.60%). *Bambusa tulda* has second highest fixed carbon (15.20 %) and *Ficus lepidosa* had minimum fixed carbon (12.20 %). Ash value of *Dalbargia sissoo* was minimum 4.4% and *Ficus lepidosa* was maximum 5.8% respectively. It was found that *Psidium guajava* had the highest calorific value (18.403 MJ kg^{-1}) and *Ficus lepidosa* has the lowest (15.952 MJ kg^{-1}) among the tested samples. Calorific value of *Bambusa tulda* was (18.401 MJ kg^{-1}) and *Camellia sinensis* was (18.400 MJ kg^{-1}). The gasifier performed satisfactorily with uprooted tea shrub (*Camellia sinensis*) and producer gas calorific value was (4.5 MJ m^{-3}) at air fuel equivalence ratio for gasification (0.27) with uprooted tea shrubs as a gasification feedstock.

In Chapter: 4 we had considered black tea drying experiment and drying kinetics modelling with producer gas generated from a mixture of *Camellia sinensis, Bambusa tulda and Psidium guajava* as gasification feed stock in equal proportion. An improved producer gas burner was redesigned for appropriate mixing of producer gas and air for combustion. At air fuel equivalence ratio (A: F = 1:1), the producer gas burner had best thermal efficiency (57%) as obtained by water boiling test. Tea drying modelling results revealed that Modified Page model was the best fit for local variety black tea while using producer gas combustion product mixed with air as a drying medium. The specific energy consumption per kilogram of made was obtained as 25.50 MJ kg^{-1} of made tea.

In the Chapter: 5, we will discuss on local solar thermal energy resources, efficient conversion technology (Solar air heater) and its performance studies. Based on previous black tea drying experimental data with producer gas, an analysis will be made for black tea drying possible hybridization of solar air heater with producer gas energy. Therefore, the details of the analytical procedure for hybridization will be discussed in this chapter. Further, the economics of renewable thermal energy application in tea drying is also analyzed through a standard procedure.

5.1 Analytical procedure of estimating component shares of solar biomass hybrid renewable energy for black tea drying

The hybrid black tea drying was considered by mixing hot air from solar air heater with combustion products of producer gas. The conceptual layout of solar biomass hybrid thermal energy application for black tea drying has been presented in Fig.5.1:

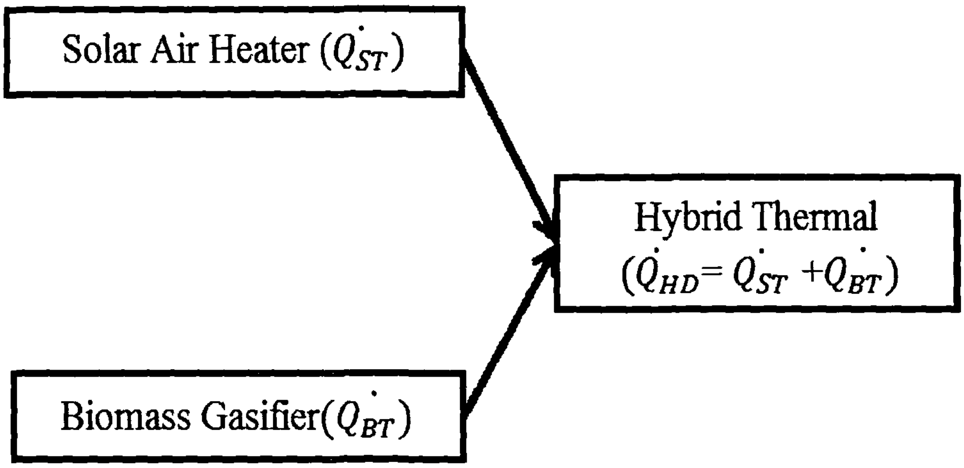

Fig.5.1 Solar-biomass energy hybridization scheme for tea drying

where, $\dot{Q}_{ST}$ is thermal energy flow rate from solar air heater, $\dot{Q}_{BT}$ is biomass thermal energy flow rate from biomass gasifier and $\dot{Q}_{HD}$ is hybrid drying energy flow rate from the combined system for black tea drying. Now thermal energy available from biomass through gasification and solar air heater is estimated from Eq. (5.1) and Eq. (5.2) below:

$$\dot{Q}_{BT} = \dot{m}_{bm} \times \eta_{gasifiction} \times CV_{bm} \times \eta_{combustion} \quad (5.1)$$

$$\dot{Q}_{ST} = I \times A \times \eta_{thermo\_hydraulic} \quad (5.2)$$

where, $\dot{m}_{bm}$ is biomass consumption rate (kg h^{-1}) of gasifier, $\eta_{gasifiction}$ is gasification efficiency (65%) of biomass gasifier, CV_{bm} is calorific value (18.40) MJ kg^{-1}) of biomass sample, $\eta_{combustion}$ is producer gas burner combustion efficiency (90%), I is average solar radiation (W m^{-2}), A is area (m^2) of solar air heater, and $\eta_{thermo\_hydraulic}$ is thermo-hydraulic efficiency (74%) of solar air heater. It may be mentioned that producer gas combustion product and air mixture were used for tea drying and therefor no heat exchanger was used. Hence, combustion efficiency was considered about 90% for producer gas burner. The total thermal energy for hybrid mode black tea drying is given by Eq. (5.3).

$$\dot{Q}_{HD} = \dot{Q}_{ST} + \dot{Q}_{BT} \tag{5.3}$$

5.2 Computation of drying efficiency in individual and hybrid modes

For low humidity and low temperature convective drying, energy efficiency of dryer may be approximated with its thermal efficiency that is given by Eq. (5.4).

$$\eta_{thermal} = \frac{T_1 - T_{wb}}{T_1 - T_{amb}} \tag{5.4}$$

Where T_1 is inlet air temperature to the dryer, T_{wb} is wet bulb temperature corresponding to dryer outlet air condition, and T_{amb} is ambient air temperature.

The system efficiency for producer gas fired solar assisted hybrid dryer is given by Eq. (5.5).

$$\eta_s = \frac{WL}{(IA\eta_{ar} + P_f + V_{pg} \times LCV)} \tag{5.5}$$

Where V_{pg} (Nm^3 h^{-1}) is volume flow rate of producer gas combusted and LCV is lower calorific value (kJ Nm^{-3}) of producer gas. P_f is dryer suction blower energy consumption (kWh), I is solar radiation (kW m^{-2}), A is area (m^2) of air heater, η_{ah} is thermal efficiency of improved air heater, W is the mass of water removed per unit time and L is theoretical amount of heat (2700 kJ kg^{-1}) required for evaporation of one kg of bound moisture. This will give the additional energy input with appropriate hybridization ratio [234].

5.3. Assessment of locally available solar energy resources

Automatic Weather Station (AWS) was used to monitoring and record climatic data at 30 days interval. AWS provided data concerning (i) wind speed (m s^{-1}), (ii) solar radiation (W m^{-2}), (iii) air temperature (°C), (iv) dew point (°C), and (v) humidity. It may be noted that AWS could provide data for the parameters at any time interval as per requirement of the experiments.

Therefore, five years (2008 to 2012) solar radiation data for Sonitpur district (Assam: India) was taken from AWS located at Tezpur University campus (latitude 26° 42′ 03″ N and longitude 92° 49′ 49″ E). The solar radiation data were available in Wm^{-2} at hourly basis. The daily average data for a particular day were calculated and then converted to $kWm^{-2}day^{-1}$. From the daily average data, monthly average of solar radiation data were calculated and analyzed to investigate the prospect of solar thermal energy utilization. Also from AWS data, the total availability of solar radiation hour (Fig.5.2) in Sonitpur District was calculated.

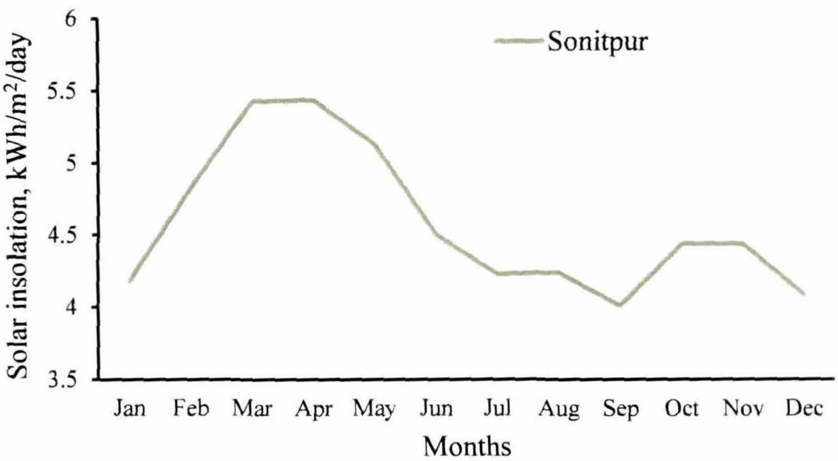

Fig.5.2 Monthly variation of solar insolation in Sonitpur district, Assam

The solar radiation data measured with the AWS indicated that on an average more than five hours per day solar radiation was available above 630 W m^{-2} and wind velocity was less than 4.5 m s^{-1}. This radiation was sufficient for testing and performance evaluation of improved designed solar air heater. Performance studies of the solar air heater was experimented by measuring continuously the velocity of hot air at outlet of duct, inlet air temperature, outlet air temperature, ambient air temperature, incident solar irradiation, wind speed and direction. The availability of solar radiation hour per day for Tezpur, Assam during the year 2008 to 2012 is shown in the Fig. 5.3 below.

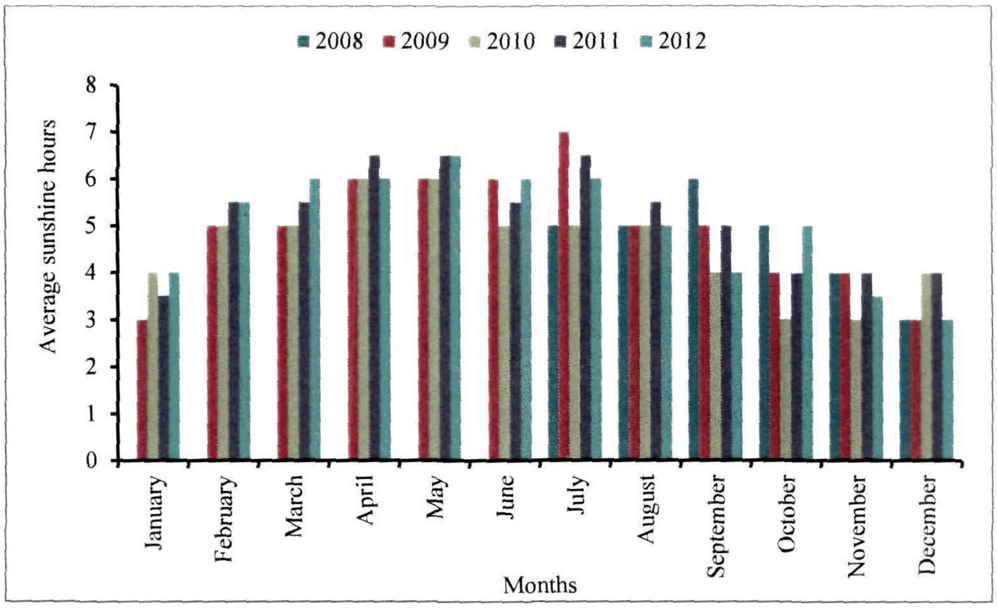

Fig. 5.3 Monthly variations of solar radiation hours per day at Tezpur

Data were available from July month for year 2008 as shown in Fig. 5.3. It was observed that the highest and lowest solar radiation hours were obtained in September (6 h/day) and in December (3 h/day) months in 2008. However, the data were available for the entire year in the year of 2009, 2010, 2011, and 2012. In the year 2009, it was observed that during the month of July, availability of solar radiation hour per day was highest (7 h/day) and lowest values were in the months of January and December (3 h/day). The availability of maximum solar radiation hours per day was observed during the months of April and May and minimum radiation for the months of October and November in the year 2010. The maximum and minimum solar radiation hours per day were in the months of May, July (6.5 h/day) and January (3.5 h/day) in the month of 2011. The corresponding radiation hours were in the month of May (6.5 h/day) and December (3 h/day) in the year 2012.

5.4 Monthly variation of tea drying thermal load

It has been observed from studies that black tea production in tea processing industries in Assam varies over the years. General trend is November, December and January to March of the succeeding year; the black tea production is almost insignificant. From middle of April to early November is considered peak period for black tea production. Accordingly, thermal load for tea drying also varies. Average variation of thermal load (%) over the year is presented in Fig.5.4. Now comparing Fig. 5.3 (Solar radiation pattern in Tezpur over the year) with Fig.5.4 (Thermal energy consumption pattern in a two million kilogram black tea production tea estate), it has been observed that a fraction tea drying thermal energy may be supplemented by solar radiation if appropriately designed solar air heater exists.

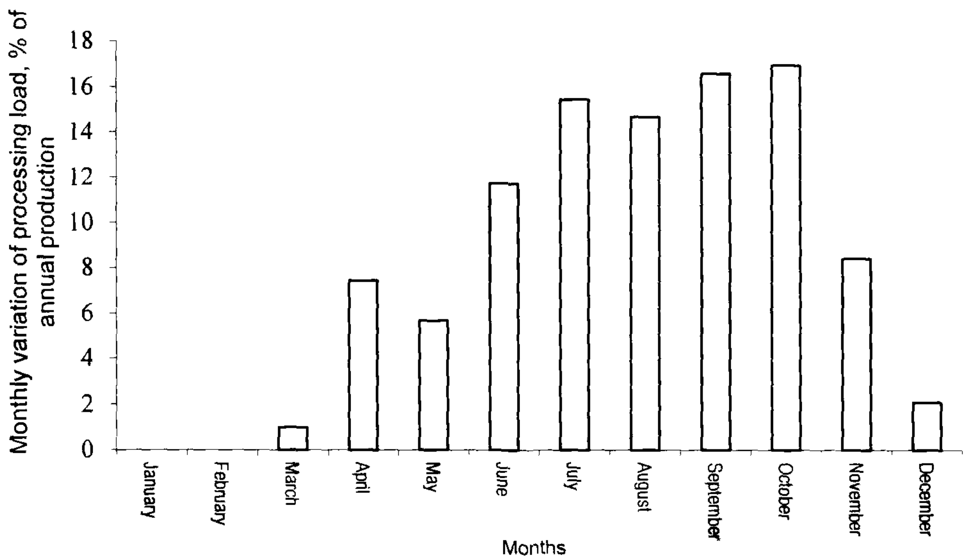

Fig.5.4 Monthly variation of processing load in a two million kg made tea factory

5.5 Solar air heater

It has been observed that some air heaters are available in India market. However, site-specific designed and low cost air heater for assisting black tea drying is still lacking. Moreover, literature on research and development and performance testing of improved solar air heaters are available [123–133]. These products are not available in market particularly for tea drying application. It has been observed that most of solar air heater absorber plate in mentioned literature had used galvanized iron or steel sheet. Therefore, a different solar thermal absorber material (Aluminum plate of 2 mm thickness) had been selected for the design. In this Chapter, an improved solar air heater has been considered for its performance evaluation in actual outdoor condition at Tezpur University campus (latitude 26° 42′ 03″ N and longitude 92° 49′ 49″ E) in the month of May-June 2012. Both the thermal performance and thermo hydraulic performance would be evaluated for the hemispherical protruded solar air heater at variable dimensionless protrusion height and pitch (roughness parameter) and Reynolds number. This series of exercise have been performed with an aim to examine the prospect of solar thermal energy in black tea drying.

5.5.1 Major components and development of solar air heater

The different components of a solar air heater had been discussed in Chapter: 2 [123-133] (literature review). Therefore, two rectangular ducts measuring 2400 (L) × 375 (W) × 37.5 (H) mm^3 was fabricated (Fig 5.5a- Fig.5.5d) at Tezpur University. The top of the air heater was covered with two number of 5 mm thickness commercial transparent glass. The other five sides of the air heater were covered with 10 mm thickness plywood boards. Moreover, the lengths of entry and exit sections were provided with 900 mm and 500 mm as per established standards [242]. The hydraulic diameter (D_h) of the solar air heater duct was calculated from Eq. (5.6):

$$D_h = \frac{2WH}{W+H} \tag{5.6}$$

where W is the duct width (mm) and H is duct height (mm). The design methodology of the solar air heater has been presented in Fig.5.5 below.

Design flowchart of solar air heater

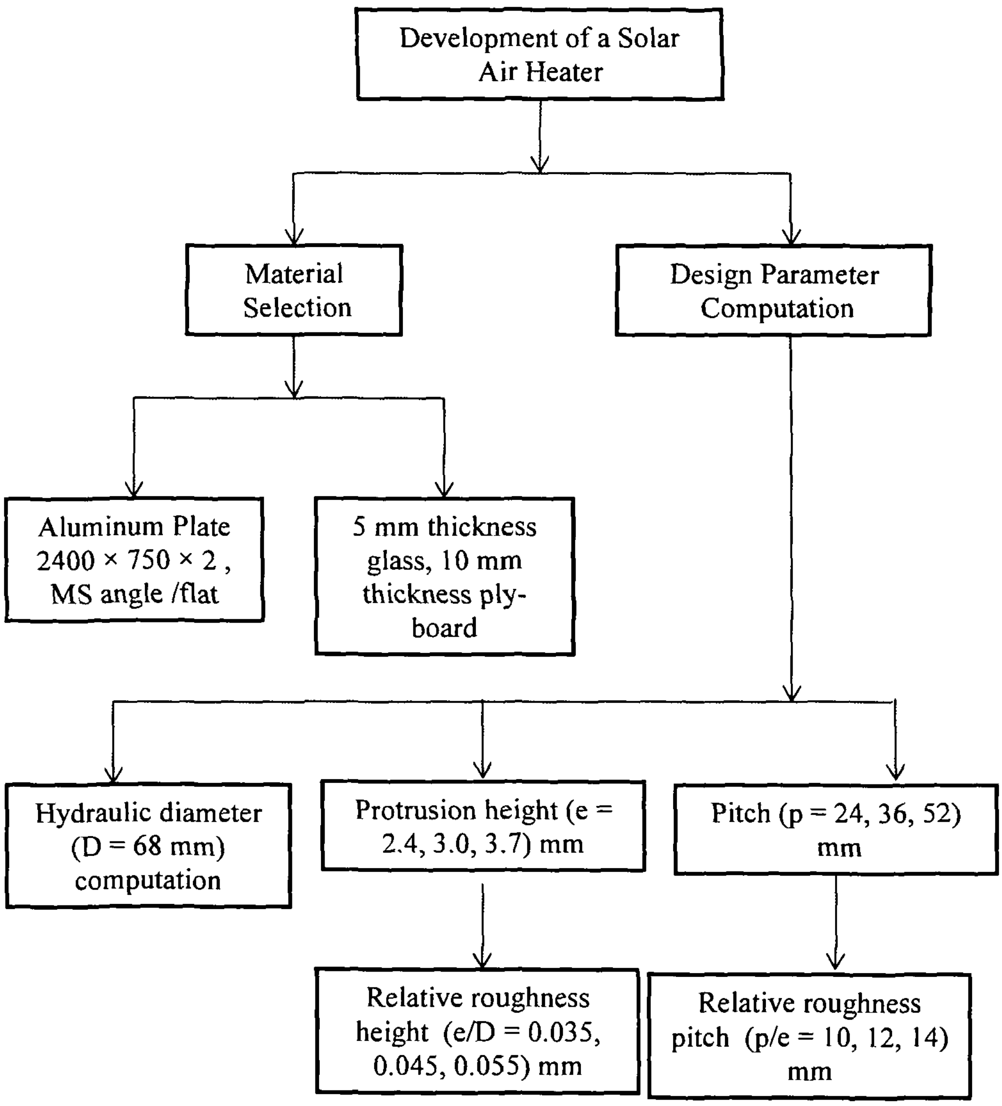

Fig.5.5 Design methodology of solar air heater thermal energy absorber

The designed and developed solar air heater absorber

The absorber plate is considered as a critical component of solar air heater design.

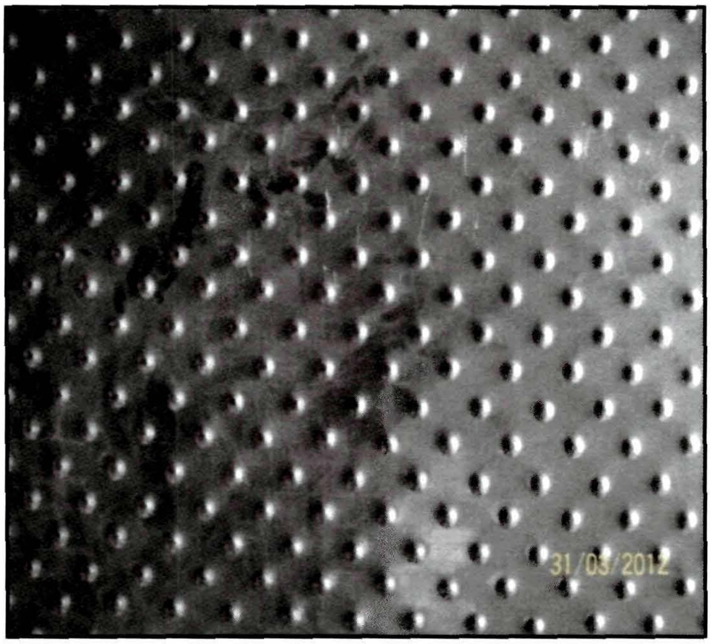

Fig.5.6a Hemispherical protrusion on aluminum sheet

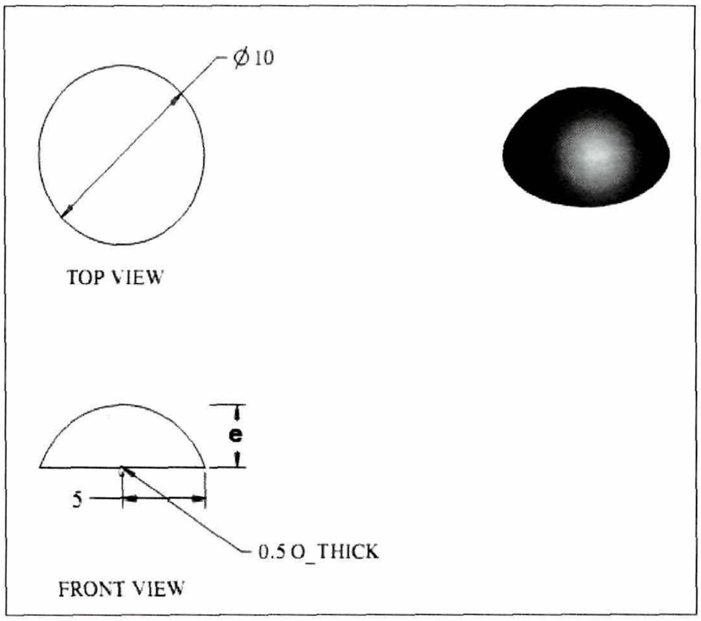

Fig.5.6b Dimension of hemispherical protrusion

The protrusion height (e) was varied as (2.4, 3.0, 3.7) mm (Fig. 5.6a and Fig.5.6b). The long way length (p) was varied as (24, 36, and 52) mm respectively (Fig.5.6c).

Nusselt number for the hemispherical protruded absorber may be calculated from experiment data of average heat transfer coefficient ($\bar{h}$), thermal conductivity (k) and hydraulic diameter (D_h) of duct as presented in Appendix: A3. Nusselt number for smooth rectangular duct is given by Dittus-Boetler (Eq. (5.7)) [233]. Roughness parameters namely $\frac{e}{D}$ and $\frac{p}{e}$ are strong function of Nusselt number for artificially roughen solar air heater. The cross section of air heater is shown in Fig.5.6d below.

$$Nu_s = 0.034Re^{0.8}\, Pr^{0.4}\, 2(\frac{R_{av}}{D}) \qquad (5.7)$$

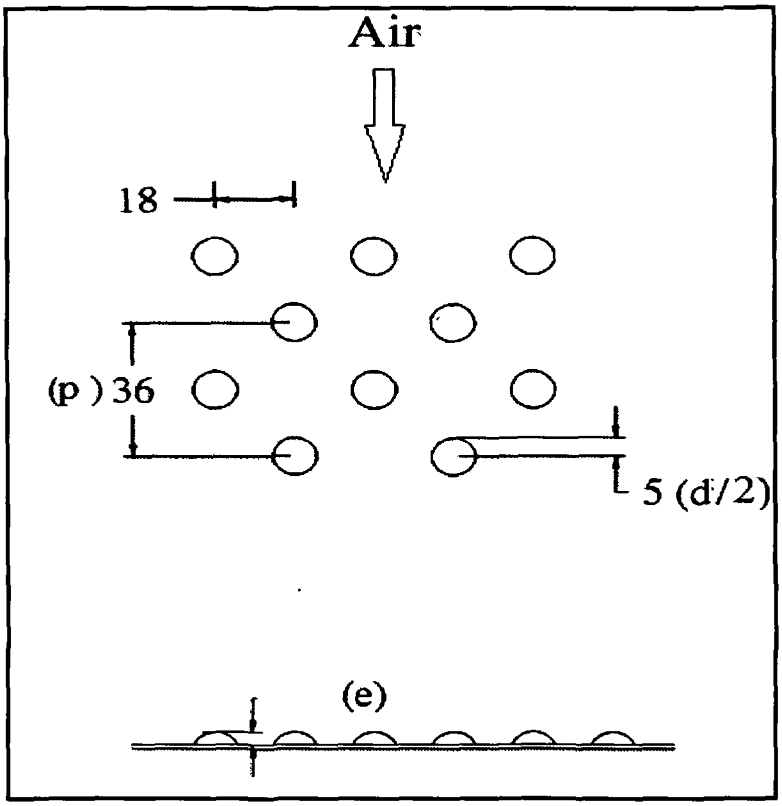

Fig. 5.6c Different dimensions of solar air heater absorber

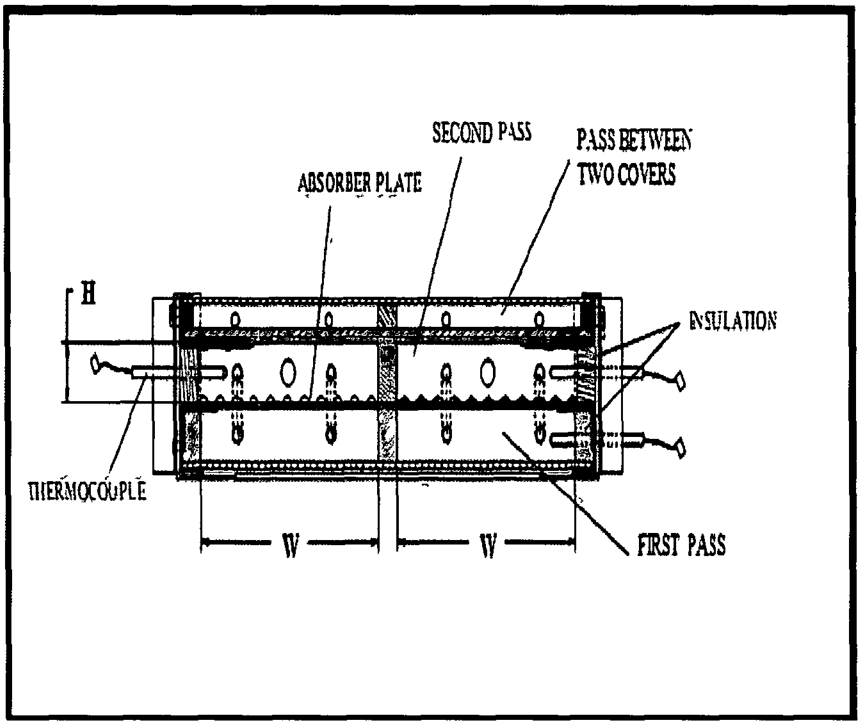

Fig.5.6d Cross sectional view of solar air heater

5.5.2 Experimental methodology

ASHRAE 93-2003 standard was followed for testing of high performance solar air heater for tea drying air [235]. One improved solar air heater of gross absorber area 1.8 m^2 was considered for present studies. The collector temperature and pressure measurement points were made to close to the collector rigid duct section. The measured variables included inlet and outlet air temperatures, ambient temperature, airflow rates, wind velocity, pressure drop and solar radiation.

The ten numbers of PT-100 type thermocouples (24 SWG) with digital display units (Electra, made in India), temperatures accuracy of 0.1°C had measured the duct air temperatures along the flow length of air. Similarly, fifteen thermocouples were pasted on the plate to measure average plate temperatures.

The mass flow rate of air was measured with the help of a calibrated hotwire anemometer (Testo 425, Made in Germany, [(0-20) m s^{-1}, resolution = 0.01 m s^{-1}, Accuracy = 0.03 m s^{-1}]. Average pressure drop across the air heater duct was measured with micro-manometer (Testo 525, Made in Germany), [(0- 200) hPa, resolution = 0.1 hPa]. Air velocity was varied by using a variable speed blower (Black and Decker, India, Maximum discharge = 3.5 m^3 min^{-1}, maximum rpm = 16000). The hotwire anemometer was calibrated with a gas turbine flow meter (Discharge: 6- 2500 m^3 h^{-1}, Linearity = $\pm 0.5\%$, Make: Rock-win, India).

The computed hydraulic diameter (D) was 68 mm for this roughen duct air heater. The relative roughness height $\frac{e}{D}$ (Fig.5.6a, Fig.5.6b) varied as 0.035, 0.045, 0.055 and relative roughness pitch $\frac{p}{e}$ varied as 10, 12, 14 during the experiments (Fig.5.6c) for total nine absorbers. The Reynolds number was varied from (3500-17000) for the experiments by using a variable speed blower. Flow of air was measured with a gas turbine flow meter.

To analyze the performance solar air heater, the following assumptions had been made. (1) The temperature difference between the plate and protrusion was neglected due to the large thermal conductivity of the absorber plate and hemispherical protrusion. (2) The thermal process in roughened air collector was approximately in steady state. (3) Centrifugal blower caused negligible rise in air temperature. (4) The glazing material had negligible heat capacity. The improved air heater performance testing experiments were normally conducted on sunny days from 9.00 a.m. to 15.00 p.m. at Tezpur University campus (latitude 26° 42′ 03″ N and longitude 92° 49′ 49″ E). The air heater experimental set up is given in Fig.5.7a and Fig.5.7b below.

Fig.5.7a Improved solar air heater: experimental setup

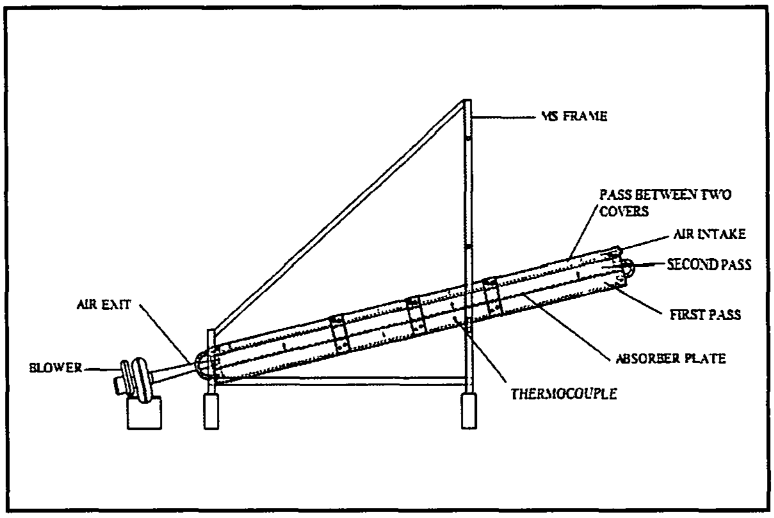

Fig. 5.7b Experimental setup of solar air heater in CAD

5.6 Economic analysis

An effort had been made to investigate economic feasibility of woody biomass based gasifier and solar air heater hybrid renewable energy system for partial substitution of conventional thermal energy in tea manufacturing. There are different procedures available in literatures for economic feasibility analysis of a new energy system. However, in the present investigation a specific procedure was followed where (i) Net present value (ii) Benefit cost ratio and (iii) Payback period pertaining to a new renewable energy technology were assessed. The difference between the present value of all future returns *(Fn1)* and present money required to make an investment *(Fn2)* with rate of interest *(i)* for *(n)* years are related with net present worth by Eq. (5.8).

$$NPV = \sum_{n=1}^{n=n} \frac{F_{n1}-F_{n1}}{(1+\iota)^n} \tag{5.8}$$

Benefit cost ratio defined as the present worth of benefit stream to present worth of cost stream. An acceptable project must have benefit cost ratio greater than one. Mathematically, benefit cost ratio is expressed as in Eq. (5.9).

$$Benefit\ cost\ ratio = \frac{\sum_{n=1}^{n=n} \frac{F_{n1}}{(1+i)^n}}{\sum_{n=1}^{n=n} \frac{F_{n2}}{(1+i)^n}} \quad (5.9)$$

The principal amount capital (P) with rate of interest i (minimum attractive rate of return, *MARR*) for n years yield future amount of money F_n given by the following Eq. (5.10) [236].

$$P = \frac{Fn}{(1+i)^n} \quad (5.10)$$

The necessary condition for attractive payback period for an investment C_0, the amount accumulated A_t in m years is given by the inequality (5.11) and a project investment has to be attractive, internal rate of return must be greater than minimum attractive rate of return (*IRR* > *MARR*).

$$PBP = \text{the smallest } m \text{ such that } \sum_{t=1}^{t=m} A_t > C_0 \quad (5.11)$$

The payback period is the total length of time from beginning of the project until the net value of the incremental production stream recovers total amount of capital investment. The following parameters were considered to carry out economic analysis of a gasifier (454 $kW_{thermal}$) cum tea dryer system [236-238].

5.7 Results and discussions

The computation for collector efficiency was performed for incident of solar radiations (average 790 W m^{-2}). Data were measured from 9.00 a.m. to 3.000 p.m. at automatic weather station of Tezpur University. Therefore, the Fig.5.8 shows variation of solar radiation and improved air heater air temperature with time from 9.00 a.m. to 3.00 p.m. The maximum out let air temperature was 65 °C around 12.00 p.m. at solar irradiance of (950) W m^{-2}. The testing was performed as per established standards [235].

Fig 6.9 shows variation of solar air preheater output air temperature and efficiency with hot air mass flow rate (kg s^{-1} m^{-2}) against collector area. It is clear that thermal efficiency increases with increase in air mass flow rate. The output temperature of hot

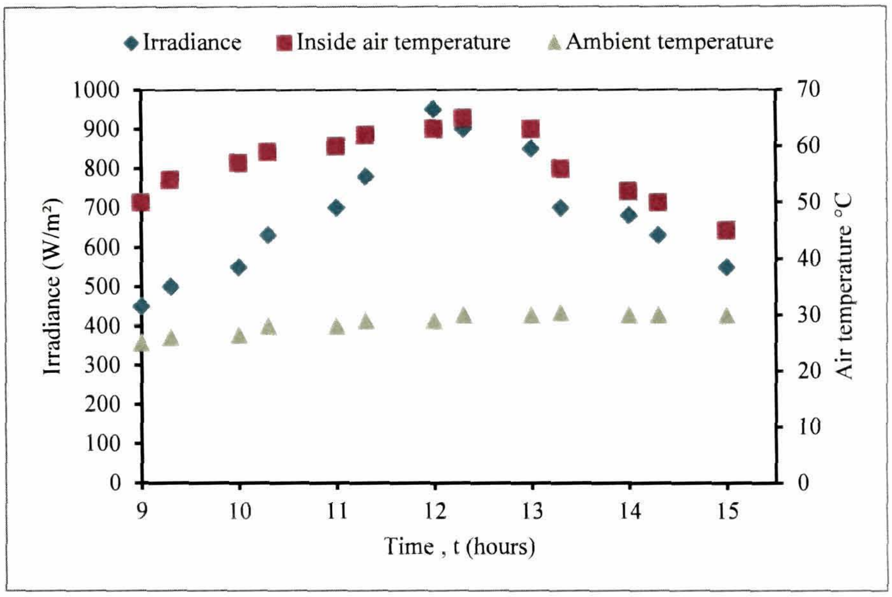

Fig.5.8 Variation of solar radiation and improved air heater air temperature with time

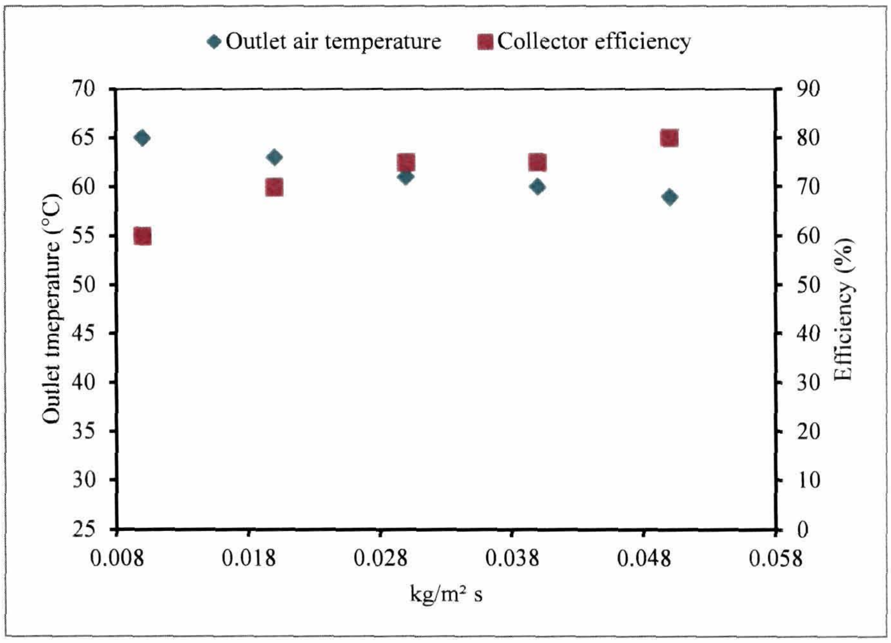

Fig.5.9 Variation of collector outlet temperature and efficiency with air mass flow rate

air decreases with increase hot air mass flow. Beyond hot air mass flows rate 0.028 kg s^{-1} m^{-2}, the falling rate of outlet temperature of air heater become steady, although collector efficiency still increases. From these data, the best operating point of solar air heater may be found out around air mass flow rate of 0.028 kg s^{-1} m^{-2}. Beyond this mass flow rate, even if there is an increase of collector efficiency, due to fall in outlet air temperature, it not economical to operate the solar air heater. Therefore, performance studies have been made at mass flow rate of 0.028 kg s^{-1} m^{-2}.

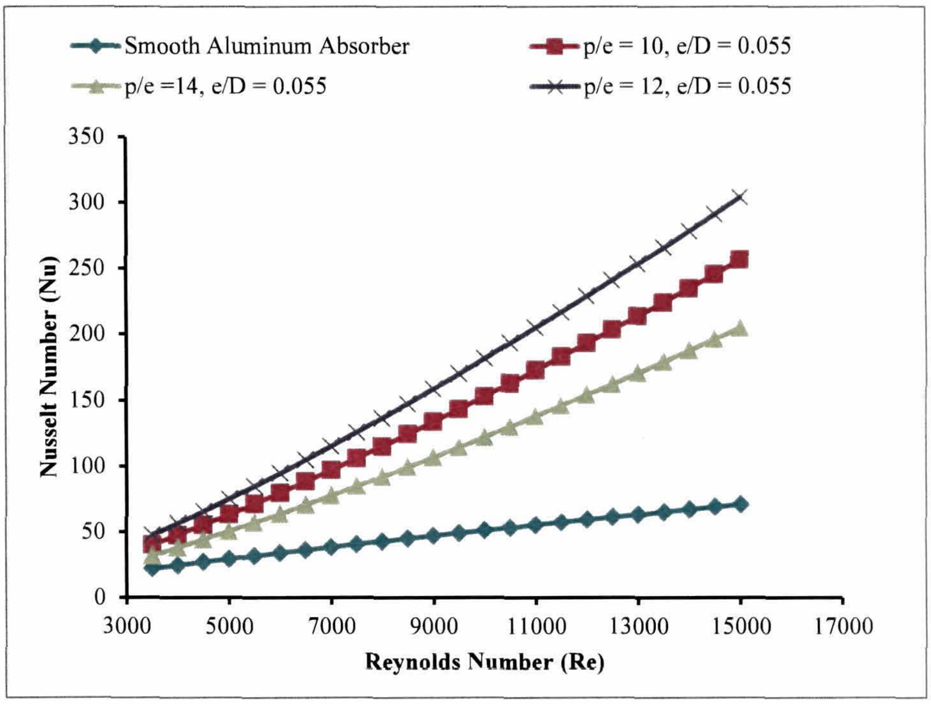

Fig.5.10 Variation of Nu number with Re number for constant e/D and variable p/e

Fig.5.10 shows the effect of variable $\frac{p}{e}$ (10-14) for fixed value of roughness parameter, $\frac{e}{D}$ (0.055). It is clear that Nusselt number is maximum for $(\frac{p}{e})$ value of 12 and it decreases in either side of 12. This might be due to separation of airflow over hemispherical protruded surface and reattachment of free shear layer occurs for $\frac{p}{e}$ (12). This gives rise to maximum heat transfer near reattachment region. Reattachment may not occur near $\frac{p}{e}$ (10 or 14) and therefore, Nusselt number is smaller in these regions. For higher value of $\frac{e}{D}$ (0.055) ratio, more reattachment of free shear layer might occur that enhances Nusselt number.

The effect of $\frac{p}{e}$ on performance of hemispherical protruded absorber has been discussed at Fig.5.11. It is seen that maximum thermal efficiency of 82% is achievable for $\frac{p}{e}$ = 12 and $\frac{e}{D}$ = 0.055. The corresponding F_0U_l and $F_0(\alpha\tau)$ are (10, 09 and 07) W $m^{-2}K^{-1}$ and 0.837, 0.721, and 0.572 for $\frac{p}{e}$ (12, 10 and 14). Similarly, Fig.5.12 shows the effect of $\frac{e}{D}$ (0.055, 0.045, 0.035) of hemispherical protruded absorber on constant $\frac{p}{e}$=12. The values of F_0U_l and $F_0(\alpha\tau)$ are (10, 09, 08) W $m^{-2}K^{-1}$ and 0.884, 0.746 and 0.664 respectively. Average solar radiation was above (790) W m^{-2} for all experiments.

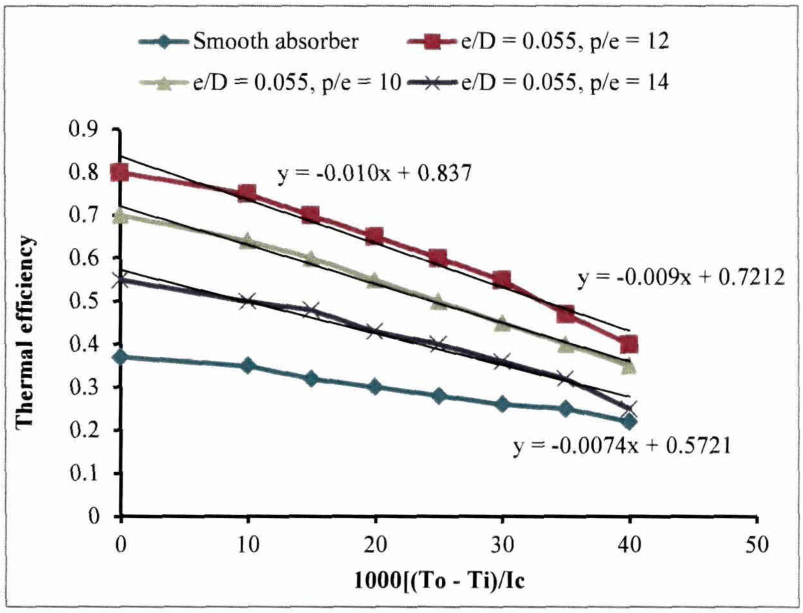

Fig.5.11 Effect of p/e on performance of hemispherical protruded air heater

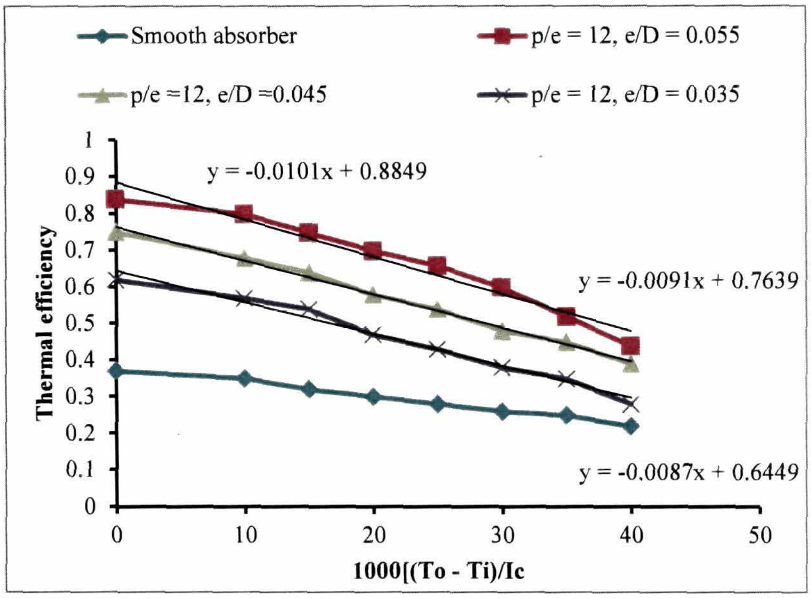

Fig.5.12 Effect of e/D on performance of hemispherical protruded solar air heater

Fig.5.13 presents variation effective efficiency of hemispherical protruded solar air heater with Reynolds number. It is clear that effective efficiency increases with Reynolds number for all three values of $\frac{e}{D}$ (0.035, 0.045, and 0.055) and attains maximum value for Reynolds number around 12000. Effective efficiency for smooth solar air heater absorber was minimum up to Reynolds number 140000 and beyond this Reynolds number, effective efficiency of smooth solar air heater become maximum. Therefore, beyond this region, there is no gain in effective efficiency of artificially roughen air heater. It is also clear that with $\frac{e}{D}$ value 0.035 and 0.055 gives maximum and minimum effective efficiency (74% and 64%) respectively around Reynolds number 12000.

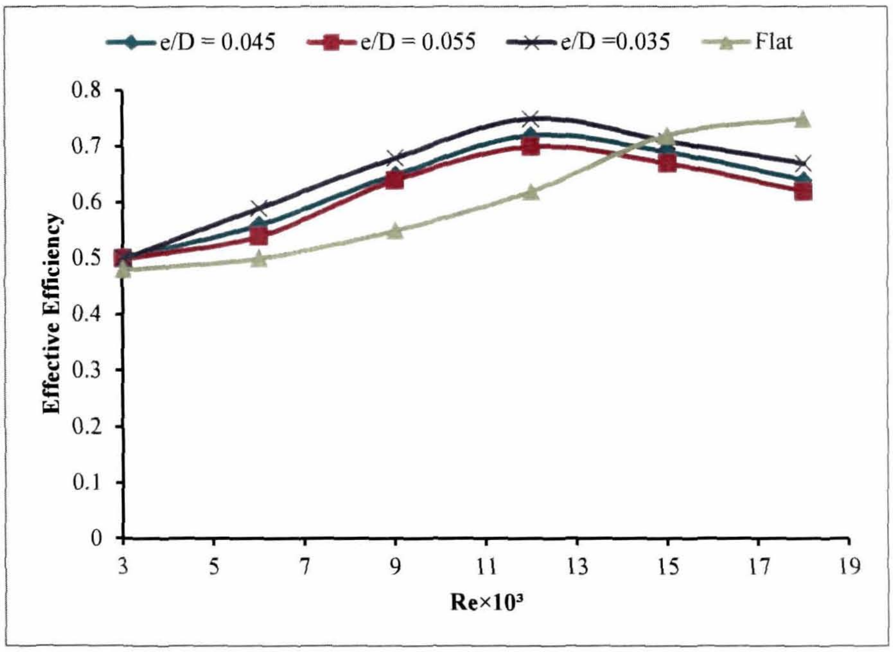

Fig.5.13 Variation of effective efficiency hemispherical protruded solar air heater with Reynolds number

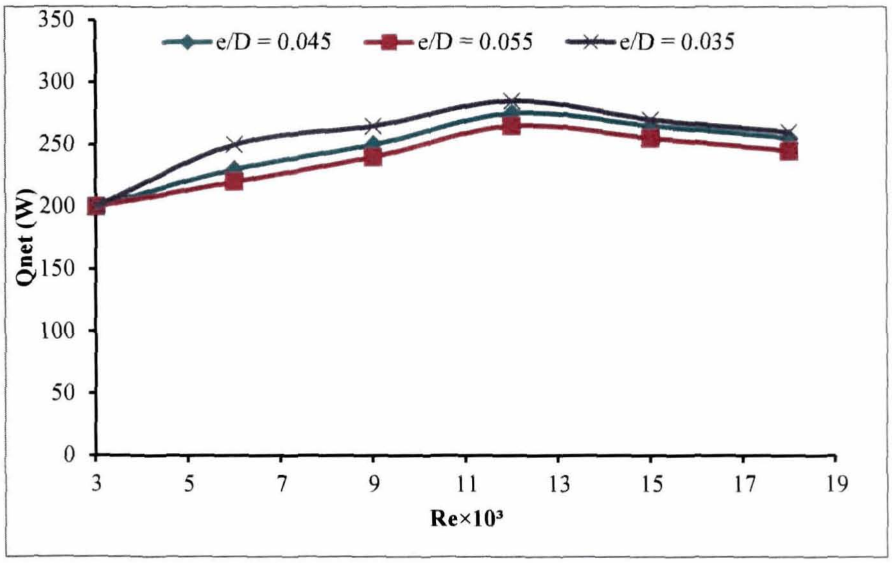

Fig.5.14 Variation of useful energy of solar air heater with Reynolds number

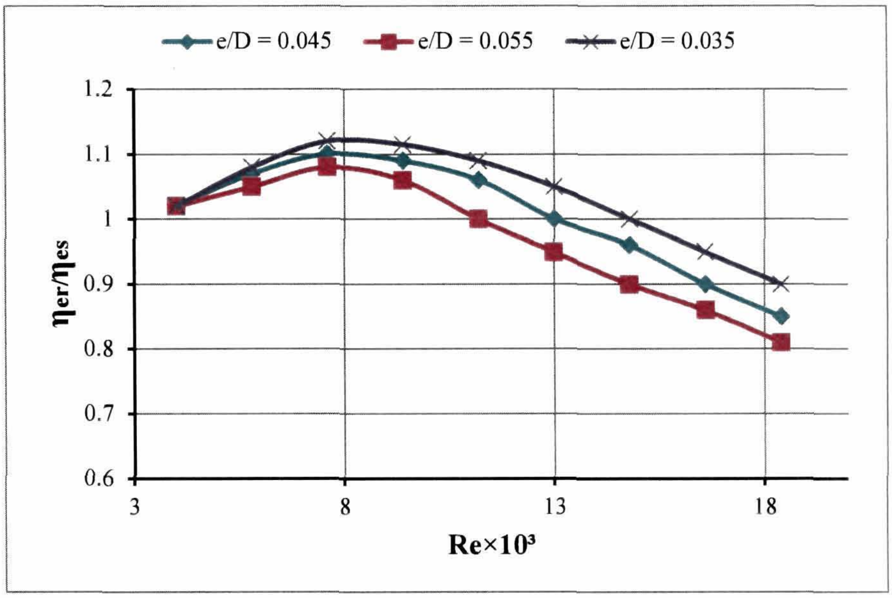

Fig.5.15 Comparison of efficiency of hemispherical protruded solar air heater with smooth air heater.

Fig.5.14 shows variation of useful energy of hemispherical protruded solar air heater with Reynolds number. It is clear that with decrease in dimensionless protrusion height ($\frac{e}{D}$: 0.055, 0.045, 0.035), useful heat gain by the hemispherical protruded solar thermal absorber increases. All three solar thermal energy absorber gain maximum energy around Reynolds number 12000 and beyond this useful energy gain decreases because of more high-grade energy is required to propel air than it acquires from roughen air heater

Fig.5.15 presents comparison of effective efficiency of hemispherical protruded solar air heater with smooth air heater. The maximum efficiency enhancement takes place for dimensionless protrusion height ($\frac{e}{D}$ = 0.035) that is about 8.9% around Reynolds number 6000-10000.The minimum efficiency enhancement about 5.5% takes place for protrusion height ($\frac{e}{D}$ = 0.055).

For performance testing of solar air heater, it has been observed that hemispherical protrusion with ($\frac{e}{D}$ = 0.035) and ($\frac{p}{e}$ = **12**) geometry gave best thermo-hydraulic efficiency 74% around Reynolds number 12000. Therefore, this configuration improved solar air heater has been selected for producer gas solar hybrid studies of black tea drying analysis.

$$Nu_{rh} = 5.2 \times 10^{-4} Re^{1.27} \left(\frac{p}{e}\right)^{3.15}$$

$$\exp(-2.12) \left[log \frac{p}{e}\right]^{p/6e} \left(\frac{e}{D}\right)^{0.33} \exp(-1.30) \left(log \frac{e}{D}\right)^{2} \qquad (5.12)$$

A modified correlation of Nusselt number had been developed from analysis of our experimental data of hemispherical protruded solar air heater as given by correlation Eq. (5.12) similar to that developed by Saini and Verma [133].

5.8 Hybridization of improved solar thermal air heater and biomass gasifier for black tea drying

To perform analytical studies of hybridization of improved solar air heater and woody biomass gasifier, the best operating condition for both the renewable energy system has been considered from experimental data [Chapter:3, Chapter:4 and Chapter:5]. The biomass gasifier was considered operating at best gasification efficiency with average calorific value producer gas 4.5 MJ m^{-3}. The maximum thermal output of the gasifier was 30 kW. Average dry biomass (moisture about 10 %) consumption rate was 8.5 kg h^{-1}. Only maximum 5 kW thermal output of producer gas was used for tea drying because of the size limitation of the tray dryer. The improved solar air heater was considered with maximum thermo-hydraulic efficiency of 74% at average radiation of 790 W m^{-2} in a sunny day in the month of May 2012 at Tezpur University campus.

5.8.1 Dryer efficiency

Fig.5.16 shows variation of tea drying efficiency and average dryer temperature with time. It is clear that at the beginning of black tea drying, the efficiency gradually increased to a maximum value (60%) then sharply decreased until completion (10%) of drying process. This is because initially some amount of thermal energy was utilized for preheating the fermented tea before start of moisture diffusion process. The dryer temperature gradually increased because of difficulty of removing internal moisture from the tea particles. At this stage, maximum amount of thermal energy was consumed if drying fluid temperature remained at initial temperature. Near completion of tea drying process, reduction of drying fluid temperature near (70-80) ° C and longer drying completion time, would reduce specific energy consumption of tea dryer. Therefore, an average tea drying efficiency 40 % may be considered.

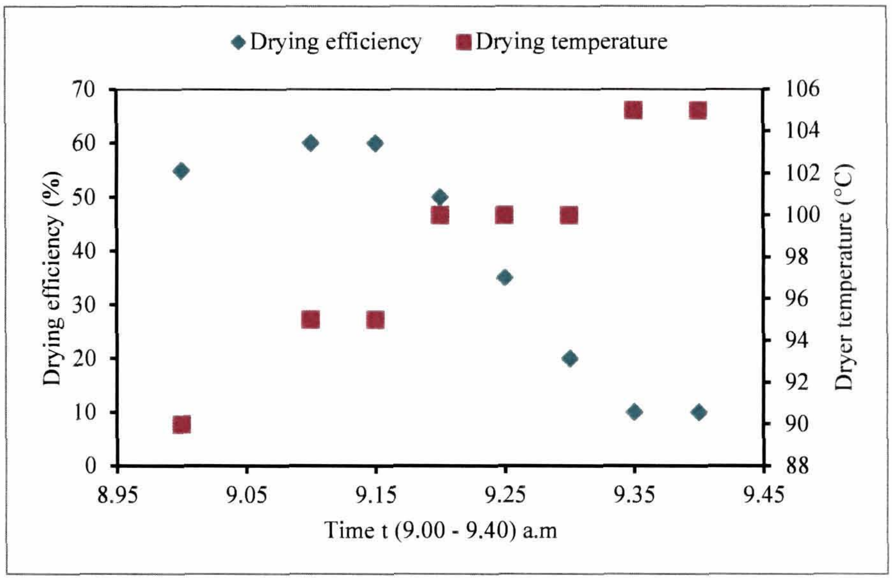

Fig.5.16 Variation of drying efficiency with drying air temperature with drying time

5.8.2 Specific energy consumption in hybrid drying

Fig.5.17 shows variation of tea drying energy from 9.00 a.m. to 2.40 p.m. considering a sunny day with available solar radiation similar to that had been presented in Fig.5.8. It is clear that specific energy consumption for per kilogram of made tea was estimated 25.50 MJ in batch drying of black tea while using both producer gas and improved solar air heater.

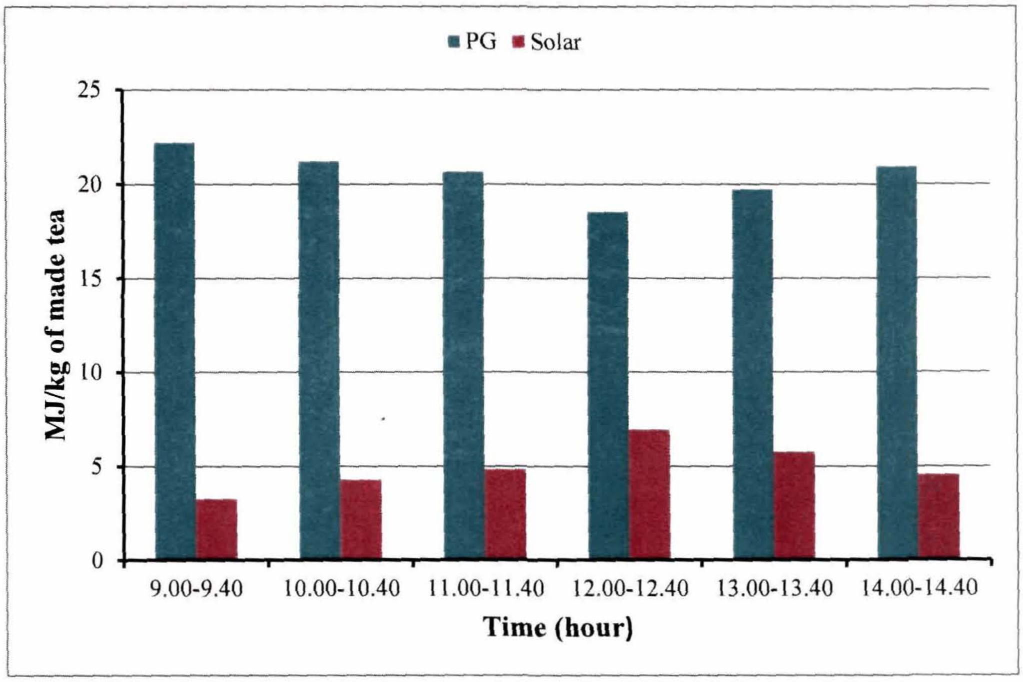

Fig.5.17 Variation of producer gas and solar thermal energy from 9.00 a.m. to 14.40 p.m

It is clear that minimum contribution of solar energy was 12.9% at (9.00- 9.40) a.m, while maximum contribution was 27.23% at (12.00 -12.40) p.m. By using five 1.65 m^2 improved solar air heater average 20% saving in biomass energy is possible.

5.8.3 Economic analysis of biomass gasification and improved solar air heater hybrid system for tea drying

Annual black tea manufactured by an average-size tea estate in Sonitpur district (Assam) was 990 t in the year 2011-2012 as computed by geographical information system mapping. Reported tea plantation areas in a FCC image (band 2, 3 and 4) were seen in dark-red to red tone depending on whether they are directly planted or appearing below shaded trees in different sizes with regular sharp edges indicating the presence of a fence around it. The average yield of black tea manufactured was assumed as 02 t ha^{-1} to compute annual black tea production for a representative average size tea estate. The total back tea production was calculated by multiplying yield of black tea by total mapped area of the tea estate [239].

Since, annual black tea manufactured by an average size tea estate in Sonitpur district (Assam) was 990 t (GIS mapping). The corresponding coal requirement is 825 t (Coal 1.35 kg kg^{-1} of black tea manufactured). It was also observed from this study that thermal efficiency was 20 % for a conventional coal fired furnace and (80-90) % for proposed producer gas fired furnace used for tea drying. Therefore, producer gas fired furnace is a better option over coal-fired system. Coal international prices was 95 \$ t^{-1}, Birol et al., [240] and that of woody biomass was 11 \$ t^{-1} in the year 2011-2012. A 454 kW thermal woody biomass gasifier was considered that could substitute 28 % of this thermal load [241]. It is estimated that by plantation of 22.5 ha *Bambusa tulda*, this thermal load of said biomass gasifer may be met [242]. If 400 m^2 of tea factory galvanized roof were converted by using black painting, plywood insulation and tempered glass enclosure to convert into solar air heater then average 20 % of biomass energy may be saved. The annual carbon-dioxide reduction 2189 t is achievable [243]. The payback period of the hybrid renewable thermal energy based system is less than fifteen month and benefit to cost ratio is 1:1 (Appendix: A8).

The limitation of improved solar air heater is that its performance may deteriorate with variation of solar radiation for an industrial scale black tea drying unit. In this case, thermal energy storage or oversized solar air heater will be useful. The solar and biomass gasifier based black tea drying is for partial substitution of conventional energy not for 100% replacement. This will reduce CO_2 emission from tea factories in Assam (India). The economic analysis was performed with data available from literature for a scaled up tea industry traditionally using inefficient coal fired furnace. However, actual payback period may be more than the computed one due to presence of real industrial tea drying system that is limitation of the study.

The focal point of the present study has been to investigate the prospect of application of locally available ten plant biomass samples in form of producer gas (biomass gasification) and solar thermal energy in the form of hot air for black tea drying as renewable energy sources and technology. Series of experiments were conducted with ten locally available biomass samples for characterization followed by details gasification studies of one biomass sample (*Camellia sinensis*). Down draft gasifier, performance had been evaluated with uprooted tea shrubs (*Camellia sinensis*) as gasification feedstock. Further three-biomass samples mixture in equal proportion was gasified. Black tea drying experimentation and modelling had been carried out with producer gas derived from three selected mixed biomass samples (*Bambusa tulda, Psidium gaujava, and Camellia sinensis*). An improved low cost solar air heater had been developed to assist hybrid tea drying system. Finally, an economic analysis had been performed for solar biomass hybrid tea drying system. The findings of all experimental studies have been summarized below.

6.1 Characterization results of three selected biomass samples for gasification

It was observed that *Psidium guajava* had the highest calorific value (18.404 MJ kg^{-1}) and *Ficus lepidosa* has the lowest (15.958 MJ kg^{-1}) amongst the tested samples by using Automatic Bomb Calorimeter. Calorific value of *Bambusa tulda* was in second position (18.403 MJ kg^{-1}). Moreover, calorific value of *Camellia sinensis* was (18.400 MJ kg^{-1}). Other eight woody biomass samples had calorific value in between *Psidium guajava* and *Ficus lepidosa*. The approximate empirical bio-chemical formula for all ten biomasses had been obtained from CHN/O analysis of data. For each atom of C, the variation of H atoms ranges between 1.866 (*Delonix regia*) and 1.580 (*Ficus lepidosa*). Such variation for N is *Azadirachta indica* (0.051) to *Camellia sinensis* (0.03). The variation of O atom is 0.698 (*Ficus lepidosa*) and 0.599 (*Bambusa tulda*).

These samples (*Bamusa tulda* and *Psidium guajava*) may be potential feedstock for gasification. The producer gas thus generated may be used for thermal applications like tea drying. However, only *Bambusa tulda* is a fast growing plant, whereas other nine plants are not as fast growing as *Bambusa tulda*.

6.2 Performance of gasifier for tea drying with (*Camellia sinensis*) up rooted shrubs as feedstock

There are potential advantages in application of gasification technology for tea manufacturing industries in Assam, India. The surplus uprooted tea branches, shrubs, shading trees are in house generation of biomass in a tea-manufacturing unit. Therefore, a downdraft gasifer performance with uprooted tea shrubs (*Camellia sinensis*) as feedstock to substitute conventional inefficient coal fired furnace have been summarized in the present studies. The uprooted tea shrub has high energy densities (18.40 MJ kg^{-1}, HHV) for gasification. It was observed that gasifier under study performed well in respect of gas quality given by gas chromatograph and calorific value at 0.27 equivalence ratios. The maximum volumes of CH_4, H_2 and CO were observed as 1.4%, 18% and 24% respectively at above equivalence ratio. The maximum calorific value of producer gas derived from (*Camellia sinensis*) was (4.5 MJ m^{-3}) as measured by Junker Gas Calorimeter at equivalence ratio (0.27). This is a satisfactory result with uprooted tea shrubs as gasifier feed stock. The maximum cold gasification efficiency was found as 65 % near air fuel equivalence ratio of 0.27 and then it declined by increasing the gas flow rate.

However, it has been observed that tea drying thermal energy requirement may not be possible by in-house generation of above biomass in a representative tea estate. Supplementary plantation of some fast growing variety trees in addition to biomass generated from tea plantation itself may be required. Wherever there is a scarcity of in house biomass production, deficit biomass may be procured from nearby market.

6.3 Improved producer gas fired premixed burner

A laboratory scale dryer was used to experiment and to model thin layer drying kinetics of local variety (Assam) black tea. An improved producer gas fired burner was redesigned for controlling appropriate air fuel equivalence ratio. At air fuel equivalence ratio (ϕ =1), a short intense blue flame was obtained. At this point, thermal efficiency of producer gas burner was maximum (57 %), obtained from water boiling test. In either side of this equivalence ratio, the burner efficiency decreased due to inappropriate air fuel ratio and diffusion flame dominated the premixed flame.

6.4 Drying kinetics of thin layer black tea drying with producer gas as a fuel

It was observed that the principal operating variables were drying medium temperatures and velocities while studying drying kinetics of black tea in a drying environment similar to an industrial tea dryer. While using producer gas fired combustion products mixed with air for black drying, Modified Page model was found as best fitted drying model for local variety tea. However, under this condition the Lewis model was as second choice for drying kinetic prediction. The drying rate constant ($k = 25.91\times10^{-4}\ s^{-1}$) exponent (n=1) as observed at 100 °C that complied with modified Page model. It was observed that both drying air temperature and velocity had influences to enhance drying rate (*k*) and exponent (*n*) in Page and Modified Page model.

The relationship of drying constant (*k*) and drying medium temperature (*T*) at constant velocity (0.65 m s^{-1}) was derived from black tea drying modelling studies as:

$$k = 6T \times 10^{-5} - 0.0038$$

The relationship of drying exponent (*n*) with drying medium temperature (*T*) at constant velocity given from black tea drying modelling studies as:

$$n = 0.01057T - 0.06$$

The effective diffusivities of tea particle during drying varied from (3.644×10^{-11} – 7.287×10^{-11}) $m^2\ s^{-1}$ in the temperature range of (80-110) °C. The activation energy for moisture diffusion was computed as (52.104 kJ mol^{-1}) from linear regression analysis data. The following relation of moisture ratio (*MR*), drying constant (*k*) and exponent (*n*) was derived from black tea drying kinetics data.

$$MR = 0.8651e^{[-(6T\times10^{-5}-0.0036)t]^{0.0106T-0.06}}$$

Producer gas fired dryer specific energy consumption was better than a conventional coal fired tea dryer. The energy consumption based on the calorific value of producer gas (4.5 MJ Nm^{-3} HHV) was found as 25.50 MJ kg^{-1} of made tea (3 % w.b.). Therefore, specific energy consumption of the dryer was approximately 10.20 MJ kg^{-1} of water removed. It may be concluded that producer gas based tea drying has great potentials, particularly application of renewable energy in tea manufacturing industries of Assam for partial fossil fuel substitution.

6.5 Improved solar air heater performance

Based on thermo-hydraulic performance of hemispherical protruded aluminium plate solar thermal absorber, the following observations were made:

1. Maximum thermal efficiency of 82% was achievable for $\frac{p}{e}$ = 12 and $\frac{e}{D}$ = 0.055. The corresponding F_0U_l and $F_0(\alpha\tau)$ were (10, 09 and 07) W $m^{-2}K^{-1}$ and 0.837, 0.721, and 0.572 for $\frac{p}{e}$ (12, 10 and 14). At constant $\frac{p}{e}$=12, with decrease in roughness height $\frac{e}{D}$ (0.055, 0.045, 0.035), the values of F_0U_l and $F_0(\alpha\tau)$ were (10, 09, 08) W $m^{-2}K^{-1}$ and 0.884, 0.746 and 0.664 respectively. Average solar radiation was above (790) W m^{-2} and air mass flow rate was 0.028 kg s^{-1} m^{-2} during experiment.

2. *Nusselt number was maximum for* $\frac{p}{e}$ *value of 12 and it decreased in either side of 12.*

3. Effective efficiency of hemispherical protruded solar air heater was 74% around Reynolds number 12000, $\frac{p}{e}$=12 and $\frac{e}{D}$ = 0.035 respectively.

4. Solar thermal energy absorber gained maximum energy around Reynolds number 12000 and beyond this useful energy gain decreased because of more high-grade energy was required to propel air than it acquired from roughen air heater.

5. The maximum (8.9%) and minimum (5.5%) efficiency enhancement take place for dimensionless protrusion height ($\frac{e}{D}$= 0.035) and ($\frac{e}{D}$ = 0.055) around Reynolds number 6000-10000.

6.6 Hybridization results

Both solar air heater and biomass gasification are viable renewable energy technologies for tea processing industries in India for substitution of conventional inefficient coal fired furnace.

A producer gas fired and improved solar air heater assisted hybrid black tea drying system had been studied. Solar radiation varied from, 450 Wm^{-2} to 950 Wm^{-2} (9.00 a.m. to 15.00 p.m.). The maximum temperature from the outlet of the improved air heater was 65 °C. The best operating point of solar air preheater may be found out around air mass flow rate of 0.028 kg s^{-1} m^{-2}.

Dryer efficiency varied maximum from (60 %) just after start of drying to minimum (10%) near completion of drying. The average drying efficiency 40 % was considered for present analysis of tea drying. Specific energy consumption for per kilogram of made tea was estimated 25.50 MJ in batch drying of black tea while using both producer gas and improved solar air heater. Minimum contribution of solar energy was 12.9% at (9.00- 9.40) a.m., while maximum contribution was 27.23% at (12.00 -12.40) p.m. By using five 1.65 m^2 improved solar air heater average 20% saving in biomass energy is possible.

For a 0.99 M kg made tea factory, 28% of tea drying thermal load may be covered by plantation of 22.5 ha *Bambusa tulda*, and thus biomass obtained from this plantation processed through biomass gasification in a 454 kW downdraft gasifier. It has been estimated that if 400 m^2 of tea factory galvanized roof were converted by using black painting, plywood insulation and tempered glass enclosure to convert into solar air heater, then average 20 % of biomass energy may be saved. The annual carbon-dioxide reduction 2189 t is achievable. The payback period of the hybrid renewable thermal energy based system is less than fifteen month and benefit to cost ratio is 1:1. Therefore, it is a very much attractive option in addition to green fuel application in tea manufacturing, emission reduction, waste utilization and clean development mechanism in tea industries.

6.7 Conclusion and future work

A new biomass gasifier coupled with improved solar air heater experimental setup for black tea manufacturing in Assam has been developed and it is sufficiently experimented for performance evaluation independently. Moreover, an analysis for this hybrid renewable energy mode black tea drying is performed. Such a renewable energy based tea drying system is expected to be most useful for partial substitution of conventional old design coal fired tea drying furnace cum air heater. *Bambusa tulda* is a first growing plant in northeast India and therefore in every aspect it is the most suitable gasification feed stock for black tea drying application. Moreover, thin layer drying kinetics study of black tea manufacturing with producer gas as fuel gave Modified Page model as best fit. Simple economic analysis for a scaled up hybrid system reveals that payback period of the system is about 1½ years.

The limitation of the present research work is that the producer gas fired tea-drying experiments and solar air heater experiments were conducted in a laboratory scale tray type tea dryer setup. Scaling up of tea drying at industrial level to get experimented data could not be performed due to non-availability of such a renewable energy powered tea drying system in Indian (Assam) tea processing industries. The computation of payback period for such a hybrid renewable energy system is based on certain assumptions and data available from literature. The actual payback period may increase depending on real industrial environment. Therefore, the following work may be carried as an extension of present studies in future.

- Application of VFBD drying experiment and modelling with producer gas.
- Thermo-physical properties determination of tea undergoing drying.
- Use of updraft gasifier for tea drying.
- High temperature solar air heater development for tea drying.
- Tea drying modelling and experimentation with solar and biomass energy.
- Energy efficiency and conservation in tea manufacturing industries in India.

REFERENCES

[1] http://www.charhai.com/world-tea-consumption/ Accessed 19/06/2013.s

[2] Tea Board of India. Production final during (2012-2013) as compared to 2011-2012 http:// http://www.teaboard.gov.in/pdf/bulletin/Production_2012-13_Final.pdf , Accessed 10/06/2013.

[3] Tea Board of India (59^{th} Annual Report) http://www.teaboard.gov.in/pdf/bulletin/59-English-AR_12-13.pdf, Accessed: 19/06/2014.

[4] Panda, H. *The Complete Book on Cultivation and Manufacture of Tea.* Asia Pacific Business Press, New Delhi, 2011.

[5] Arunachalam, K. *A Handbook of Indian Tea*, Pondichery:1^{st} Eds, 1995.

[6] Tomlins, K.I., Mashingaidze, A. Influence of withering, including leaf handling, on manufacturing and quality of black tea – a review. *Food Chem.* **60(4)**, 573-580, 1997.

[7] Ullah M.R. A reappraisal of withering process in black tea manufacture. I. Physical and chemical wither and their effects on tea liquor. *Two and a Bud.* **31**, 20-24, 1984a.

[8] Orchard, J.E. Technical Report 1988-91. ODA TCO, Tea Research Foundation of Kenya, P.O. Box 820, Kericho, Kenya, pp. 126.

[9] Kramer, J.P. and Kozlowski, T.T. *Physiology of Woody Plants*, Academic Press, London, 1989.

[10] Jonson, A.L. *Tea Planter Handbook,* Tea Research Foundation Central Africa, P.O. Box: 51, Mulanje, Malawi, 1990.

[11] Muthumani. T., Senthil Kumar, R.S. Influence of fermentation time on development of compounds responsible for quality in black tea. *Food Chem.* **101**, 98-102, 2007.

[12] Ni, J.N., Zhou, H. Energy consumption and conservation in tea processing in China. *Renew Energ.* **2**(1), 1-5, 1992.

[13] Baruah, D.C., Bhattacharyya, P. C. Energy utilization pattern in the manufacturing of black tea. *Agricultural Mechanization in Asia Africa and Latin America.* **27**(4), 65-70, 1996.

[14] Balachandran, S., Rudramoorthy, R. Energy efficiency improvement in air heater of a tea unit – A case approach. *J Sci Industrial Res.* **67**, 151-153, 2008.

[15] Yoshitomi, H., Nakano, F., Takiya, H., Tanaka, S. Development of energy saving method for primary drying tea roller (part 1) - comparison of heat recovery devices. *J Jap Soc Agri Machinery.* **52**(1), 51-60, 1990.

[16] Kishor, N., Yadav, L.S. Coal, and oil energy requirement for drying fermented tea leaves. *New Agriculturist* (Allahabad, India). **12** (1/2): 81-83, 2001.

[17] Temple, S. J. Water in tea. *Quarterly Newsletter - Tea Research Foundation (Central Africa).* **119**, 10-11, 1995.

[18] Zilva, R. de. The energy crisis in tea plantation. *J National Inst Plantation Manage.* **1, 2**, 127-135, 1981.

[19] Sadeghi, M., Khoshtaghaza, M. H. Vibration effect on particle bed aerodynamic behavior and thermal performance of black tea in fluidized bed dryers. *J Agri Sci Technol.* **14**(4), 781-788, 2012.

[20] Temple, S.J. Dryer bedplate material. *Tea Research Foundation (Central Africa), Mulanje, Malawi, Quarterly Newsletter - Tea Research Foundation (Central Africa).* **123**, 27-30, 1996.

[21] Temple, S.J., Whittle, A.M., Khumalo, F.R.B. Fluid bed drying of tea - experimental work and practical implications. In: Proceedings of the 1st Regional Tea Research Seminar, Tea Research Foundation of Central Africa, Mulanje, Malawi. 136-143, 1995.

[22] Basu, R. P. Drying of tea. *Two and a Bud.* **20**(1), 27-33, 1973.

[23] Shah, R.M., Goyel S.K., Rudolph, V., Keey R.B. Drying characteristics of tea fluidized on a vibrating bed (Part II) - handling of dust grades & its impact on quality. In: Proceedings of the 9th International Drying Symposium, Gold Coast, Australia, Volume A. 391-400, 1994.

[24] Yoshitomi, H., Nakano, F., Takiya, H., Suzuki, K. Drying characteristics of tea leaves : Effect of primary drying conditions on tea drying. *J Jap Soc AgriMachinery*. **49**(3), 197-206, 1987.

[25] Norman, J.G.S. A tea drier house with integrated exhaust. *Agri Eng.* **45**(3), 86, 1990.

[26] Pandiaraj, G.T.S., Pandiaraj, G.P. Drier efficiency, heat balance, and flue gas analysis. *Tea Research Institute, United Planters' Association of Southern India (UPASI), Valparai, India, Bulletin.* **44**, 45-50, 1991.

[27] Kanagaratnam, N. The introduction of a rotary drier in the manufacture of China tea in Malaya. *Malayan Agricl Journal*. **38**, 174-176, 1955.

[28] E. M. Experience with endless belt gas-heated driers. *Schweizerische Landwirtschaftliche Monatshefte*. **20**, 55-56, 1942.

[29] Temple, S.J., Boxtel, A.J.B. van. Modelling of fluid bed drying of black tea. *J Agric Eng Res*. **74**, 203-212, 199.

[30] Dong, S.L. Leaf temperature moisture content model for tea dryer. *T Chinese Soci Agric Machinery*. **20**(4), 44-48, 1989.

[31] Yoshitomi, H. Drying characteristics of tea leaves. Moisture diffusion coefficients of tealeaves. *J Jap Soc Agri Machinery*. **48** (3/4), 303-308, 1986.

[32] Kamanu, J.N. The keeping quality of black tea fired to different moisture content levels in a fluid bed dryer. *Tea Research Foundation of Kenya, Kericho, Kenya, Tea*. **24**(1), 21-28, 2003.

[33] Shinde, A., Das, S., Datta, A. K. Quality improvement of orthodox and CTC tea and performance enhancement by hybrid hot air-radio frequency (RF) dryer. *J Food Eng.*. **116** (2), 444-449, 2013.

[34] Law, R., Harvey, A., Reay, D. Opportunity of low-grade heat recovery in U K food processing industry. *Appl Therm Eng.* **53**(1), 188-196, 2013.

[35] Aneke M, Agnew B, Underwood C, Wu H, Masheiti, S. Power generation from waste heat in a food processing application. *Appl Therm Eng.* **36**(1), 171-180, 2012.

[36] Jekayinfa, S. O, Bamgboye, A. I. Estimation of energy requirement in cashew (Anacardium occidentale L.) nut processing operation. *Energy.* **31**(15), 1305-1320, 2006.

[37] Roman, F., Nagle, M., Leis, H., Janjai, S., Mahayothee, B., Haewsungcharoen, M., Muller, J. Potential of roof-integrated solar collectors for preheating air at drying facilities in North Thiland. *Renew Energ.* **34**(7), 1661-1667, 2009.

[38] Kalogirou S. The potential of solar industrial process heat applications. *Appl Energ.* **76**, 337-381, 2003.

[39] Kapur, T., Kandpal, T.C. & Garg, H.P. Energy demand and supply options for primary processing of rice in India. In: World Renewable Energy Congress. 946-949, 1996.

[40] Imre, L. Technical and economic evolution of solar drying. *Drying Technol.* 4(4), 503-512, 1986.

[41] Marculescu, C., Ciuta, S. Wine industry waste thermal processing for derived fuel properties improvement. *Renew Energ.* 57, 645-652, 2013.

[42] Ramırez, C.A., Patel, M., Blok, K. From fluid, milk to milk powder energy use and energy efficiency in the European dairy industry. *Energy.* **31**, 1984-2004, 2006.

[43] Kumar, S., Senanayake, G.C., Visvanathan, C., Basu, B. Desiccated coconut industry of Sri Lanka: opportunities for energy efficiency and environmental protection. *Energ Convers Manage.* **44**, 2205-2225, 2003.

[44] Muller, D.C.A., Marechal, F.M.A., Wolewinski, T., Roux, P.J. An energy management method for the food industry. *Appl Therm Eng*. 27, 2677-2786, 2007

[45] Paton J, Khatir Z, Thompson H, Kapur N, Toropov V. 2013. Thermal energy management in the bread baking industry. *Appl Therm Eng*. **53**, 340-347, 2013.

[46] Singh, S., Kumar, S. Solar drying for different test conditions: Proposed framework for estimation of specific energy consumption and CO_2 emissions mitigation. *Energy*, **51**, 27-36, 2013.

[47] Ma, C. M., Chen, M.H., Hong, G.B. Energy conservation status in Taiwanese food industry. *Energ Policy*. 50, 558- 463, 2012.

[48] Abdelaziz, E.A., Saidur, R., Mekhilef, S. A review on energy saving strategies in industrial sector. *Renew Sust Energ Rev*. 15, 150-168, 2011.

[49] García-Maraver, A, Zamorano, M, Ramos-Ridao, M, Díaz, L. F. Analysis of olive grove residual biomass potential for electric and thermal energy. *Renew Sust Energ Rev*. **16**, 745-751, 2012.

[50] Ammar, Y., Joyce, S., Norman, R., Wang, Y., Roskilly, A.P. Low-grade thermal energy sources and uses from the process industry in the UK. *Appl Energ*, **89**, 3-20, 2012.

[51] Xu, T., Flapper, J. Energy use and implications for efficiency strategies in global fluid-milk processing industry. *Energ Policy*. **37**, 5334-5341, 2009.

[52] Muller, D.C.A., Marechal, F.M.A., Wolewinski, T, Roux, P.J. An energy management method for the food industry. *Appl Therm Eng*. **27**, 2677-2686, 2007.

[53] Ramirez, C.A., Blok, K., Neelis, M., Patel, M. Adding apples and oranges: The monitoring of energy efficiency in the Dutch food industry. *Energ Policy*. **34**, 1720-1735, 2006.

[54] Tengfang, Xu. T., Joris Flapper, J., Kramer, K.J. Characterization of energy use and performance of global cheese processing. *Energy*. **34**, 1993-2000, 2009.

[55] Turner, J. Sustainability issues in tea sectors: A comparative analysis in six leading countries. Amsterdam: SOMO; 2008.

[56] Palaniappan, C., Subramanian, S. V. Economics of solar air pre-heating in South Indian tea factories: A case study. *Sol Energ*. **63**(1): 31–37, 1998.

[57] Koneswaramoorthy, S., Mohamed, M. T. Z., Galahitiyawa, G. Developing and evaluating solar energy techniques for tea drying. *J National Sci Foundation* . **32** (1 & 2): 49-60, 2004.

[58] Ramasamy, V., Rajendiran, A. R. Solar energy for tea processing. *Newsletter – UPASI Tea Research Institute*. **2**(2), 4-5, 1993.

[59] Jayah, T.H., Aye, L., Fuller, R.J., Stewart, D.F. Computer simulation of a downdraft wood gasifier for tea drying. *Biomass Bio-energy*. **25**(4), 450-469, 2003.

[60] Dasappa, S. Biomass gasification for energy needs of tea industry 2004. *Int J Tea Sci.* **3** (3/4), 83-94, 2004.

[61] Basu, P. *Biomass Gasification and Pyrolysis Practical Design and Theory*. Kidlington, Oxford; Academic Press, 2010.

[62] Smooth LD, Smith PJ. *Coal Combustion and Gasification*. Plenum Chemical Engineering Series, New York, 1985.

[63] Blasi, C.D. Combustion and gasification rate of lignocelluloses char. *Prog Energ Combust*. **35**(2), 121-140, 2009.

[64] Walker, P.L., Rusinko, F., Austin, L.G. Gas reaction in carbon. *Adv Catal*. **11**, 133-221, 1959.

[65] Petersen, L., Werther, J. Experimental investigation and modelling of gasification of sewage sludge in a circulating fluidized bed. *Chem Eng Process*. **44**(7), 717-736, 2005.

[66] Probstein, R.F., Hicks, R.E. *Synthetic Fuels*. Dover Publication, 2006.

[67] Loppinet-Serani, A., Aymonier, C., Cansell, F. Current and foreseeable application of super critical water for energy and environment. *Chem Sus Chem*.**1**, 486-503, 2008.

[68] UNFCCC. *Clarification of Definition of Biomass and Consideration of Changes in Carbon Pools due to a CDM Project Activity*. EB-20, Appendix: 18, 2005.

[69] Bergman, P.C.A., Boersma, A.R., Kiel, J.S.A., Prins, M.J., Ptasinski, K.J., Janssen, F.J.J.G. *Torrefaction for Entrained Flow Gasification of Biomass*. Energy Centre of the Netherlands, ECN Report, ECN-C-05-067, 2005a.

[70] Klass, D.L. *Biomass for Renewable Energy, Fuels and Chemicals*. Academic Press, Boston, 1998.

[71] Miline, T. Pyrolysis: The thermal behaviour of biomass below 600 °C (Chapter: 5). In: Reed T.B. et al. eds., *Encyclopaedia of Biomass Thermal Conversion*, 3rd Ed. Biomass Energy Foundation Press, Golden Colorodo, 2002, 96-131.

[72] Diebold, J.P., Bridgewater, A.V. Overview of fast pyrolysis of biomass for the production of liquid fuels. In: *Development in Thermochemical Biomass Conversion*, A.V. Bridgewater & D.G.B. Boocock et al. eds., Blackaie Academic and Professional, 1997, 5-27.

[73] Desch, H.E., Dinwoodie, J.M. *Timber: Its Structure Properties and Utilization*, 6th ed., Macmillan Press, 1981.

[74] Maclean, J.D. Thermal conductivity of wood. T Am Soc Heating Ventilation Eng. **47**, 323-354, 1941.

[75] Kitini, O., Hall, C.W. *Biomass Hand Book*. Gordon and Breach Science Publisher, 1989.

[76] Jenkins, B.M. Physical properties of biomass. In: *Biomass Handbook*, O. Kitani, & C.W. Hall et al., eds., Gordon and Breach Science Publisher, Amstradam, 1989,

[77] Perry, R.H., Green, D.W. *Perry's Chemical Engineers Handbook*, 7^{th} ed., McGraw Hill, New York, 1997.

[78] Dutta, P.P., Baruah, D. Gasification of tea (Camellia sinensis (L.) O. Kuntze) shrubs for black tea manufacturing process heat generation in Assam, India. *Biomass Bioenerg.* **66**, 27-38, 2014.

[79] Singh, R.N., Jena, U., Patel, J.B., Sharma, A.M. Feasibility study of cashew nut shells as an open core gasifier feedstock. *Renew Energ.* **31**, 481-487, 2006.

[80] Jayah, T.H., Aye, L., Fuller, R.J., Stewart, D.F. Computer simulation of a woody downdraft gasifier for tea drying. *Biomass Bioenerg.* **25**, 459-469, 2003.

[81] Bhoi, P.R., Singh, R.N., Sharma, A.M., Patel, S.R. Performance evaluation of open core gasifier on multi fuels. *Biomass Bioenerg.* **30**, 575-579, 2006.

[82] Pathak, B.S., Patel, S.R., Bhava, A.G., Bhoi, P.R., Sharma, A.M., Shah, N.P. Performance evaluation of an agricultural residue based modular throat type down draft gasifier for thermal application. *Biomass Bioenerg.* **32**, 72-77, 2008.

[83] Dutta, P. P., Jain, B.C., Knowar, D. and Baruah, D.C. Experimental heat transfer study of a woody biomass gasifier. In: *Proceeding of 4^{th} SEE Forum Meeting and Renewable Energy Asia*, V.K. Vijay, H.P., Garg et al. eds. Narosa, New Delhi, 2008, 998-905.

[84] Masek, O., Konno, M., Hosokai, S., Sonoyama, N., Norinaga, K., Hayashi, J. A study on pyrolytic gasification of coffee grounds and implications to allothermal gasification. *Biomass Bioenerg.* **32**, 78-89, 2008.

[85] Wilson, L., John, R.G., Mhilu, C.F., Yang, W., Blasiak, W. Coffee husk gasification using high temperature air-steam agent. *Fuel Process Technol.* **91**, 1330-1337, 2010.

[86] Zainal, Z.A., Rifau, A., Quadir, G.A., Seetharamu, K.N. Experimental investigation of a downdraft biomass gasifier. *Biomass Bioenerg.* **23**, 283-289, 2002.

[87] Tippayawong, N., Chaichana, C., Promwangkwa, A., Rerkkriangkrai, P. Gasification of cashew nut shells for thermal application in local food processing factory. *Energ Sustain Dev.* **15**, 69-72, 2011.

[88] Dasappa, S., Sridhar, H.V., Paul, P.J., Mukunda, H.S. Biomass gasification – a substitute to fossil fuel for heat application. *Biomass Bioenerg* **25** (6), 637 – 649, 2003.

[89] Dasappa, S., Paul, P.J., Mukunda, H.S., Rajan, N.K.S., Sridhar, G., Sridhar, H.V. Biomass gasification technology – a rout to meet energy needs. *Curr Sci India.* **87** (7), 908-916, 2003.

[90] Patel, S.R., Bhoi, P.R., Sharma, A.M., Shah, N.P. Field testing of SPRERI's open core gasifier for thermal application. *Biomass Bioenerg.* **30**(6), 580-583, 2006.

[91] Panwar, N.L., Rathore, N.S., Kurchania, A.K. Experimental investigation of open core downdraft biomass gasifier for food processing industry. *Mitigation Adaptation Strategies and Global Change.***14**, 547-556, 2009.

[92] Singh, R.N., Patil, K.N., Ramana, P.V. Performance evaluation of biomass gasifier based thermal backup for solar dryer. *SESI Journal.* **9**, 115-122, 1999.

[93] Botheju, W.S., Amarathunge, K.S., Mahmad, M.T.Z. Modelling Moisture desorption isotherm and thermodynamic properties of fermented tea *dhool* (Camellia sinensis var. assamica). *Drying Technol.* **26**(10), 1294-1299, 2008.

[94] Basunia, M.A., Abe, T. Thin layer solar drying characteristics of rough rice under natural convection. *J Food Eng.* **47**(4), 295-301, 2001.

[95] Can, A. Drying kinetics of pumpkin seeds. *Int J Energ Res.* **24**(11), 965-975, 2000.

[96] Kiranoudis, C.T., Maroulis, Z.B., Tasami, E., Marinos-Kouris, D. Drying kinetics of some fruits. *Drying Technol.* **15**(5), 1399-1418, 1997.

[97] Dutta, P.P., Baruah, D.C. Drying modelling and experimentation of Assam black tea (*Camellia sinensis*) with producer gas as a fuel. *Appl Therm Eng.* **63**, 495-502, 2014.

[98] Handerson, S.M. Progress of developing the thin layer drying equation. *Transactions of ASAE.* **17**(6), 1167-1172, 1974.

[99] Whitaker, T., Barre, H.J., Hamdy, M.Y. Theoretical and experimental studies of diffusion in spherical bodies with a variable diffusion coefficient. *Transactions of ASAE.* 12(5), 668–672, 1969.

[100] Crank, J. *The Mathematics of Diffusion.* Claredon Press: Oxford, England; 1975.

[101] Ece, M.C., Cihan, A. A liquid diffusion model for drying rough rice. *Transaction of ASAE.* **15**, 156-159, 1993.

[102] Dimartas, C., Ayhan, T., Kaygusuz, K. Drying behaviour of hazelnut, *J Sci Food Agri.* **76**(4), 559-564, 1998.

[103] Crisp, J., Woods, J.L. The drying properties of rapeseed, J Agri Eng Res. **57**, 89-97, 1994.

[104] Parry, J.L. Mathematical modelling and computer simulation of heat and mass transfer in agricultural grain drying. J Agri Eng Res. **32**(1), 1-29, 1985.

[105] Sharaf-Eldeen, Y.I., Blaisdell, J.L., Hamdy, M.Y. A model for ear corn drying. *Transactions of ASAE.* **23**(5), 1261-1265, 1980.

[106] Henderson, S.M., Pabis, S. Grain drying theory I: Temperature effect on drying coefficient. *J Agri Eng Res.* **6**(3), 169-174, 1969.

[107] Watson, E.L., Bhargava, V.K. Thin layer studies on wheat. *Canadian J Agri Eng.* **16**(1),18-22, 1974.

[108] Moss, J.R., Otten, L. A relationship between colour development and moisture content during roasting of peanut. *Canadian Inst Food Sci Technol.* **22**, 34-39, 1989.

[109] Madamba, P.S., Driscoll, R.H., Buckle, K.A. Thin layer drying characteristics of garlic slices. *J Food Eng.* **299**(1), 75-97, 1996.

[110] Lewis, W.K. The rate of drying of solid materials, *Ind Eng Chem.* **13**,427, 1921.

[111] Bruce, D.M. Exposed layer barely drying, Three model fitted to new data upto 150°C. *J Agr Eng Res.* **32**(4), 337-347, 1985.

[112] Wang, C. Y., & Singh, R. P. Use of variable equilibrium moisture content in modelling rice drying. *Transaction of ASAE.* **78**(6), 6505, 1978.

[113] Hutchinson, D., Otten, L. Thin layer air drying of soybeans and white beans, *J Food Technol.* **18**(4), 507-524, 1983.

[114] Agrawal, Y.C, Singh, R.P. Thin Layer Studies on Short Grain Rice. *Transaction of ASAE.* **77**, 3531, 1977.

[115] Overhault, D.G., White, G.M., Hamilton, H.E., Ross, I.J. Drying soybean with heated air. *Transactions ASAE.* **16**(1), 112-113, 1973.

[116] Keey, R.B. *Drying Principle and Practice.* Pregoman Press, New York, 1972.

[117] Klein, S.A. Calculation of flat plate collector loss coefficient. *Sol Energ.* **17**(1), 79-80, 1975.

[118] Kalogirou, S. *Solar Energy Engineering: Processes and System.* Elsevier, Oxford, 2009.

[119] Ramadan, M.R.I., El-Sebaii, A.A., Aboul, E.S., El-Bialy. E. Thermal performance of a packed bed double pass solar air heater. *Energy* **32**, 1524-1535, 2007.

[120] Sopian, K., Supranto, Daud, W. R. W., Yatim, B, & Othman., M.Y. Thermal performance of the double pass solar collector with and without porous media. *Renew Energ.* **18**(4), 557-564, 1999.

[121] Bharadwaj, S.S., Singh. D., Bansal. N. K. Design and thermal performance of a matrix solar air heater. *Energy Convers Manage.* **21** (4), 253-256, 1981.

[122] Shoemaker, M. J., Notes on solar collectors with unique air permeable media. *Sol Energ.* **5**, 138-141, 1961.

[123] Mishra, C.B., Sharma, S.P., Performance study of air heated packed bed solar energy collectors. *Int J Energ.* **6** 153-157, 1981.

[124] Choudhuri, C., Garg, H.P. Performance of air heating collectors with packed air flow passage. *Sol Energ.* **50** (3), 205-221, 1993.

[125] Chau, K.V., Henderson, S.M. Performance of matrix solar collector for heating air. *T ASME.* **20**(3), 558-561, 1997.

[126] Kolb, A., Winter, .E.R.F., Viskanta, R. Experimental studies on solar air collector with metal matrix absorber. *Sol Energ.* **65** (2), 91-98, 1999.

[127] Tong. L.S., London. A.L., Heat transfer and flow friction characteristics of woven-screen and cross-rod matrices. *T ASME* **79**, 1558-1570, 1957.

[128] Kays. W.M.. London. A.L. *Compact Heat Exchangers*. McGraw Hill. New York , 1964.

[129] Hamid, Y.H.. Beckman. W. A. Performance of air cooled radiative heated screen matrices. *J Eng Gas Turbine Power.* **93** (2), 221-224, 1971.

[130] Bhusan, B., Singh, R. Nusselt number and friction factor correlations for solar air heater duct having artificially roughened absorber plate. *Sol Energ.* **85**, 1109-1118, 2011.

[131] Hans, V.S., Saini, R.P., Saini, J.S. Performance of artificially roughened solar air heaters-a review. *Renew Sust Energ Rev.* **13**, 1854-1869, 2009.

[132] Varun, Saini, R.P., Singal, S.K. A review on roughness geometry used in solar air heaters. *Sol Energ.* **81**, 1340-1350, 2007.

[133] Saini, R.P., Verma, J. Heat transfer and friction factor correlations for a duct having dimple-shape artificial roughness for solar air heaters. *Energy* **33**, 1277-1287, 2008.

[134] Vennard, J.K., Street, R.L. *Elementary Fluid Mechanics*. John Wiley & Sons, New York, 1982.

[135] Landau, L.D., Lifshitz, E.M. *Fluid Mechanics*, Vol. 6. Butterworth-Heinemann, Oxford, 2000.

[136] Prasad, K., Mullick, S.C. Heat transfer characteristics of a solar air heater used for drying purposes. *Appl Energ.* **13**, 83-93, 1983.

[137] Prasad, B.N., Saini, J.S. Effect of artificial roughness on heat transfer and friction factor in a solar air heater. *Sol Energ.* **41**, 550-560, 1988.

[138] Saini, R.P., Saini, J.S. Heat transfer and friction factor correlations for artificially roughened ducts with expended metal mesh as roughness element. *Int J Heat Mass Tran.* **40** (4), 973-986, 1979.

[139] Emerson, W.H. Heat transfer in a duct in region of separated flow. In: *Proceeding of Third International Heat Transfer Conference*. 267-275, 1966.

[140] Edwards, F.J., Sheriff, N. The heat transfer and friction factor characteristics for forced convection air flow over a particular type of rough surface. In: *Proceeding of International Heat Transfer Conference, ASME.* 415-425, 1961.

[141] Dipperey, D.F., Sabersky, R.H. Heat and momentum transfer in smooth and rough tubes at various Prandtl number. *Int J Heat Mass Tran.* **6**(5), 329-353, 1963.

[142] Sheriff, N., Gumley, P. Heat transfer and friction properties of surface with discrete roughness. *Int J Heat Mass Tran.* **9**(12), 1297-1320, 1966.

[143] Webb, R.L., Eckert, E.R.G., Goldstein, R.J. Heat transfer and friction in tubes with repeated rib roughness. *Int J Heat Mass Tran.* **14**(4), 601-617, 1971.

[144] Dutta, P.P., Keot, A., Gogoi, A., Bhattacharjee A., Saharia, J., Sharma, N., Baruah, D.C. A Study on some techniques for improving thermo-hydraulic performance of a solar air heater. *Int J Emerging Technol Adv Eng.* **3**(3), 225-233, 2013.

[145] Dutta, P.P., Saharia, J., Sarma, N., Baruah, D.C. Thermal performance studies of a rectangular duct solar air heater with hemispherical protrusion. In: Proceeding of *22th National and 11th International ISHMT-ASME Heat and Mass Transfer Conference*. IITkgp, December 27-31, 2013.

[146] Prasad, B. N. Thermal performance of artificially roughen solar air heater. *Sol Energ.* **91**(1), 59-67, 2013.

[147] Varun, Saini, R.P., Singal, S.K. Investigation of thermal performance of solar air heater having roughness elements as a combination of transverse ribs on absorber plate. *Renew Energ.* **33**(6), 1398-1405, 2008.

[148] Peng, D., Zhang, X., Dong, H., Lv, K. Performance study of a novel solar air collector. *Appl Therm Eng.* **30**(16), 2594-2601, 2010.

[149] Ho, C.D., Yeh, H.M., Chen, T.C. Collector efficiency of upward type double-pass solar air heaters with fins attached. *Int Commun Heat Mass.* **38**(1), 49-56, 2011

[150] Hans, V.S., Saini, R.P. and Saini, J.S. Performance of artificially roughened solar air heaters-a review. *Renew Sust Energ Rev.* **13**(8), 1854-1869, 2009.

[151] Saini, R.P., Verma, J. Heat transfer, and friction factor correlations for duct having dimple shape artificial roughness for solar air heaters. *Energy.* **33** (8), 1277-1287, 2008.

[152] Akpinar, E.K., Kocyigit F. Experimental investigation of thermal performance of solar air heater having different obstacles on absorber plates. *Int Commu Heat Mass Tran.* **37**(4), 416-421, 2010.

[153] Bhushan, B., Singh, R. A review on methodology of artificial roughness used in duct of solar air heaters. *Energy.* **35** (1), 202-212, 2010.

[154] Khattab, N.M. Evaluation of perforated plate solar air heater. *Int J Sol Energ.* **21**, 45-62, 2000.

[155] Languri, E.M., Taherian, H., Hooman, K., Reisel, J. Enhanced double-pass solar air heater with and without porous medium. *Int J Green Energ.* **8**, 643-654, 2011.

[156] Imbriale, M., Panelli, M., Cardone, G. Heat transfer enhancement with natural convection with ribs. *Quant Infra-Red Tomography.* **9** (1), 55-67, 2012.

[157] Bharadwaj, G., Kaushal, M., & Goel, V. Heat transfer and friction characteristics of an equilateral triangular solar air heater duct using inclined continuous ribs as roughness element on the absorber plate. *Int J Sust Energ.* **32** (6), 515-530, 2013.

[158] Rallabandi A.P., Yang, H., Han J.C. Heat transfer and pressure drop correlations for square channels with 45 deg ribs at high Reynolds numbers. *J Heat Tran.* **131**, 1-10, 2009.

[159] Saha, S. K., Dutta, A. Thermo-hydraulic study of laminar swirl flow through a circular tube fitted with twisted tape. *J Heat Tran.* **123**, 417-427, 2001.

[160] Saha, S.K. Thermo-hydraulics of laminar flow through rectangular and square ducts with axial corrugation roughness and twisted tapes with oblique teeth. *J Heat Tran.* **132**, 1-10, 2010.

[161] El-Sebaii, A.A. Aboul-Enein, S.,.Ramadan, M.R.I,. Shalaby, S.M, Moharram, B.M. Thermal performance investigation of double pass-finned plate solar air heater. *Appl Energ.* **88**, 1727-1729, 2011.

[162] Aharwal, K.R. B.K. Gandhi, B.K., Saini, J.S. Experimental investigation on heat-transfer enhancement due to a gap in an inclined continuous rib arrangement in a rectangular duct of solar air heater. *Renew Energ.* **33**, 585-595, 2008.

[163] Mohammed, H.A., Abed A.M, Wahid, M.A. The effects of geometrical parameters of a corrugated channel with in out-of-phase arrangement. *Intl Commun Heat Mass*. **40**, 47-57, 2013.

[164] Tiwari, G.N. *Solar Energy fundamentals, Design, Modelling and Applications*, Narosa Publishing House, New Delhi, India, 2008.

[165] Dutta, P. P., Saharia, J., Sarmah, N., Baruah D.C., Dutta B., Das, R. Studies on some solar thermal energy absorber for hot air generation. In: *Proceeding of International Seminar, Workshop on Energy, Sustainability (ISWESD-2012)*, 146-150, 2012.

[166] Cortes, A., Piacentini, R. Improvement of the efficiency of a bare solar collector by means of turbulence promoters. *Appl Energy*. **36** (4), 253-256, 1990.

[167] Gupta, D., Solanki, S.C., Saini, J.S. Thermo hydraulic performance of solar air heaters with roughened absorber plates. *Sol Energ*. 61(1):33-42, 1997.

[168] Leon, A., M., Kumar, S. Design and performance evaluation of a solar assisted biomass drying system with thermal storage, *Dying Technol*. **26**, 936—947, 2008.

[169] Hirunlabh, J., Paraboon, T, Namprakai, P., Khedari, J., Pairintra, R. A new type of modular dryer combining solar energy and producer gas, *Drying Technol*. **15** (3 & 4), 1203-1211, 1997.

[170] Gupta, M.K., Kaushik, S.C. Exergetic utilization of solar energy for feed water preheating in a conventional thermal power plant, *Int J Energy Res*. **33**, 593 – 604, 2009.

[171] Lokeswaran, S., Eswaramoorthy, M. Experimental study on a solar dyer system with a biomass back up heater, *Energ Source Part A*. **35**, 467- 475, 2013.

[172] Prasad, J., Vijay, V.K., Tiwari, G.N., Sorayan, V.P.S. Study on performance evaluation of hybrid dryer for turmeric (Curcuma long L.) drying at village scale. *J Food Eng.* **75**, 497 – 502, 2006.

[173] Bena, B., Fuller, R.J. Natural convection solar dryer with biomass backup heater, *Sol Energ.* **72** (1), 75-83, 2002.

[174] Kholmirzaev, N.S., Khairiddinov, B.E., Kim, V.D. Heat balance of cotton dryer with combined fuel sun recuperative heat supply. *Appl Sol Energ.* **45**(1), 21-24, 2009.

[175] Srinivas, T., Reddy, B.V. Hybrid solar-biomass power plant without energy storage. *Case Study Therm Eng.* **2**, 75-81, 2014.

[176] Lopez-Vidana, E.C., Mendez-lagunas, L.L., Rodriguez-Ramirez, J. Efficiency of a hybrid solar-gas dryer. *Sol Energ.* **93**, 23-31, 2013.

[177] Hossain, M.A., Bala, B.K. Drying of hot chilli using solar tunnel dryer. *Sol Energy* **81**, 85-92, 2007.

[178] Sreekumar, A. Techno-economic analysis of a roof-integrated solar air heating system for drying fruit and vegetables. *Energ Convers Manage.* **51**, 2230-2238, 2010.

[179] Palaniappan, C., Subramanian, S.V. Economics of solar air pre-heating in South Indian tea factories: A case study. *Sol Energ.* **63**(1), 31-37, 1998.

[180] Madhlopa, A., Ngwalo, G. Solar dryer with thermal storage with biomass backup heater. *Solar Energ.* **81**, 449-462, 2007.

[181] Khanna, M.L. Design data for solar heating of air using a heat exchange and storage system. *Solar Energ.* **11**, 142-145, 1967.

[182] Ayensu, A. Dehydration of food crops using a solar dryer with convective heat flow. *Sol Energ.* **59**, 121-126, 1997.

[183] Aboul-Enein, S., El-Sebaii, Ramadan, M.R.I., El-Gohary, H.G. Parametric study of solar air heater with and without thermal storage for solar drying. *Renew Energ.* **21**, 505-522, 2000.

[184] Prasad, J., Vijay, V.K. Experimental studies on drying of *Zingiber officinale, Curcuma l. and Tinosopora cordifolia* in solar–biomass hybrid drier. *Renew Energ.* **30**, 2097–2109, 2005.

[185] Hossian, M.A., Amer, B.M.A., Gottschalk, K. Hybrid solar dryer for quality dried tomato. *Drying Technol.* **26**, 1591- 1601, 2008.

[186] Chavan, R.B., Yakupitiyag, A, Kumar, S. Mathematical modelling of drying characteristics of Indian Mackerel (Rastrilliger kangurta) in solar biomass hybrid cabinet dryer. *Drying Technol.* **26**, 1552-1562, 2008.

[187] Kumar, S., Bhattacharya, S.C. Technology packages: *Solar, Biomass and Hybrid Dryers, Renewable Energy Technologies in Asia.* Regional Energy Resources Information Centre (RERIC), AIT, Thailand, 44-60, 2005.

[188] Gunasekaran, K., Shanmugam, V., Suresh, P. Modelling and analytical study of hybrid solar dryer integrated with biomass dryer for drying *Coleus Forskohlii* stems. *IACSIT Coimbatore Conferences, 2012.*

[189] Othman M.Y.H., Sopian, K., Yatim, B., Daud, W.R.W. Development of advanced solar assisted drying systems. *Renew Energ.* **31**,703–709, 2006.

[190] Reyes, A., Mahn, A., Cubillos, F., Huenulaf, P. Mushroom dehydration in a hybrid-solar dryer. *Energ Convers Manage.* **70**, 31-39, 2013.

[191] Boughali, S., Benmoussa, H, Bouchekima, B, D. Mennouche, D., Bouguettaia, H., Bechki, D. Crop drying by indirect active hybrid solar – Electrical dryer in the eastern Algerian Septentrional Sahara. *Sol Energ.* **83**, 2223-2232, 2009.

[192] Farkas, I. Integrated use of solar energy for crop drying. *Drying Technol.* **31**, 866-871, 2013.

[193] Leon, M.A., Kumar, S., Bhattacharya, S.C. A comprehensive procedure for performance evaluation of solar food dryer. *Renewable and Sustainable Energy Review* **3**, 367-393, 2002.

[194] Luh B.S., Woodfoof, J.G. *Commercial Vegetable Processing*. The Avi Publishing Company. USA. 1975.

[195] Mastekbayeva, G.A., Leon, M.A., Kumar, S. Performance evaluation of a solar tunnel dryer for chilli drying, in: Asean Seminar and Workshop on Solar Drying Technology, Phitsanulok, Thailand, 1998, 15–26.

[196] Tokar, G.M. Food drying in Bangladesh. Agro-based industries and technology project (ATDP), IFDC, Dhaka 1213, and December, 1997. Available from: http://www.agrobengal.org/special/fooddry.htm. 1997

[197] Pengpad, S, Rakwichian, W. Development of an air recycle solar drying system for continuous banana drying, in: Asean Seminar and Workshop on Solar Drying Technology, Phitsanulok, Thailand, 1998. 27–34.

[198] Nathakaranakule, S. A comparative study of various methods of banana drying, in: Proceedings of ASEAN Seminar on Drying Technology. 1997, 660–667.

[199] Hughes, K.V., Willenberg, B.J. Quality for Keeps—Drying Foods. University of Missouri-Columbia Human Environmental Sciences publication GH1562—Reviewed May 15, 1994. Available from: http://muextension.missouri.edu/xplor/hesguide/foodnut/gh1562.htm.

[200] Mahapatra, A.K., Imre, L. Role of solar agricultural drying in developing countries. *International Journal of Ambient Energy* **2(4)**, 1990, 205–210.

[201] Vargas TV, Camacho SA. Drying of fruits and vegetables—experiences in Bolivia. Publication of Energetica (Bolivia) and FAKT (Germany), 1996.

[202] Leniger, H.A., Beverloo WA. *Food Process Engineering*. USA: D. Reidel Publishing Company, 1975.

[203] Crapiste, G.H., Rotstein, E. Design and performance evaluation of dryers. In: Valentas Kenneth J, Rotstein Enrique, Singh Paul, editors. *Handbook of Food Engineering Practice*. New York: CRC Press; 1997.

[204] Soponronnarit S, Dussadee N, Hirunlabh J. Computer simulation of solar-assisted fruit cabinet dryer. *RERIC International Energy Journal,* **14(1)**, 1992.

[205] *Annual Book of ASTM Standard.* American Society for Testing of Materials. Philadelphia, 1983, p. 19103.

[206] Mettanant, V., Basu P, Bulter J. Agglomeration of biomass fed fluidized bed gasifier and combustor. *Canadian J Chem Eng.* **87**, 656-684, 2009.

[207] Buragohain, A. K. *Identification of plants and birds of Assam.* Tezpur University, Assam, India, 2010.

[208] Dutta, P.P., Pandey, V., Sen, S., Das, A.R., Nath, A. and Bruah, D.C. Fuel characteristics of some indigenous plant. *Int J Emerg Technol Adv Eng.* **3**(3): 570-576, 2013.

[209] Reed, T.B., Das, A. *Hand Book of Biomass Downdraft Gasifier Systems.* Golden Co; Biomass Energy Foundation Press; 1988.

[210]Ankur. Ankur biomass gasifier model WBG-10 in scrubber gas mode for thermal applications. Vadodara (India): ASCENT, 20, 2008.

[211] Inserf. Junker gas calorimeter (Category No.IRI 023). Chennai (India): Instrumentation and Refrigeration India, 2008.

[212] Rockwin. Fuel gas turbine flow meter. Ghazibad (India): Rockwin Flow meter India (P) Limited, 2008.

[213] Shivaki. Temperature data-logger. New Delhi (India): Sonics Control System, 2008.

[214] Singh, R.N., Patil, K.N., Ramana, P.V. Performance evaluation of biomass gasifier based thermal backup for solar dryer. *SESI Journal.* **9**, 115-22, 1999.

[215] Sokhansanj, S., Jayas, D.S. Drying of foodstuffs, In: Majumdar AS, editor. *Hand Book of Industrial Drying.* 3rd ed. London; CRC Press, 550-55, 2006.

[216]*Bureau of Energy Efficiency Code for Dryer.* Ministry of Power. Government of India, 2006.

[217]Park, R.M., Hoersch, M. *Manual on use of Thermocouples in Temperature Measurement*. 4th ed. West Concohocken, ASTM; 1993.

[218] Holman, J.P. *Experimental Methods for Engineers*.7th ed. New Delhi, The McGraw-Hill Companies; 2007.

[219] Heldman, R.D., Lund, B.D. *Hand Book of Food Engineering*: 2nd ed. London; CRC Press; 2007.

[220] Parikh, P.P. (IIT Bombay, Department of Mechanical Engineering). *Qualifying, Testing and Performance Evaluation of Biomass Gasifier and Gasifier-Engine System*. Test procedure no. I: Ministry of New and Renewable Energy, Govt. Of India, New Delhi, Report No: 203-01-04/97-BM, 2000.

[221]Sheth, N.P., Babu, V.B. Experimental studies on producer gas generation from wood waste in a downdraft biomass gasifier. *Bio-resource Technol.* **100**, 3127-3133, 2009.

[222]Dutta, P.P., Pandey, V., Das, A.R., Sen, S., Baruah, D.C. Down draft biomass gasification modelling for some indigenous biomass for thermal application. In: *Proceeding of 4th International Conference on Advances in Energy Research*, IIT Bombay, 166-175, 2013.

[223] ASHRAE Standard. *ASHRAE Hand Book Fundamentals*. Atlanta, GA: American Society of Heating Refrigeration and Air -conditioning Engineers; 2009.

[224] Wu, C.Y., Chen, K.H., Yang S.Y. Experimental study of porous metal burner for domestic stove application. *Energ Convers Manage*. **77**, 380-388, 2014.

[225] Jone, H.R.N. *The Application of Combustion Principles to Domestic Gas Burner*. Taylor and Francis, London, 2005.

[226]Zhang, Q., Litchfield, J.B. An optimization of intermittent corn drying in a laboratory scale thin layer dryer. *Drying Technol.* **9**(2), 383-395, 1991.

[227] Panwar, N.L., Rathore, N.S. Design and performance evaluation of a 5 kW

producer gas stove. *Biomass Bioenerg.* **32**, 13-49-1352., 2008.

[228]Akpinar, E.K. Mathematical modelling of thin layer drying process under open sun of some aromatic plants. *J. Food Eng.* 77(4), 864-870, 2006.

[229] Panchariya, P.C., Popovic, D., Sharma, A.L. Thin layer modelling of black tea drying process. *J Food Eng.* **52**, 349-357, 2002.

[230] Hati Baruah, D. Investigation of Microwave Assisted Hot Air Drying Behaviour of CTC Tea (Camellia sinensis). PhD Thesis, Tezpur University, 2013.

[231] Temple, S.J., Boxtel, A.J.B.V. Modelling of fluidized bed drying of black tea. *J Agri Eng Res.* **74**(2), 203-212, 1999.

[232]Simal. S., Femenia, A., Garau, M.C., Rossello, C. Use of exponential Page's and Diffusion Models to simulate drying kinetics of kiwi fruits. *J Food Eng.* **79**(4), 323-328, 2005.

[233]Han J.C., Park, J.S., Lei C.K. Heat Transfer Enhancement in Channels with Turbulence Promoters. *Trans ASME J Eng Gas Turbine Power.* **107**(30), 628-635, 1985.

[234]Majumdar, A.S. *Hand Book of Industrial Drying.* 3rd ed. London; CRC Press, 2006.

[235]ANSI/ASHRAE Standard 93-2003, *Methods of Testing to Determine the Thermal Performance of Solar collectors.* ISSN 1041-2336, ASHRAE, Inc., 1791 Tullie Circle, Ne, Atlanta, GA30329, 2003.

[236] Turner, W.C., Doty, S. *Energy Management Hand Book.* 6th ed. Boca Raton; CRC Press; 2006.

[237]Rathore, N.S., Panwar, N.L., Chiplunkar, Y.V. Design and techno-economic evaluation of biomass gasifier for industrial thermal application. *Afr J Env Sci Technol.* **3**(1), 06-12, 2009.

[238]Siemons, R.V. Identifying a role for biomass gasification in rural electrification in developing countries: the economic perspective. *Biomass Bioenerg.* **20**(4), 271-285, 2001.

[239]Project Team natural resource census: national land use and land cover analysis using multi-temporal LISS-III (LULC-LII: 50K) e Project manual. Hyderabad: National Remote Sensing Centre; Document No.: NRSA/RSGIS-A/NRC/NLULCL3/TECHMAN/R02/JANUARY. 2006.

[240] Birol, F. *World Energy Outlook 2010.* International Energy Agency, France, 2010.

[241] Rural Energy [Internet]. Hyderabad (India): Indian Development gateway; 2011. Energy production; 2011, 01 August. [Cited 2012 June 14]. Available from: http://www.in dg.in/rural-energy/technologies-under-rural energy/energy production/ biomass gasification for thermal and electrical applications/.

[242] http://nbm.nic.in/ap_roadmap.html (Accessed on 08/05/2014).

[243] Resources [Internet]. Madison (Wisconsin): Leonardo Academy; 2011; Pollution Calculator; 2011, June 14 [Cited 2012 June 14]. Available from: // http://www.cleanerandgreener.org/resources/pollutioncalculator.html

[244]Duffie, J.A., Beckman, W.A. *Solar Engineering for Thermal Processes*, 3rd Eds. Wiely Inter-science, New York, 2006.

[245]Prasad, B.N., Saini, J.S., Thermo-hydraulic optimization of artificially roughened solar air heaters. In: *Proceeding of NSEC*, Solar Energy Society of India, Hyderabad, 1988.

[246] Karthikeyan, R., Rathnasamy, R. Thermal performance of Pin-Fin arrays. *Int J Adv Eng Sci Technol.* **10**(1), 125-138, 2011.

[247] Fath, H.E.S. Thermal performance of a simple design solar air heater with built-in thermal energy storage system. *Energ Convers Manage.* **36(10)**, 989–997, 1995.

[248] Ahmad, A., Saini, J.S., Verma, H.K. Thermo hydraulic performance of packed-bed solar air heaters. *Energ Consers Manage* **37(2)**, 205–214, 1996.

[249] Tiris, C., Ozbalta, N., Tiris, M., Dincer, I. Thermal performance of a new solar air heater. *Int Communi Heat Mass Trans* **22(3)**, 411–423, 1995a.

[250] Rachmat, R., Horibe, K., Suzuki, K. Experimental performance of an FRP solar drying house. *AgricEng J.* **7(3&4)**, 159–170, 1998.

[251] Brenndorfer, B., Kennedy, L., Bateman, O., Trim, D.S., Mrema, G.C., Brobby, C.W. *Solar dryers—their Role in Post-harvest Processing.* London: Commonwealth Science Council, 1987.

[252]Tiris, C., Tiris, M., Dincer, I. Investigation of the thermal efficiencies of a solar dryer. *Energ Convers Manage* **36(3)**, 205–212, 1995b.

[253] Rakwichian, W., Thadnium, V., Wiengmoon, B. Introduction to a solar dryer for the vegetable drying industry. Paper presented in: Asean Seminar and Workshop on Solar Drying Technology, Phitsanulok, Thailand. 113–118, 1998.

[254] Jannot, C. The evaporative capacity as a performance index for a solar drier-air heater. *Sol Energ.* **63(6)**, 387–391, 1998.

1. **Journal Publications**

- Dutta, P.P, Baruah, D.C. (2014). Modelling and Experimental Studies of Black Tea Using Producer Gas as Fuel. *Applied Thermal Engineering,* 63: 495-502.
- Dutta, P.P., Baruah D.C. (2014). Gasification of up rooted Tea Shrubs for Process Heat generation in Tea Manufacturing, *Biomass and Bioenergy*, 66: 27-38, 2014. (http://dx.doi.org/10.1016j.biombioe.2014.03.062
- Dutta, P.P, Baruah, D.C. (2014). Possibility of Biomass gasification in Tea Manufacturing Industries. *International Journal of Renewable Energy Technology*, 5(4): 310-322.
- Dutta, P.P., Pandey V., Das A.R., Sen, S., Baruah D.C. (2014). Downdraft Gasification Modelling and Experimentation of Indigenous Biomass for Thermal Application, *Energy Procedia,* 54: 21-34
- Dutta, P.P., Pandey V., Sen S., Das A.R., Nath A., Baruah D.C. (2013). Fuel characteristics of some indigenous plant. International Journal of Emerging Technology and Advanced in Engineering, 3(3): 570-576.
- Dutta, P.P., Keot A, Gogoi A, Bhattacharjee A., Saharia J., Sharma N., Baruah D. (2013). A study on some techniques for improving thermo-hydraulic performance of solar air heater. International Journal of Emerging Technology and Advanced Engineering, 3(3): 225-233.

2. **Conference Proceedings**

- Dutta, P.P, Saharia J., Sarmah, N., Baruah D.C. 2013. Thermal Performance Studies of a Rectangular Duct Solar Air Heater. 22th National and 11th International Conference of ISHMT, ASME, Heat and Mass Transfer Conference, IITKgp. (28-31/12/2013)
- Dutta, P.P., Pandey, V., Das, A.R., Sen, S., Baruah, D.C.2013. Downdraft Gasification Modelling of Indigenous Biomass for Thermal Application. IVth International Conference on Advances Energy Research, IIT Bombay , 10/12/2013-12/12/2013.

- Dutta P.P., Das A., Pandey V. (2013). Fuel Characteristics of Some Locally Available Biomass as a Potential Gasification Feedstock for Thermal Applications. International Conference Energy System Modelling, 09-11/12/2013, NIT, Durgapur.
- Dutta P.P., Saharia J., Sarmah N., Baruah D.C., Dutta B. (2012). Studies on Some Solar Thermal Collectors. International Seminar and Workshop on Energy, Sustainability, and Development, 12-14/10/2013, Sibsagar College.
- Dutta P.P., Baruah D.C. (2012). A Fluidized Bed tea Dryer Power with Producer Gas. International Seminar and Workshop on Energy, Sustainability, and Development, 12-14/10/2013, Sibsagar College.
- Dutta P.P., Baruah D.C. (2011). Performance Testing of a Renewable Energy Based Tea Dryer. National Conference on Water, Energy and Biodiversity, 20-22/08/2011 at Institution of Engineers, Tripura State Centre.
- Dutta P.P., Baruah D.C. (2011). Thermal Analysis of a Fluid Bed Tea Dryer. ICORE, Tezpur University, 02- 04/11/2011.

Appendix A1: Experimental uncertainty analysis of measuring variables

Errors and uncertainties in the experiments may arise from instrument selection, circumstance, calibration, environment, observations and readings, and test planning [217]. Appropriate instrument were used to measure different variables such as tea dryer different temperatures, relative humidity, and weight losses of fermented tea etc. Let w_R is the uncertainty in the result and $w_1, w_2, \ldots, w_n$ are the uncertainties in the independent variables of the function. Then uncertainties in the independent variables are all with same odds. Therefore, uncertainty in result is comprised of all these odds given as follows [218].

$$w_R = \sqrt{[\{\frac{\partial R}{\partial x_1} w_1\}^2 + \{\frac{\partial R}{\partial x_2}\}^2 + \{\frac{\partial R}{\partial x_3} w_3\}^2]}$$

The total uncertainty in measurement of drying air inlet temperature, outlet temperature, average tray temperature, and ambient temperature may arise from thermocouples and digital thermometer (data logger), connection points and readings. Total temperatures measurement uncertainty is:

$= [(w_{thermcouples})^2 + (w_{datalogger})^2 + (w_{connection\ point})^2 + (w_{reading})^2]^{½} = [0.25^2 + 0.15^2 + 0.1^2 + 0.2^2]^{½} = 0.37$

The total uncertainty in the measurement of time of temperature and time of mass loss values may result from oscillation of time meter and reading as:

$= [(w_{oscillation})^2 + (w_{reading})^2]^{½} = [0.00032^2 + 0.1^2]^{½} = 0.10$

The total uncertainty in measurement of mass loss may arise from digital balance, reading, and friction of tray. It is as follows:

$= [(w_{digital\ balance})^2 + (w_{reading})^2 + (w_{friction})^2]½ = [(0.03)^2 + (0.01)^2 + (0.45)^2]½ = 0.45$

The total uncertainty in measurement of air velocity may arise from anemometer, reading, and air leaking as:

$= [(w_{anemometer})^2 + (w_{reading})^2 + (w_{leaking})^2]½ = [(0.02)^2 + (0.\ 1)^2 + (0.1)^2]½ = 0.14$

Appendix A2: Statistical analysis of different thin layer models

Model	Temp. (°C)	R^2	k1(× 10^{-4})	A1	RMSE (× 10^{-5})	χ^2 (× 10^{-9})	k(× 10^{-4})	n /A
The Page model	80	0.935			3.82	1.72	4.08	1.16
	90	0.940			2.46	0.72	5.75	1.18
	100	0.945			2.27	0.61	6.81	1.25
	110	0.930			38.08	171.4	7.12	1.28
The Henderson and Pabis model	80	0.954			1.09	0.141	16.51	1.25
	90	0.935			2.46	0.716	23.37	1.20
	100	0.965			0.492	0.029	30.40	1.10
	110	0.968			0.375	0.017	33.91	1.00
Lewis model	80	0.956			1.25	0.185	12.76	
	90	0.967			0.66	0.052	18.29	
	100	0.968			0.61	0.043	25.91	
	110	0.970			0.35	0.023	33.91	
Modified Page model	80	0.956			0.84	0.083	15.95	0.8
	90	0.959			0.64	0.048	21.52	0.85
	100	0.969			0.49	0.029	25.91	1
	110	0.968			0.43	0.022	30.81	1.1
Two term model	80	0.934	17.92	0.40	2.01	0.478	17.35	0.90
	90	0.925	27.15	0.45	27.75	90.97	34.69	0.95
	100	0.887	45.82	0.55	1387	227000	24.07	1.0
	110	0.878	48.95	0.60	13868	227000	21.82	1.1

Appendix A3: Heat transfer study of solar air heater

According to the assumptions made on the physical model, the heat balance of the solar collector may be given as below [244].

$$Q_s(\tau\alpha) = I_c F(\tau\alpha) = Q_u + Q_{cl}$$

Heat loss of collector Q_{cl} is given by:

$$Q_{cl} = FU_{cl}(T_p - T_a)$$

$$U_{cl} = U_b + U_s + U_t$$

$$Q_u = \dot{m}C_p(T_o - T_i) = I_c F(\tau\alpha) - FU_{cl}(T_p - T_a)$$

$$\eta = \frac{Q_u}{Q_s} = (\tau\alpha) - U_{cl}\frac{T_p - T_a}{I_c} = F_R[(\tau\alpha) - U_{cl}\frac{T_i - T_a}{I_c}]$$

$$= A - B\frac{T_i - T_a}{I_c}$$

But for conventional solar air heater the above expression cannot be used since T_i is approximately equal to T_a. Therefore, the above equation may be modified based on collector heat gain factor (F_o) relating to air exit temperature [152].

$$\eta = F_0[(\tau\alpha) - U_{cl}\frac{T_0 - T_a}{I_c}]$$

The average convective heat transfer coefficient ($\bar{h}$) from hemispherical protruded roughen absorber and air flowing over it is given by following equation, where $\overline{t_p}$ and $\overline{t_a}$ are average aluminum absorber temperature and ambient air temperature respectively.

$$\bar{h} = \frac{mC_p(t_0 - t_i)}{A_c(\overline{t_p} - \overline{t_a})}$$

It was observed that variation of absorber temperatures along the flow direction was linear. Moreover, the variation of temperature in normal direction of airflow was incredibly small. The variation of flowing air temperature over the absorber plate was linear. Now the convective heat transfer coefficient ($\bar{h}$) is related with Nusselt number of artificially roughen (hemispherical protrusion) solar thermal absorber by following relation:

$\overline{Nu} = \frac{\bar{h}D}{k}$

The collector performance parameter heat removal factor (F_R) and collector efficiency factor (F') related with other variable as suggested by Duffi and Beckman [244].

$$F_R(\tau\alpha) = F_0(\tau\alpha)\left[\frac{\frac{mC_p}{A_c}}{\frac{mC_p}{A_c}+F_0\,U_l}\right]$$

$$F_R\,U_l = F_0U_l\left[\frac{\frac{mC_p}{A_c}}{\frac{mC_p}{A_c}+F_0\,U_l}\right]$$

$$F' = GC_p\left[ln\frac{F_0\,U_l}{F_R\,U_l}/U_l\right]$$

Thermo hydraulic performance of solar air heaters

The thermal efficiency of a solar air heater increases with increase in mass flow rate and with higher mass flow rate, and friction losses become higher. This increases the energy expenditure required to propel the air through the collector. Thus, it is necessary to consider the energy expenditure in the blower along with the useful energy gain [247, 249]. Cortes and Piacentini [166], Gupta et al. [167] proposed "effective efficiency", η_{eff} as:

$$\eta_{eff} = \frac{(q_u - \frac{P_m}{c})}{IA_p}$$

where c is the conversion factor to account for the conversion of high-grade mechanical energy to thermal energy and it is given by:

$$c = \eta_F\eta_m\eta_{tr}\eta_{th}$$

where η_F is the efficiency of the fan, η_m is efficiency of the motor, η_{tr} is the efficiency of the electric transmission from the power supply, and η_{th} is the efficiency of thermal conversion of the power plant.

The rate of useful thermal energy may be obtained from the equation:

$$q_u = F'[I(\tau\alpha) - \frac{U_L(t_o - t_i)}{2}]A_p$$

where, $F' = \frac{h}{(h + U_L)}$

The rate of useful energy gain of a solar air heater with artificial roughness may also be calculated by the following equation.

$$q_u = hA_p(t_{pm} - t_{fm})$$

or

$$q_u = mC_p(t_o - t_i)$$

The mechanical power consumed is given by following relation:

$$P_m = \mathrm{VA\Delta P}$$

where

$$\Delta P = \frac{2fLV^2\rho}{D}$$

Therefore,

$$P_m = \frac{VA2fL_cV^2\rho}{D} = V(WH)2fL_cV^2\rho/[\frac{2WH}{W+H}] = \rho f L_c V^3(W + H)$$

For artificially roughened solar air heaters friction factor (f)with mentioned geometry is given by following relation [133].

$$f = 0.1911(\frac{e}{D})^{0.196}(\frac{W}{H})^{-0.093} \quad (Re)^{-0.165}\exp[-0.993(1 - \beta/70)^2]$$

Substituting for power consumption, P_m , and for the rate of useful energy gain, q_u , the effective efficiency of a solar air heater can be calculated as:

$$\eta_{eff} = \frac{\{F[I(\tau\alpha) - U_L(t_o - t_i)/2]A_p - \rho f L_c V^3(W+H)/c\}}{IA_p}$$

The above equation may be used for determination of effective efficiency for a solar air heater with smooth absorber plate. The friction factor and heat transfer co-efficient for a solar air heater with a smooth absorber plate may be obtained from the Blasius and the Dittus-Boelter equations [233], respectively as:

$$f_s = 0.079(Re)^{-0.25}$$

$$h_s = 0.023\left(\frac{k}{D}\right)(Re)^{0.8}(\mathrm{Pr})^{0.6}$$

Thus for a solar air heater with smooth absorber plate:

$$F_s' = \frac{h_s}{h_s + U_L}$$

$$\eta_{eff} = \frac{\left\{F_s'\left[I(\tau\alpha) - \frac{U_L(t_o - t_i)_s}{2}\right]A_p - \frac{\rho f_s L V^3 (W+H)}{c}\right\}}{I A_p}$$

The pressure loss due to flow through the hemispherical protruded array is represented by a friction factor (f), based on the Darcy's relationship and it can be rewritten as:

$$f = \frac{2\Delta P}{(L_c/d)\left(\frac{m}{A_{ff}}\right)^2 (1/\rho)}$$

where,

$$A_{ff} = W(H + C) - N_x ed$$

This was considered by Karthikeyan and Rathnasamy [246].The values of the efficiency were computed for a set of system and operating parameters (absorber plate with hemispherical protrusion, relative roughness height, mass flow rate) for a given duct geometry.

Appendix A4: Air heater performance

Fig.A4.a shows that for constant $\frac{p}{e}$ (12), increased in $\frac{e}{D}$ (0.055) value caused augmentation of heat removal factor (F_R) for same Reynolds number. Similar trend was observed in case of collector efficiency factor (F'). For a given value of $\frac{p}{e}$ (12), Reynolds number and increased value of $\frac{e}{D}$ (0.045-0.055), there was an augmentation of Nusselt number 2.67 and 3.62 with respect to a smooth collector.

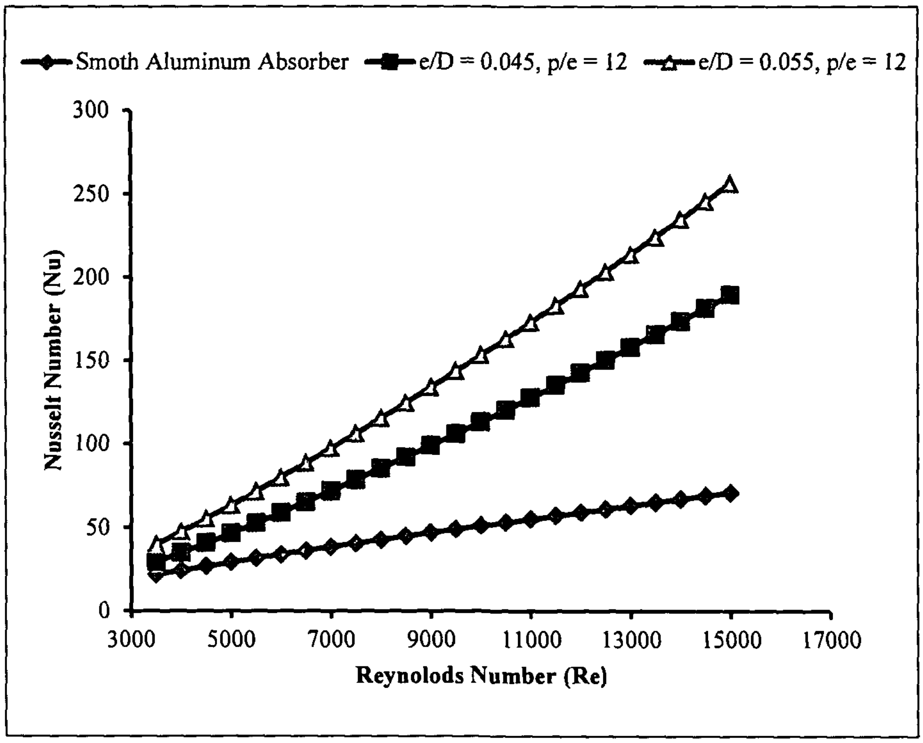

Fig.A4.a: Variation of Nusselt number with Reynolds number for constant p/e (12) and variable e/D

Fig. A4.b shows performance of the roughen collector compared to smooth collector for mass flow rate (0.0208 kg s^{-1} m^{-2}) of air over unit absorber area for $(\frac{p}{e})$ =12 and $(\frac{e}{D})$ = 0.055. The values of F_0U_l for roughen and smooth collectors were computed as 10 $Wm^{-2}K^{-1}$ and 3 $Wm^{-2}K$ and $F_0(\tau\alpha)$ as 0.837 and 0.377 respectively.

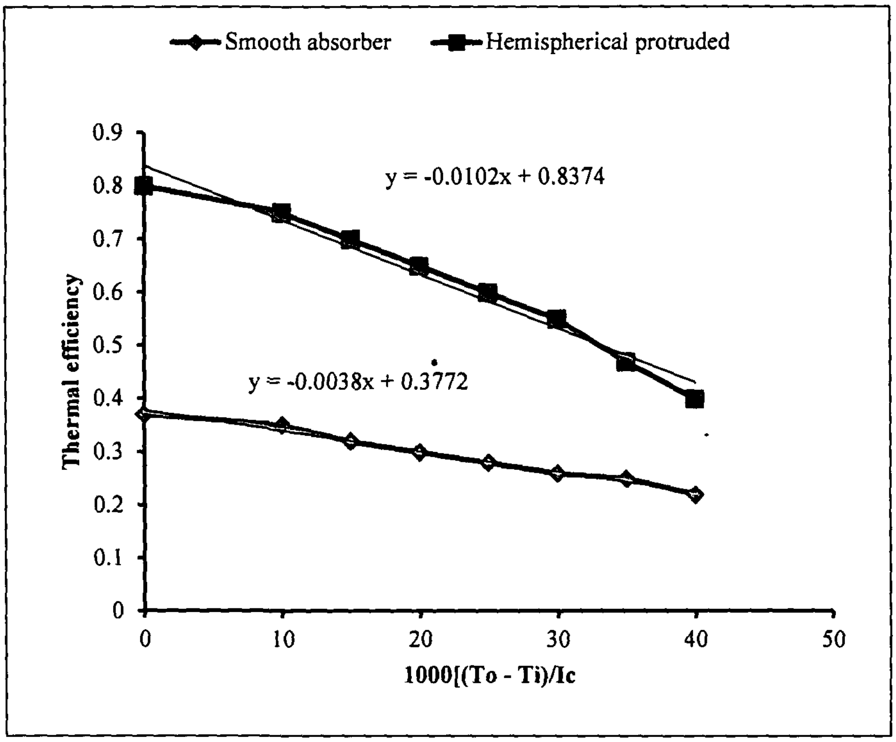

Fig.A4.b: Performance of improved solar air heater

Collector efficiency versus the temperature parameter $(T_o - T_a)/I_c$ for three different mass flow rates have been presented (Fig. A4.c). The efficiencies for hemispherical protrusion were computed as 80 %, 70 %, and 60 % at mass flow rates of $\dot{m}1$= 0.0417, $\dot{m}2$= 0.0313, and $\dot{m}3$ = 0.0208 kg $s^{-1}m^{-2}$ respectively. It was observed that efficiency decreased as temperature parameter increased. Efficiency increased at higher mass flow rate because of the fact that it changed fluid flow from laminar to turbulent region.

The F_R, F_o, F' values was increased with increase in mass flow rate of air. Collector heat removal factor (F_R) varied from 0.42 to 0.50, F' varied from 0.45 to 0.75 and F_O varied from 0.55 to 0.80 with the air mass flow rate of (0.0208 – 0.0417) kg s^{-1} m^{-2} (Fig.A4.d).

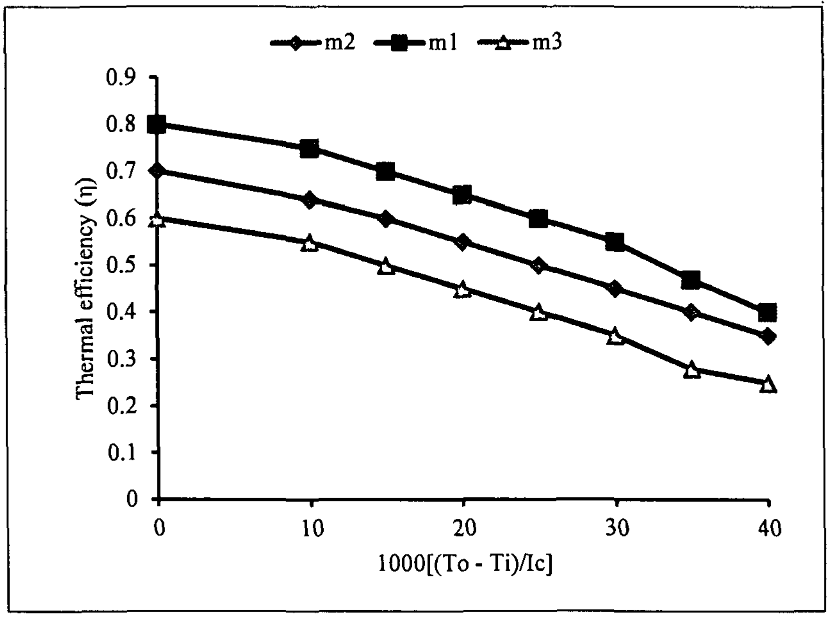

Fig.A4.c: Variations of collector efficiency with temperature parameter for hemispherical protrusion

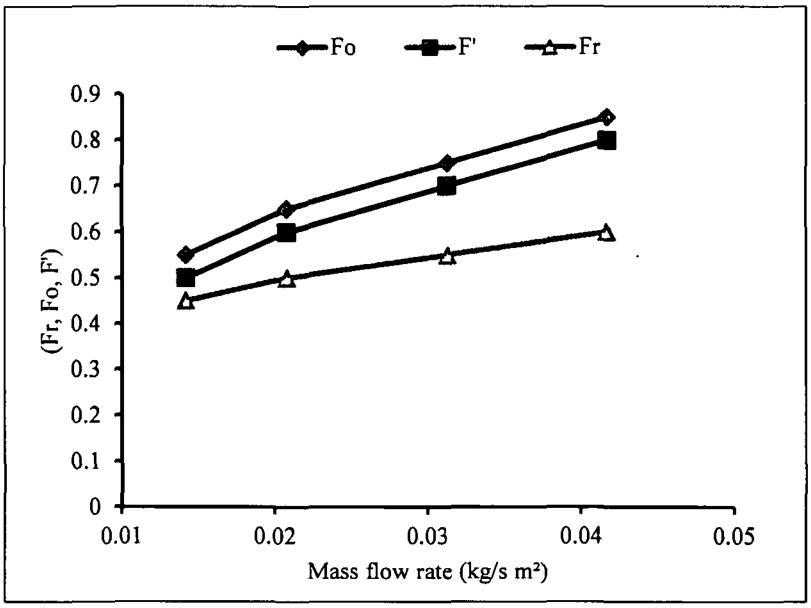

Fig.A4.d: Heat gain factor for hemispherical absorber

Appendix A5: Dryer

The dryer was made of mild steel angle, flat and sheet; ply board as insulator, and steel-wired perforated trays. It was mainly consisted of three principal sections as shown below. They are producer gas combustion chamber cum mixing chamber, drying section and heat exchanger for waste heat recovery. The dryer was a portable unit with overall dimension as 1.22 m × 0.61 m × 1.52 m fuelled by 5 kW thermal out of a WBG-10 biomass gasifier. The drying chamber had height of 0.533 m, breadth of 0.38 m and width of 0.61 m. Ten numbers of steel wire screen perforated trays of dimensions 0.57 m× 0.25 m× 0.13 m were installed one above another and the direction of hot air flow was perpendicular to the trays orientations. The burner of the dryer was modified appropriately for combustion of producer gas with best thermal efficiency. Producer gas flow from the gasifier was controlled to get desired tea drying air temperature in the tray dryer (80-110 °C) for the entire experimentation.

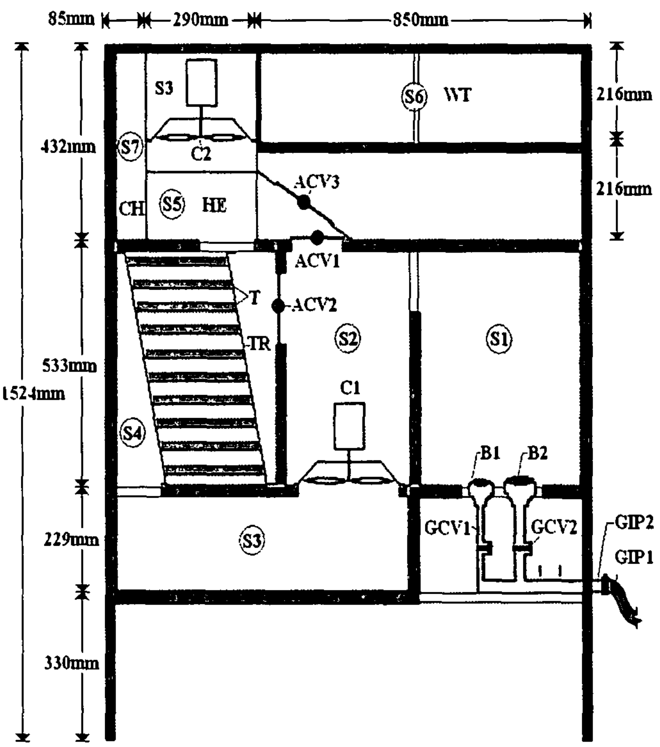

Chambers
S1:Combustion Section
S2:Mixing Section
S3:Compressor Section
S4:Drying Section
S5:Heat exchanger Section
S6:Withering section
S7:Exhaust
Gas inlet pipes
GIP1:Gas inlet flexible hose pipe
GIP2:Gas inlet GI inlet pipe
Gas Control valves
GCV1: Main burner control valve
GCV2: Additional burner control valve
Air control valves
ACV 1: Fresh air control valve
ACV 2: Recirculation air control valve
ACV 3: Withering air control valve
Burners
B1: Main burner (25 mm diameter)
B2: Additional burner (12.5 mm)
Compressors
C1: Hot air Compressor
C2: Fresh air Compressor
Other components
TR: Tray rack
T : Trays
HE: Heat exchanger
WT: Withering trough
CH: Chimney

Fig. A5 Different views of tray dryer

Appendix A6: Dryer efficiency

Efficiency may be expressed by dryer efficiency, heat collection efficiency or collector efficiency, specific moisture extraction rate and pickup efficiency.

Collector efficiency or *heat collection efficiency* (η_{hc}) is a common measure of collector performance in a solar dryer [250, 251]. Collector efficiency is defined as by following equation, where Q_a , Q_c are energy absorbed by drying air (kWh) and solar radiation (kWh) striking the collector area respectively.

$$\eta_{hc} = \frac{Q_a}{Q_c}$$

Pick-up efficiency is defined as the efficiency of moisture removal by the drying air from the product. Pick-up efficiency generally decreases with decreasing moisture content in the product [252, 253]. Pick up efficiency is given by the following equation.

$$\eta_p = \frac{h_0 - h_\iota}{h_{as} - h_\iota} = \frac{W}{\rho V t (h_{as} - h_\iota)}$$

Where h_ι, h_0, and h_{as} are absolute humidity of air (%) at inlet, outlet and adiabatic saturation point, W is weight of water evaporated (kg) from the drying product, V is volumetric air flow rate (m^3 s^{-1}) and t is time in second.

Drying (or system) efficiency indicates the overall thermal performance of the drying system, including collector efficiency and dryer (or drying chamber) efficiency. The system efficiency of a solar dryer is a measure of how effectively the input energy (solar radiation) to the drying system is used in drying the product [234]

$$\eta_s = \frac{WL}{IA + P_f}$$

Drying efficiency is commonly used to represent dryer performance. Major factors affecting drying system efficiency include air temperature rise in the drying chamber, airflow rate, wind speed and collector/dryer design, which directly or indirectly relate to overall thermal losses in the system. A few authors have also attempted to rate the performance of dryers using 'Performance Indices'. *Evaporative Capacity* is one such performance index suggested by Jannot and Coulibaly [254], which considers the effect of ambient air temperature and humidity on the performance of a solar dryer.

Appendix A7: Tea drying thermal energy consumption pattern in some representative black tea manufacturing industries in Assam

Table A7.a Energy consumption pattern in selected tea factories

Factory	MT (M kg/y)	Fuel (withering)	Fuel (drying)	Coal (Mkg y^{-1})	Natural gas (kg y^{-1})	Oil (kg)
F1	2.100	Oil/Gas	Gas/Oil	0	490292	112627
F2	0.0098	Oil	Oil	0	0	4845
F3	1.50	Oil/Gas	Gas/Oil	0	386890	85789
F4	1.30	Oil/Gas	Gas/Oil	0	405000	88789
F5	1.208	Oil/Gas	Gas/Oil	0	395987	86745
F6	1.249	Oil/Gas	Gas/Oil	0	398950	86867
F7	1.350	Oil/Gas	Gas/Oil	0	405467	87987
F8	1.633	Oil/Gas	Gas/Oil	0	456793	90567
F9	1.694	Oil/Gas	Gas/Oil	0	467832	91456
F10	2.272	Oil/Gas	Gas/Oil	0	556789	121578
F11	1.200	Oil	Coal	1.3	0	95890
F12	1.000	Oil	Coal	1.2	0	89765
F13	0.9500	Oil	Coal	1.1	0	85000
F14	1.5000	Oil	Coal	1.6	0	105600
F15	1.8000	Oil	Coal	1.9	0	108976

Table A7.b :Thermal efficiency of black tea drying and total fuel cost

Factory	MJ kg^{-1} MT	Thermal efficiency	Annual Gas Cost $(\$)^{\#}\times10^4$	Annual oil/ $(\$)^{\#}\times10^4$	Annual coal cost $(\$)^{\#}$	Total cost $(\$)\times10^4$
F1	10.64	0.52	25.33	7.77	0	33.10
F2	20.42	0.27	0.00	0.33	0	0.33
F3	11.67	0.48	19.99	5.92	0	25.91
F4	14.06	0.40	20.93	6.13	0	27.05
F5	14.78	0.38	20.46	5.99	0	26.44
F6	14.40	0.39	20.61	6.00	0	26.61
F7	13.53	0.41	20.95	6.07	0	27.02
F8	12.39	0.45	23.60	6.25	0	29.85
F9	12.20	0.46	24.17	6.31	0	30.48
F10	11.05	0.50	28.77	8.39	0	37.16
F11	29.83	0.19	0	6.62	169000	2352.
F12	31.87	0.18	0	6.20	149500	21.14
F13	31.25	0.18	0	5.87	138957	19.76
F14	29.03	0.19	0	7.29	208000	28.09
F15	27.67	0.20	0	7.52	240500	31.57

Coal Price = \$ 0.13 kg^{-1} , Oil price = \$ 0.69 kg^{-1} , Natural gas price = \$ 0.31 Nm^{-3}

Appendix: A8 Solar and biomass gasifier economic analysis results

Table A8.a :Parameters used for estimate of payback period

No	Description of parameter	Amount (US $)
1.	Initial investment of 454 kW (WBG-150) down draft gasifier for thermal mode [241]	15000
	Cost of 400 m^2 improved air heater (\$30 m^{-2}) [179]	12000
2.	Interest one initial investment (@ 10 %)	2700
3.	Depreciation (@ 20 %) for 10 years	540
4.	Repair and maintenance cost (@ 20 %)	270
5.	Cost of electricity to run the accessories of gasifier (8 kW h day^{-1} × 250 days × 0.1 \$ $(kWh)^{-1}$	200
6.	Fuel cost (Wood, 100 kg h^{-1} × 15 h day^{-1} × 250 days × 11 \$ t^{-1}) [7] – 20 % biomass save from air heater	[4125 – 825] 3300
7.	Labour cost (2 × 2 \$ day $^{-1}$ × 250 days)	1000
	Total investment in first year	**35010 $**
8.	Cost of operation per day	9.34 \$ h^{-1}
Cost of operation by coal fired furnace for equivalent heating		
1.	Annual black tea production in an average size tea estate	990 t
2.	Total coal requirement (@ 1.35 kg kg^{-1}) made tea	1366 t
3.	Equivalent coal requirement (28 %)	374 t
4.	Annual cost of coal (374 t × 95 \$ t^{-1})	35551$
5.	Cost of electricity to run ID and FD fan etc., (15 kW h day^{-1} × 250 days × 0.1 \$ $(kWh)^{-1}$)	375$
6.	Labour cost 2 × 2 \$ day $^{-1}$ × 250 days)	1000
7.	Total cost	36926 $
8.	Cost of operation per day	9.85 \$ h^{-1}

Table A8.b: Cash flow (US $) for heating system of a tea dryer

Year	Present worth	PW of cash outflow	Cash inflow	PW of cash inflow	NPV
0	27000	270000	0	0	-27000
1	35114	31921.82	36926	33569.09	1647.27
2	35114	29019.83	36926	30517.36	1497.52
3	35114	26381.67	36926	27743.05	1361.38
4	35114	23983.33	36926	25220.95	1237.62
5	35114	21803.03	36926	22928.14	1125.11
6	35114	19820.94	36926	20843.76	1022.83
7	35114	18019.03	36926	18948.88	929.84
8	35114	16380.94	36926	17226.25	845.31
9	35114	14891.76	36926	15660.23	768.46
10	35114	13537.97	36926	14236.57	698.60

Table A8.c: Payback period

Cash inflow	Present worth	Cumulative cash flow
36926	33569	33569
36926	30517	1545
36926		
	Payback period	1 year 1 months
	Benefit: Cost ratio	1.10